

**Study on Natural Disaster Reduction and Recovery  
Based on Mathematical Engineering Approach**

January 2021

Division of Safety Systems Construction Engineering,  
Graduate School of Engineering,  
Kagawa University

Shiori Kubo



## ABSTRACT

### Study on Natural Disaster Reduction and Recovery Based on Mathematical Engineering Approach

Shiori KUBO

Nowadays, various natural disasters have caused tremendous damages to Japan. It is necessary not only to take disaster prevention and mitigation measures to take appropriate evacuation actions in the event of a disaster and minimize human damage but also to discuss the provision of the information for quick recovery and relief activities after a disaster. In this study, the evacuation simulation considering the flooding state by a storm surge on the basis of the result of flooding analysis is conducted so as to grasp the proper evacuation behavior when a storm surge occurs. Many agents get caught in the flooding in front of the evacuation site and cannot complete evacuation when there is an evacuation spot in a low-altitude area or an area prone to flooding. Next, the additional evacuation simulation in which the agent grasps the flooding state beforehand is carried out under the same conditions as those used in the analysis in which the agent doesn't grasp the flooding state in advance so as to understand the effect of grasping the inundation place beforehand on the evacuation action. When the agent grasped the flooded state in advance, they can complete the evacuation in a short time without being caught in the flooding. At the same time, the evacuation completion rate is much higher than that in the case where the flooded state is not grasped in advance. The damage situation on the road is extracted using SAR image and road edge data in order to grasp the damaged area on the road necessary for a smooth recovery and relief activities after the disaster since the purpose of this study is not only to provide the useful information on disaster mitigation measures, but also to promptly grasp the disaster area immediately after a disaster and to provide the information of leading to more rational recovery activities. As the results of grasping the disaster situation using SAR images, it is found that the extensive changes such as flooded areas can be extract by the method of additive color mixture used in this study.

The results of flooding analysis and evacuation simulation can be utilized for the improvement of the usefulness of the hazard map, the utilization for disaster prevention education, and the disaster-resistant city development planning. In addition, the results of the satellite image analysis are possible to be important information for quick recovery activities by utilizing it to grasp the damage situation of the road area in the event of a disaster Based on the above, it becomes possible to consider the disaster reduction and recovery measures in large-scale cities, which cannot be grasped by experiments.

Keywords: Storm surge, Rainfall disaster, Flooding analysis, Evacuation simulation, Multi-agent simulation, Method of additive color mixture, Satellite image analysis

# Contents

<b>1</b>	<b>Introduction</b>	<b>1</b>
1.1	Background . . . . .	1
1.2	Object . . . . .	4
1.3	Thesis organization . . . . .	5
<b>2</b>	<b>Basic theory</b>	<b>6</b>
2.1	Flooding analysis . . . . .	6
2.2	Evacuation simulation . . . . .	9
2.3	Satellite image analysis . . . . .	12
<b>3</b>	<b>Flooding analysis of storm surge</b>	<b>15</b>
3.1	Introduction . . . . .	15
3.2	Analysis summary . . . . .	15
3.3	Boundary conditions . . . . .	18
3.4	Results of flooding analysis . . . . .	19
3.5	Conclusions . . . . .	24
<b>4</b>	<b>Evacuation simulation during storm surge</b>	<b>25</b>
4.1	Introduction . . . . .	25
4.2	Simulation summary . . . . .	26
4.3	Results of evacuation simulation . . . . .	29
4.3.1	Results of evacuation simulation: Case of the flooding state is or is not reflected . . . . .	29
4.3.2	Results of evacuation simulation: Case of agent grasped or don't grasp the flooding state in advance . . . . .	39
4.4	Conclusions . . . . .	48
<b>5</b>	<b>Satellite image analysis during heavy rainfall</b>	<b>49</b>
5.1	Introduction . . . . .	49
5.2	Analysis summary . . . . .	50
5.3	Results of satellite image analysis . . . . .	50
5.3.1	Extraction of damaged areas by the method of the additive color mixture . . . . .	50
5.3.2	Extraction of road area in addition processing images . . . . .	55
5.3.3	Extraction results of damaged areas in the road area . . . . .	57
5.4	Conclusions . . . . .	64

<b>6 Discussion and conclusions</b>	<b>65</b>
<b>REFERENCES</b>	<b>68</b>
<b>Acknowledgment</b>	<b>73</b>

# List of Tables

3.1	Analysis conditions . . . . .	17
4.1	Walking speeds and standard deviations of agent . . . . .	28
4.2	Simulation cases . . . . .	28
5.1	Condition of satellite image shooting . . . . .	50

# List of Figures

2.1	City model with the passable road . . . . .	11
2.2	Raster data . . . . .	11
2.3	Vector data . . . . .	11
2.4	City model which is reflected the flooding state . . . . .	13
3.1	Expected to be flooded by storm surge <sup>22)</sup> . . . . .	16
3.2	Analysis mesh . . . . .	16
3.3	Ground elevation . . . . .	17
3.4	Boudary condition . . . . .	18
3.5	Flooding state (T=1200 sec) . . . . .	19
3.6	Flooding state (T=1500 sec) . . . . .	20
3.7	Flooding state (T=1800 sec) . . . . .	21
3.8	Flooding state (T=2100 sec) . . . . .	22
3.9	Flooding state (T=2400 sec) . . . . .	22
3.10	Flooding state (T=2700 sec) . . . . .	23
4.1	Initial placements of agents and evacuation spots . . . . .	27
4.2	Evacuation condition of Case 1 (T=1800s) . . . . .	29
4.3	Evacuation condition of Case 2 (T=1800s) . . . . .	30
4.4	Evacuation condition of Case 1 (T=2100s) . . . . .	31
4.5	Evacuation condition of Case 2 (T=2100s) . . . . .	32
4.6	Evacuation condition of Case 1 (T=2400s) . . . . .	33
4.7	Evacuation condition of Case 2 (T=2400s) . . . . .	33
4.8	Evacuation condition of Case 1 (T=3600s) . . . . .	35
4.9	Evacuation condition of Case 2 (T=3600s) . . . . .	35
4.10	Evacuation condition of Case 1 (T=7200s) . . . . .	36
4.11	Evacuation condition of Case 2 (T=7200s) . . . . .	36
4.12	The evacuation completion rate . . . . .	37
4.13	Number of evacuees by evacuation spot . . . . .	37
4.14	Evacuation condition of Case 3 (T=1800s) . . . . .	40
4.15	Evacuation condition of Case 4 (T=1800s) . . . . .	40
4.16	Evacuation condition of Case 3 (T=2100s) . . . . .	42
4.17	Evacuation condition of Case 4 (T=2100s) . . . . .	42
4.18	Evacuation condition of Case 3 (T=2400s) . . . . .	43

4.19	Evacuation condition of Case 4 (T=2400s) . . . . .	44
4.20	Evacuation condition of Case 3 (T=3600s) . . . . .	45
4.21	Evacuation condition of Case 4 (T=3600s) . . . . .	45
4.22	Evacuation condition of Case 3 (T=7200s) . . . . .	46
4.23	Evacuation condition of Case 4 (T=7200s) . . . . .	47
5.1	Satellite image of before a disaster (Gray scale) . . . . .	51
5.2	Satellite image of after a disaster (Red scale) . . . . .	51
5.3	Satellite image of before a disaster (Gray scale) . . . . .	52
5.4	Satellite image of after a disaster (Cyan scale) . . . . .	52
5.5	Satellite image using additive color mixture . . . . .	53
5.6	The estimated inundation range at Mabi-cho . . . . .	54
5.7	The estimated flooding stage color map around Mabi-cho <sup>44)</sup> . . . . .	54
5.8	Vector data of road edge . . . . .	55
5.9	Distinguishing road parts . . . . .	55
5.10	Extraction of road parts in satellite images . . . . .	56
5.11	Emphasizing colored parts . . . . .	56
5.12	Aerial photogrammetry after a disaster (Near Kurashiki makibi support school) <sup>45)</sup> . . . . .	57
5.13	Extraction of damaged area on road (Near Kurashiki makibi support school) . . . . .	58
5.14	Extended figure (East side of Kurashiki makibi support school) . . . . .	58
5.15	Extended figure (Near prefectural highway 281) . . . . .	59
5.16	Extended figure (Near Oda river) . . . . .	59
5.17	Aerial photogrammetry after a disaster (North side of Route 486) <sup>45)</sup> . . . . .	60
5.18	Extraction of damaged area on road (North side of Route 486) . . . . .	61
5.19	Extended figure (Near Yata elementary school) . . . . .	61
5.20	Aerial photogrammetry after a disaster (South side of Oda river) <sup>45)</sup> . . . . .	62
5.21	Extraction of damaged area on road (South side of Oda river) . . . . .	62
5.22	Extended figure (South side of Oda river) . . . . .	63
5.23	Extended figure (Intersection of Madani and Oda river) . . . . .	63



# 1 . Introduction

## 1.1 Background

### Past disaster cases

Nowadays, the disaster-preventions such as the communication of disaster information like an occurrence of an earthquake and a flooding state and the technology development of observations have been conducted since the various natural disasters have caused tremendous damages to Japan. However, it is assumed that there are still many problems about the disaster-preventions such as the evacuation behavior since the 2011 off the Pacific coast of Tohoku Earthquake had a desperately serious influence on the lives of Japanese citizens and the serious human and material damages occurred. Many studies related to the evacuation behavior especially during tsunami flooding have been conducted since the experience of the earthquake and tsunami as referred to above and the anticipation of occurring a giant earthquake and tsunami around Nankai Trough. It is necessary to consider the measures that isn't only the tsunami, but the collapse of rivers and ponds due to heavy rain and the flooded caused by storm surge in the areas that are unlikely to be severely damaged by Nankai megathrust earthquakes or Tokyo Metropolitan Earthquake that may occur in the future. For example, the levee of Kinugawa River was broken for about 200 m, the serious damages were caused: two persons died, more than forty persons were injured, and the number of houses which collapsed full or half was more than 5000 buildings<sup>1)</sup>. At that time, the alert of evacuation advisor had announced in some areas before the levee of Kinugawa River collapsed. However, many residents got caught in the water of the river or was forced to stay home in the region which was included the area near the point of breaking the levee since the alert of evacuation advisor wasn't announced in this area<sup>1)</sup>. Additionally, more than 1000 residents were isolated by flooding around the designated evacuation spot to which they evacuated, although many residents evacuate to this spot<sup>2)</sup>. Therefore, there is room for reconsidering the evacuation behavior and the location of the evacuation spot when the flooded area spreads by occurring a storm surge or breaking the levee of a river or an irrigation tank as well as the evacuation behavior on the occurrence of the tsunami.

Besides, it is necessary to discuss the flooding damages and the evacuation behavior with considering the flooding state in the area facing an inland sea such as Takamatsu City caused by a storm surge associated with typhoon than a tsunami since it is expected that the high of the highest wave is less than 4.0 m and the arrival time of the highest wave is about 3.0 hours when the enormous earthquake occurs along Nankai Trough<sup>3)</sup>. The season's 16th and 23rd typhoons in 2004 caused tremendous damages to Takamatsu City. In August 2004, the maximum tide level at the Takamatsu port was recorded. Then, two persons died and

the number of houses which inundated above floor level was 5877 buildings and below floor level was 10088 buildings by the season's 16th typhoon<sup>4</sup>). At that time, many residents could not complete evacuating to a certain evacuation spot and stayed at home since the alert of evacuation advisor was delayed in the region where serious damages occurred, and the designed evacuation spot is flooded although the alert of evacuation advisor was announced<sup>5</sup>). While 10 residents evacuated to an evacuation spot only 100 meters away from their homes, they got caught in the flooding, 8 people died and one person went missing in Sayo-cho, Sayo District, Hyogo Prefecture during the heavy rain occurred in August 2009<sup>6</sup>). However, if they had grasped an adequate flood condition, made a rapid decision to evacuate and behaved a proper and expeditious evacuation under these situations, it was possible to minimize the human casualties. Additionally, it is necessary for residents to raise their awareness of disaster prevention on a daily basis and to grasp how far the flood area will expand and how deep the flood will reach when a storm surge occurs.

## **Disaster prevention measures: hazard maps**

Takamatsu City officially announced, "Takamatsu disaster prevention map"<sup>7</sup>) which indicates the maximum water depth due to flooding and the dangerous factors for each disaster so as to minimize the damages when the disaster occurs. However, the flooding region and depth which change with time aren't written down on the hazard map. Therefore, it is possible that the residents can't evacuate properly if they evacuate based only on the hazard map when the storm surge occurs. According to the questionnaire was conducted for Higashiyama-cho and Kawasaki-mura, Higashiiwai District, Iwate Prefecture in which serious damage caused by heavy rain in the last 30 years, the respondent of "I had seen the hazard map" was 53%<sup>8</sup>). That is to say, only half of the residents are aware of the hazard map. Moreover, 52% of respondents who answered, "I have seen the hazard map" (that is 27% of all respondents) answered "The hazard map was useless". Among those who responded to this question, there were multiple opinions such as "Unrealistic designation of evacuation spots on hazard maps" and "Hazard maps weren't consider flooding from tributaries". That is to say, they were not suited to the actual situation of each region. Although the hazard map is a useful tool for residents to know the disaster prevention information around their homes, it is desirable to provide a more valuable hazard map by adding information such as evacuation spots and routes suitable for the target area, the necessary time for evacuation, and disaster conditions which change with the passage of time. It is also possible to provide the disaster prevention information to residents by not only the hazard map but also the disaster prevention workshop and citizen lecture conducted by the local governments, the students of local universities, etc. The provision of such useful hazard maps and the implementation of disaster prevention workshops will make residents think about disaster prevention, and it will be possible to develop human resources who can think about and actively work not only on actions in disasters but also on recovery activities afterwards.

## **Disaster prevention recovery measures**

In addition, not only disaster prevention and mitigation measures, but also the necessary information for restoration/relief activities are necessary to discuss. When the heavy rainfall disaster in the Kanto-

Tohoku region occurred in September 2015, obstacles such as abandoned vehicles and rubble hindered the movement of the drainage pump vehicle, which posed a problem for restoration<sup>9)</sup>. At that time, the removal of sediment on specific roads and the moving of abandoned vehicles according to be grasped the disaster situation by the disaster prevention helicopter can operate the drainage pump vehicle. However, it took more than two days to move it. This is because a lot of time to decide which road to move the vehicle. When the heavy rainfall disaster occurred in July 2018, one resident didn't know that the river levee near her home had collapsed but returned home temporarily from the evacuation spot, then she got caught in sudden flooding<sup>10)</sup>. It became an issue to quickly grasp the damage situation after the disaster. At this disaster, if information about the disaster situation had been shared at the evacuation spot, this situation would haven't occurred. In summary, it is necessary to quickly grasp the damage situation immediately after the disaster for recovery activities, and also necessary not only to share information with experts and local governments, but also to disseminate information that is easy to understand to residents in the future.

## 1.2 Object

It is necessary to discuss what kind of behavior evacuee should do and the proper choice of the evacuation routes at the time of occurring a disaster so as to minimize the damage. However, it is difficult to get the flooding situation which changes with time and to grasp the information of the evacuation spots and routes which are available even if the hazard map is utilized. Therefore, it is difficult to grasp the difference of flooding state between areas and the region which is flooded in a short time. It is necessary to grasp the proper evacuation behavior when the flooded area spreads over a wide area and the evacuation behavior that the evacuee should take then as has mentioned in Section 1.1. Moreover, it is necessary to grasp the proper location of the evacuation spot since the situation in which the evacuation spot was flooded by a water disaster as mentioned in the first section. In addition, it is necessary not only to take disaster prevention and mitigation measures to take appropriate evacuation actions in the event of a disaster and minimize human damage but also to discuss the provision of the information for quick recovery and relief activities after a disaster.

In this study, the storm surge flooding simulation is conducted and the evacuation behavior considering the flooding state which changes with the passage of time obtained by flooding analysis were simulated. Additional simulations in which the agent grasps the areas flooded at an early stage and deeper than other areas in flooding analysis are defined as the impassable area in advance are carried on. The area is expected to be flooded and the effects on the selection of the evacuation site and route is grasped by these simulations. The purpose of this study is to reduce the long-term disaster mitigations by the suggestion of the proper location of evacuation spot and proper evacuation route for a future city planning. Additionally, the damage situation is grasped by analyzing the satellite image of before and after the disaster. In particular, the damage situation on the road is grasped since the purpose of this study is to enable quick activities after a disaster by focusing on the road which is important during restoration and relief activities. For the analysis, SAR images which can be taken and grasped even in the bad weather such as a storm surge and heavy rain were used. SAR images are analyzed using the method of additive color mixture which requires few processing steps and can extract the damaged area relatively quickly and easily.

## 1.3 Thesis organization

As shown in the previous section, in this study, the storm surge flooding analysis is conducted and evacuation behavior considering the flooding state which is the results of the flooding analysis is simulated as disaster prevention and mitigation measures. Additionally, the damage situation during the heavy rain disaster of the road area is extracted using the satellite image of before and after the disaster. This thesis is summarized these studies and consisted of the following six chapters.

In Chapter 1, the situation during a disaster occurred in recent years, current disaster countermeasures, and their issues are discussed and the purpose of this study is clarified. In Chapter 2, the basic theory of the flooding analysis, evacuation simulation, and satellite image analysis method are described. In Chapter 3, 3D flooding analysis is conducted and the flooding state changing with time at the time of storm surge occurred in the past is discussed. The flooding state at the time of the disaster and the result of this analysis are compared and are generally correlated. That is to say, the numerical analysis method used in this study is justified. The analysis result is useful as information on new disaster mitigation measures since it becomes easier to visually grasp the flooding state changing with time by animating the result. In Chapter 4, the evacuation behavior considering the flooding state which is the result of the flooding analysis is conducted and the evacuation behavior during the storm surge flooding is discussed. It shows that the evacuees can't complete the evacuation due to the early flooding even if there are evacuation spots around the flooded areas shown in the previous chapter. Moreover, the evacuation simulations in which the agent recognized the part of the flooding state in advance are conducted in order to discuss the effect of the prior recognizing of the disaster situation using hazard maps, etc. on the evacuation behavior. These simulations show that the prior recognizing of flooded areas is effective in taking appropriate evacuation behavior. Additionally, early evacuation and evacuation at home is necessary to consider in the areas where there are few evacuation spots and flooding at an early stage. In Chapter 5, the result of grasping the damage situation at the time of heavy rain disaster using the SAR images not affected by the shooting time and weather condition by the method of the additive color mixture is shown. This result will be useful in the disaster area because it becomes possible to clearly interpret whether the damage on the road is due to sediment or flooding. In Chapter 6, this thesis is summarized and future works is described.

## 2 . Basic theory

### 2.1 Flooding analysis

#### Governing equation

In this study, for the purpose of the provision of the useful information that leads to disaster mitigation, the numerical simulations are conducted to grasp the damage at the time of disaster occurred in the past. Flooding analysis of a storm surge is carried out using OpenFOAM<sup>11)</sup>, a computational fluid dynamics (CFD) software, is used for the flooding analysis of a storm surge so as to grasp the flooding state at any time due to storm surge. OpenFOAM equips interFoam, the solver for multi-phase flow analysis in which the volume of fluid (VOF) method. IHFoam in the wave-making source for the multi-phase flow analysis solver interFoam is employed for the storm surge flooding analysis. This solver covers the incompressible, unsteady, and isothermal fluid. The governing equations in the IHFoam include the Navier Stokes equation, continuity equation, and advection equation, respectively, as follows:

$$\rho \frac{\partial \mathbf{v}}{\partial t} + \rho \mathbf{v} \cdot \nabla \mathbf{v} = -\nabla p + \mu \nabla^2 \mathbf{v} + \rho \mathbf{F} \dots\dots\dots (2.1)$$

$$\nabla \cdot \mathbf{v} = 0 \dots\dots\dots (2.2)$$

$$\frac{\partial \alpha}{\partial t} + \nabla \cdot (\alpha \mathbf{v}) = 0 \dots\dots\dots (2.3)$$

where the parameters  $\rho$ ,  $\nu$ ,  $p$ ,  $\mu$ ,  $F$ ,  $t$  and  $\alpha$  are density, flow velocity vector, pressure, the viscosity coefficient, external force vector, time and the volume fraction of the liquid phase, respectively. Regarding the value of  $\alpha$ , the whole of the intended cell is the gas phase when the value of  $\alpha$  is "0". Also, this cell is the liquid phase when the value of  $\alpha$  is "1". Moreover, the density, the viscosity coefficient and the kinematic viscosity coefficient are shown as follows equations:

$$\rho = \alpha \rho_l + (1 - \alpha) \rho_g \dots\dots\dots (2.4)$$

$$\mu = \alpha \mu_l + (1 - \alpha) \mu_g \dots\dots\dots (2.5)$$

$$\nu = \alpha \nu_l + (1 - \alpha) \nu_g \dots\dots\dots (2.6)$$

It should be noted that  $\rho_l$ ,  $\rho_g$ ,  $\mu_l$ ,  $\mu_g$ ,  $\nu_l$  and  $\nu_g$  are the density, the viscosity coefficient and the kinematic viscosity coefficient about the liquid phase and gas phase, respectively.

Navier-Stokes equation whose third term of the right side is divided into the external force term " $F_s$ " and the gravity term " $g$ " is shown as the following equation.

$$\rho \frac{\partial \mathbf{v}}{\partial t} + \rho \mathbf{v} \cdot \nabla \mathbf{v} = -\nabla p + \mu \nabla^2 \mathbf{v} + \rho \mathbf{F}_s + \rho \mathbf{g} \dots\dots\dots (2.7)$$

The external force is expressed by CSF (Continuum Surface Force) model<sup>12)</sup> which was proposed by Brackbill et.al as the following equation.

$$\mathbf{F}_s = \sigma \kappa \mathbf{n} \dots\dots\dots (2.8)$$

where the parameters  $\sigma$ ,  $\kappa$  and  $n$  are the surface tension coefficient, the curvature of interface and the normal unit vector on the free surface, respectively. Then, the curvature of the interface which is the divergence of the normal unit vector is shown as  $\kappa = -\nabla \cdot n$ . Moreover, the viscosity term which is the second term of the right side is shown as  $\nabla \tau$  by using the viscous stress tensor "  $\tau = \mu \nabla^2 v$ ". Therefore, Navier-Stokes equation is defined as the following equation in this study.

$$\rho \frac{\partial \mathbf{v}}{\partial t} + \rho \mathbf{v} \cdot \nabla \mathbf{v} = -\nabla p + \nabla \tau + \rho \mathbf{F}_s + \rho \mathbf{g} \dots\dots\dots (2.9)$$

In this analysis, the advection equations for the liquid and gas domains are solved so as to deal with these phases. In this equation, the flow velocity vector at the liquid and gas phases is shown as  $v_l$  and  $v_g$ .

$$\frac{\partial \alpha}{\partial t} + \nabla \cdot (\alpha \mathbf{v}_l) = 0 \dots\dots\dots (2.10)$$

$$\frac{\partial \alpha}{\partial t} + \nabla \cdot ((1 - \alpha) \mathbf{v}_g) = 0 \dots\dots\dots (2.11)$$

The flow velocity vector  $\mathbf{v}$  is shown as the following equation by using  $v_l$  and  $v_g$  in the same way as the density and the viscosity coefficient.

$$\mathbf{v} = \alpha \mathbf{v}_l + (1 - \alpha) \mathbf{v}_g \dots\dots\dots (2.12)$$

Eq.2.12 is substituted to Eq.2.10.

$$\frac{\partial \alpha}{\partial t} + \nabla \cdot (\mathbf{v}) - \nabla \cdot ((1 - \alpha) \mathbf{v}_g) = 0 \dots\dots\dots (2.13)$$

Moreover, the above equation is rewritten as the following equation by Eq.2.10 and Eq.2.13.

$$\nabla \cdot (\mathbf{v}) - \nabla \cdot (\mathbf{v}_g) + \nabla \cdot ((\mathbf{v}_g - \mathbf{v}_l) \alpha) = 0 \dots\dots\dots (2.14)$$

The relative velocity "  $v_c$ " which is the difference of the flow velocity between liquid phase and gas phase is shown as "  $v_c = v_l - v_g$ " and substituted into Eq.2.14.

$$\nabla \cdot (\mathbf{v}) - \nabla \cdot (\mathbf{v}_l - \mathbf{v}_c) - \nabla \cdot (\alpha \mathbf{v}_c) = 0 \dots\dots\dots (2.15)$$

The advection equation is shown as Eq.2.16 in which Eq.2.15 is multiplied by the value of  $\alpha$  and Eq.2.10 is substituted to Eq.2.15.

$$\frac{\partial \alpha}{\partial t} + \nabla \cdot (\alpha \mathbf{v}) + \nabla \cdot ((1 - \alpha) \alpha \mathbf{v}_c) = 0 \dots\dots\dots (2.16)$$

## Wave-making Source

As mentioned above, "ihFoam" in which the wave-making source is added to "interFoam" is employed in this simulation. In this stage, the wave which is used in this simulation applies "Stokes 2nd order" according to the reference into consideration of the actual wave height and water depth. In the storm

surge flooding simulation, the height of surface elevation  $\nu$  and the velocity  $V(u, v, w)$  are defined by the following equations.

$$\eta = \frac{H}{2} \cos(\theta) + k \frac{H^2}{4} \frac{3 - \sigma^2}{4\sigma^3} \cos(2\theta) \dots\dots\dots (2.17)$$

$$u = \frac{H}{2} \omega \frac{\cosh(kz)}{\sin(kh)} \cos(\theta) + \frac{3}{4} \frac{H^2 \omega k \cosh(2kz)}{4 \sinh^4(kh)} \cos(2\theta) \dots\dots\dots (2.18)$$

$$v = \frac{H}{2} \omega \frac{\cosh(kz)}{\sin(kh)} \cos(\theta) + \frac{3}{4} \frac{H^2 \omega k \cosh(2kz)}{4 \sinh^4(kh)} \sin(2\theta) \dots\dots\dots (2.19)$$

$$w = \frac{H}{2} \omega \frac{\sinh(kz)}{\sin(kh)} \cos(\theta) + \frac{3}{4} \frac{H^2 \omega k \sinh(2kz)}{4 \sinh^4(kh)} \sin(2\theta) \dots\dots\dots (2.20)$$

where  $\mu$ ,  $H$ ,  $\theta$ , and  $V$  are wave height, the water depth on the wave-making surface, wave phase and the velocity vector having velocity components,  $u$ ,  $v$  and  $w$  of  $x$ ,  $y$  and  $z$  directions, respectively. The wave constant  $k$  is defined as  $k = 2\pi/L$  relative to wavelength  $L$ . Moreover,  $\sigma = \tanh(kh)$ .

### Pressure-velocity coupling method

In this simulation, the pressure and the velocity are calculated by using the Navier-Stokes equation and the equation of continuity. PIMPLE method is employed so as to calculate pressure and velocity since the incompressible fluid is employed in this analysis. PIMPLE method consists of SIMPLE (Semi-Implicit Method for Pressure-Linked Equation) and PIMPLE (Pressure-Implicit with Splitting of Operators) methods. In SIMPLE method, the predicted value of the pressure is offset until this value converges after the predicted values of pressure and velocity are calculated by these initial values. Whereas the number of times to offset the predicted value of the velocity is once, the predicted value of the pressure is offset until this value converges. On the other hand, in PISO method, the predicted values of the pressure and velocity are offset until these values converge after these predicted values are calculated by the initial values of them in the same way as SIMPLE method. PIMPLE method is the method in which SIMPLE method is incorporated in the timestep of PISO method. In addition, the finite volume method is utilized for the space discretization of the governing equations. Where, the time term and the convection term are discretized by the 1st order forward difference method and 2nd order TVD (Total Variation Diminishing) method, respectively. The unsteady term is interpolated by linter interpolation method. Then, the gradient for vector field is kept from oscillating by using coefficient  $\phi = 1.0$ .



## 2.2 Evacuation simulation

### Regarding to MAS

In this study, for the purpose of the provision of the useful information that leads to disaster mitigation, the evacuation simulation, which reflects the inundation situation shown by the flooding analysis, was performed to describe the evacuation behavior under inundation in the event of a storm surge. The evacuation simulator<sup>13)14)</sup> developed by Earthquake Research Institute, the University of Tokyo is employed in the evacuation behavior simulation and operated by a multi-agent system (MAS). In the MAS, complicated phenomena can be reproduced by defining only the interaction between the individual elements into a rule. MAS, the system which independent individual agents depend on each other consists of "Agent" and "Environment". "Agent" is acted independently on the basis of the mechanism of decision-making and action plan since "Agent" acts independently without the direct intervention by something such as a human. On the other hand, "Environment" is the object which has an influence such as a time and space on "Agent". Therefore, "Agent" acknowledges "Environment" and acts autonomously on the basis of the individual attribute in order to accomplish the purpose of "evacuate" in MAS.

### Agent model design

Thus, the rule which is the action between each "Agent" is made in order to be reproduced the complex phenomenon in MAS<sup>15)16)</sup>. For example, when the agent evacuates, it is expected the evacuation routes are congested due to a decrease in walking speed by overtaking and stopping. It is necessary that the ability data of the moment and intellect are expressed these evacuee's behaviors. Then, the ability of the moments which are the walking speed and the visual field, and the ability of the intellect is the criterion evaluation which is about the overtaking and the stopping. Based on the above, the three functions, "see", "think" and "move", are designed. As for "see" function, the visual field is set in order to decide the moving direction after watching other agents, the wall and the evacuation route in the visual field. As for "think" function, it has the option by which the walking speed and the moving direction are decided. The agent evacuates to the evacuation spot by "move" function using the walking speed and the moving direction which is decided in "think" function. In "think" function, the decision of the overtaking is contained. The agent decides whether to the overtaking other agents forcibly or stopping. Then, it is possible that the roadblock is caused due to occur a lot of the overtaking. In this simulation, the three conditions about the overtaking are set <sup>13)</sup>. Regarding the first condition, the agent doesn't overtake when the right and left side of the intended agent is blocked by the other agents. Regarding the second condition, the agent overtakes to the direction that isn't blocked when the one side or the other of the intended agent is blocked by another agent. Regarding the third condition, the agent decides which side the agent overtakes the front agent depending on the positional relationship with the front agent when both sides of the intended agent isn't blocked. The agent stops 0.5 sec with 50% of a probability when the agent overtakes the front agent.

Additionally, there are four kinds of the agent which is "Resident", "Non-Resident", "Official", and "Car". First, "Resident" in this simulation have good knowledge of the local area and individually evacuate

to the designated evacuation by themselves. Second, "Non-Resident" isn't familiar with the local area and able to evacuate without the evacuation guiding person. Third, "Official" is the evacuation guiding person. Finally, "Car" is the agent who evacuates to use the car. In this study, "Resident" is only employed. Agents are randomly generated and placed in the city model and they typically have different walking speeds because the average speed and arbitrary standard deviation are given to each agent in the numerical formulation. Then, the agents are classified by gender and age based on the population data in the target area<sup>17</sup>), and then, the regional characteristics of the evacuation behavior which is influenced by the difference in the population distribution of each area are reflected by assigning different walking speeds and standard deviation to each agent.

## City model design

The city model(**Fig.2.1**) consists of the raster data which is high-definition two dimensions grid (**Fig.2.2**) and the vector data which indicates the passable area(**Fig.2.3**). The vector data connect the passable area and the evacuation spot and the agent acts on the basis of this vector data in the evacuation simulation. On the other hand, the raster data is composed of the passable area, the impassable area, and the evacuation spot. The evacuation and flooding state in the city are recognized easily by using the raster data when the result of evacuation simulation is visualized. In the city model, which is utilized in the evacuation simulation, the area where the flooding depth obtained by the flooding analysis exceeds a threshold value, as well as to the area with structure as the impassable area and another area are set as the passable area.

## Evacuation simulation cases

As mentioned in the first section, there were two evacuation simulation cases: (a) when the agent was aware in advance of the flooded area and (b) when the agent was unaware. In either case, the agent evacuates to the nearest evacuation spot through the quickest route from the initial placement. However, the agent may not always find the quickest route or evacuate when the evacuation route is blocked by the flooding. When confronted with the area being flooded, the agent must return to the bifurcation point in the road, and from there, the agent must search a new evacuation route. Accordingly, the agent in case (b) has to search for another evacuation route every time a chosen route is flooded or when many roads around the route are inundated, whereas the agent in case (a) can search for the quickest route and evacuate while avoiding routes that are likely to be flooded.

The judge of the passable or not by flooding is conducted on the basis of the value of  $\alpha$  which is the volume fraction of the liquid phase. As will be described in detail later, the area is impassable if the value of  $\alpha$  at each node in the ground, which has the information such as the coordinate in order to compose the analysis mesh is more than the fixed value. Also, the area is passable if the value of  $\alpha$  is less than the fixed value. In this study, as mentioned above, the city model is made by the raster data which is constructed two dimensional grids. Then, this data is composed of the two numbers which are "zero" and "one". "zero" means the passable area, "one" means the impassable area. The city model in which the intricate configurations such as the road and the impassable area are reflected is structured by these numbers. Then, the flooding area and the impassable area such as the building are expressed by

"one" which means the impassible area. Thus, the two city models are combined in order to reflect the flooding state. One is considered the flooding state, and another isn't. Then, the impassible area such as the building is expressed by "two", the flooding area is expressed by "one", and the impassible area is expressed by "zero".

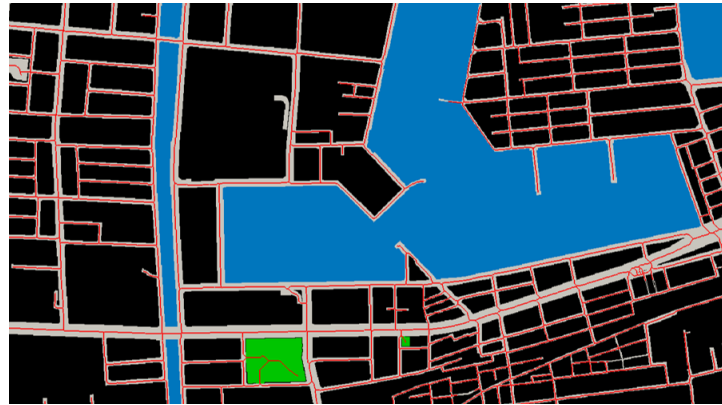


**Fig.2.1** City model with the passable road



**Fig.2.2** Raster data



**Fig.2.3** Vector data

## 2.3 Satellite image analysis

### Regarding to grasp a disaster situation

The purpose of this study is not only to provide the useful information on disaster mitigation measures, but also to promptly grasp the disaster area immediately after a disaster and to provide the information of leading to more rational recovery activities. Therefore, in addition to flooding analysis and evacuation simulation, the damage situation in the heavy rain disaster is grasped by image analysis. Aerial photography and satellite image taken by aircraft and drone are mainly used to grasp the damage situation. First, while it is easy to interpret the damaged situation and to get detailed information using aerial photography it is difficult to take aerial photography at night or in bad weather. It is considered to be useful when a landslide disaster or earthquake occurs during the day when the weather is good, but it is not suitable during heavy rain or storm surge occurs due to a typhoon. Next, satellite images are classified into optical satellite image and Synthetic aperture radar (SAR) image. The former is an image object taken with sunlight and the latter by using microwave reflection. Optical satellite image can be taken in a wider area than aerial photography since it is taken by satellite. However, it is difficult to take optical satellite image at night or in bad weather since it is taken with sunlight like aerial photography. SAR image can not only be taken over a wide area due to be taken by satellite, it but also can be taken regardless of the weather due to can be taken by the reflection of microwaves emitted by it. Therefore, SAR image is often used to grasp the damage situation during heavy rain disasters and storm surge disasters. In this study as well, SAR image is used to grasp the damage situation by heavy rain.

### SAR image analysis method

SAR is the observation system that irradiates microwaves to the ground and analyzes the signal from the ground. As has mentioned above, it is possible to observe the object at night or in bad weather, which is difficult to observe with sunlight such as optical satellite and aerial camera since SAR image observe the reflected intensity using microwaves. However, SAR image is more difficult intuitively to interpret than aerial photography and optical satellite image since the SAR image is a monochrome image showing the reflection intensity of the microwaves. In order to resolve such problems, the method of additive color mixture which is extracted the changing area by the disaster in the two images before and after the disaster as a color change, is used to interpret the damage situation. In the method of additive color mixture, the pre-disaster image is converted to red scale and the post-disaster image is converted to cyan scale. Then, the RGB values of the two images are added. The method of adding processing is shown in Fig.2.4 and Eq.2.21.

$$be(R, G, B) + af(r, g, b) = mix(R + r, G + g, B + b) \dots\dots\dots (2.21)$$

The numerical values in Fig.2.4 indicate the RGB values of each pixel. In Eq.2.21,  $be(R, G, B)$  indicates the color at any pixel before the disaster, and  $R, G, B$  indicate the magnitude of Red, Green, Blue, respectively.  $af(r, g, b)$  indicates the color at any pixel after the disaster, and  $r, g, b$  also indicates the magnitude of Red, Green, Blue, respectively. Then, the numerical value of each color takes a value of 0

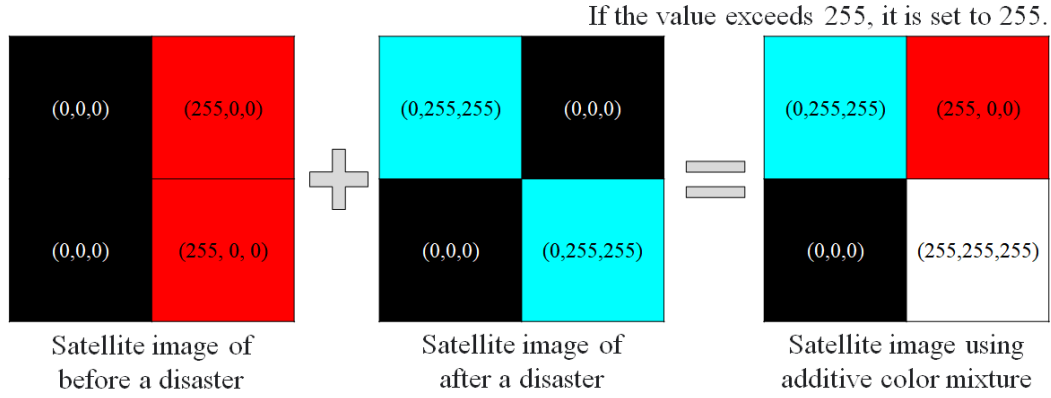


**Fig.2.4** City model which is reflected the flooding state

or more and 255 or less. As a specific example, when a vegetated or water area becomes a bare area by a disaster, RGB value changes from close to black  $(R, G, B) = (0, 0, 0)$  to cyan  $(r, g, b) = (0, 255, 255)$  like a top left pixel of 3 images in Fig.2.4. From Eq.2.21, the pixel value of the area which vegetated or water area becomes a bare area by the disaster becomes  $(0, 255, 255)$  and the color becomes close to cyan after adding the RGB values of both images. In addition, when a bare area becomes a water area by a disaster, RGB value changes from close to red  $(R, G, B) = (255, 0, 0)$  to black  $(r, g, b) = (0, 0, 0)$  like a top right pixel of 3 images in Fig.2.4. From Eq.2.21, the pixel of the area which a bare area becomes a water area by the disaster becomes  $(255, 0, 0)$  and the color becomes close to red after the RGB values of both images. In a water area such as a paddy field, pond, and river which doesn't change status by a disaster, RGB value doesn't changes from close to black  $(R, G, B) = (0, 0, 0)$  like a bottom left pixel of 3 images in Fig.2.4. Therefore, from Eq.2.21, the pixel of the area which doesn't change status by the disaster such as a water area (e.g. paddy field, pond, and river) doesn't change from  $(0, 0, 0)$  and also the color doesn't change from black after adding the RGB values of both images. At the structure which doesn't change status by a disaster, RGB value changes from close to red  $(R, G, B) = (255, 0, 0)$  to cyan  $(r, g, b) = (0, 255, 255)$  like a top right pixel of 3 images in Fig.2.4. From Eq.2.21, the numerical value of such place's pixel becomes  $(255, 255, 255)$  and the color becomes close to white after adding the RGB values of both images. Therefore, the area that changes before and after a disaster is indicated by either cyan or red in the image after adding the RGB values of both images.

### Extraction method of road part in satellite image

Not only the area of changing before and after the disaster is extracted, but also the disaster situation on roads is grasped from the image after adding the RGB values of both images since the purpose of this study is to grasp the damage situation on the roads necessary for smooth recovery and relief activities after the disaster. As will be described in detail later, in order to extract the damage situation on the road, the satellite image is classified into two areas, one is inside the road edge and the other is outside using the road edge data provided by the Geospatial Information Authority of Japan. The procedure for extracting the road part is shown below.

1. Convert the road edge from vector data to raster data.
2. Inside or outside the road, that is to say, the road or not is distinguished by the road edge raster data created in 1.

After creating an image distinguished whether or not as the road, it is converted to the same resolution as the satellite image.

3. Only the road part is extracted from the image created in 2. and the additive color mixed image

Through the above procedure, the road part is extracted from the additive color mixed image, that is to say, the damaged situation in the road area is extracted.

## 3 . Flooding analysis of storm surge

### 3.1 Introduction

It is necessary to grasp the damage situation during the disaster so as to provide the proper evacuation behavior and spot considering the disaster situations. In terms of the water disaster out of the various disasters, the flooding situation is predicted and verified by many inundation or flooding analyses such as the inside water inundation analyses<sup>18)19)</sup> and a tsunami or storm surge flooding analyses<sup>20)</sup>. It is referred by Oshita et al. that the non-structural measure like a hazard map for the unexpected large-scale disaster in case of a storm surge or a tsunami as well as structural measure is more effective since the structural measure should require the enormous cost and time<sup>21)</sup>. That is to say, the non-structural measure may lead to reduce the disasters. The reference suggested that the detailed data like the flooding area, the maximum depth of flooding and the flow velocity of a tsunami or storm surge should be added to a hazard map after these flooding simulations. As has already mentioned in Chapter 1, the flooding simulation was conducted for many prefectural and city governments such as Takamatsu City and the map showing areas for flooding from a tsunami or a storm surge was produced on the basis of the simulation and it opened to the public<sup>22)</sup>. Indicating the area and maximum depth of flooding in the hazard map leads to directly help evacuation behavior in an emergency. However, the flooding situations of a tsunami or a storm surge may change as times go by after hitting. Thus, it is necessary to grasp the area where there is a possibility of flooding in advance in order to take appropriate evacuation behavior. Therefore, it is necessary to carry on the evacuation simulation reflecting the flooding by flooding disaster and to discuss the evacuation behavior concerning the flooding situation at any time. In this chapter, the flooding analysis of a storm surge is carried out using a sort of CFD software "OpenFOAM" to grasp the flooding state changing from hour to hour when a storm surge occurs.

### 3.2 Analysis summary

#### Target area

In this research, the flooding analysis is conducted in the area indicated by the black framework in the hazard map of Takamatsu city shown in **Fig.3.1**. In this analysis area, the southern area from the area whose flooding depth is expected more than 1.1 m and less than 2.1 m is the natural landform from **Fig.3.1**. However, the northern area from this area is the artificial landform.

## Analysis model

As for the analysis domain for the storm surge flooding analysis, the height of the analysis area from the ground level to the top is set to 10.0 m in a three-dimensional space since the maximum flooding depth in this analysis area with the 16th and 23rd typhoons of 2004 reached approximately 3.1 m<sup>23)</sup>. The digital elevation model (DEM) with 5.0m interval, provided by the Geospatial Information Authority of Japan, is employed for the bottom surface of the analysis domain to enhance analysis precision. The depth of the seafloor surface without digital elevation data is determined according to the port planning map<sup>24)</sup> in Takamatsu city. In the analysis mesh, the coordinates indicating east, west, south, and north positions at the 5.0 m intervals that constituted the topography are set as the nodes for generating the analysis mesh (Fig.3.2). Additionally, the time-step  $\delta t$  is automatically adjusted such that the Courant number can't

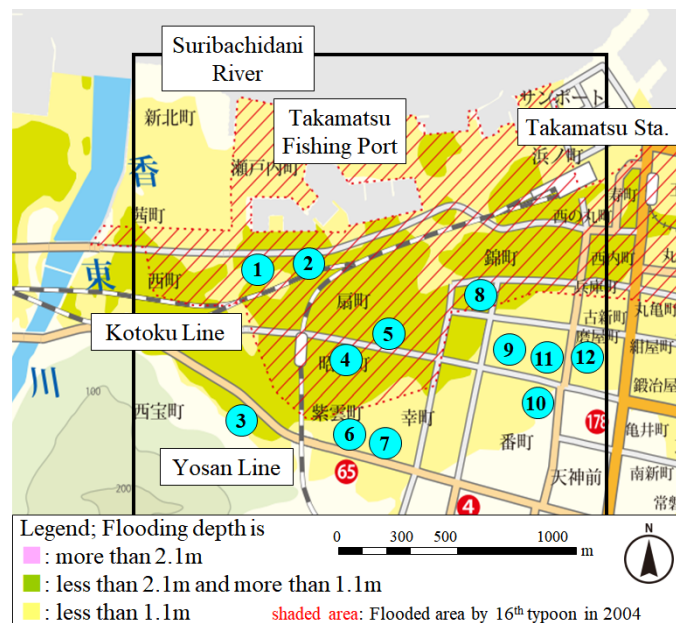


Fig.3.1 Expected to be flooded by storm surge<sup>22)</sup>

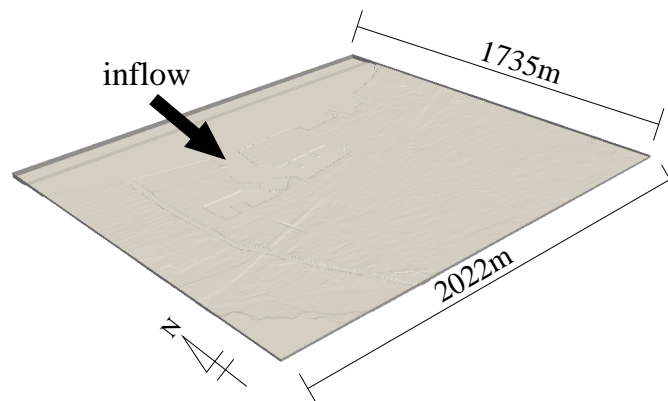


Fig.3.2 Analysis mesh



exceed 0.3, and a solid mesh size is set to approximately  $5.0 \text{ m} \times 5.0 \text{ m} \times 1.0 \text{ m}^{25}$ ).

$$Co = \frac{\delta t |U|}{\delta x} \dots\dots\dots (3.1)$$

In this equation,  $\delta t$ ,  $|U|$ , and  $\delta x$  are time step, velocity through the cell and the cell size in the direction of water flow, respectively. In this analysis, the flooding analysis of the storm surge area is conducted under the 3D analysis domain having the ground (bottom) surface and top surface as already noted above. In this analysis mesh, the levee which is higher than 1.0 m is reflected in the analysis mesh on the basis of the DEM. Moreover, the various conditions related liquid and gas phase and related analysis model are provided in **Table3.1**. Additionally, the figure of the altitude in analysis area is shown in **Fig.3.3**. It is expected that the flooding area will spread according to elevation as the probable flooding area in a hazard map and the area with a low elevation in an elevation map are almost the same.

**Table3.1** Analysis conditions

Liquid phase	Dynamic coefficient of viscosity ( $\text{m}^2/\text{s}$ )	$1.00 \times 10^{-6}$
	Density ( $\text{kg}/\text{m}^3$ )	1000
Gas phase	Dynamic coefficient of viscosity ( $\text{m}^2/\text{s}$ )	$1.48 \times 10^{-5}$
	Density ( $\text{kg}/\text{m}^3$ )	1
Surface tension coefficient ( $\text{kg}/\text{s}^2$ )	0.07	
Acceleration of gravity ( $\text{m}/\text{s}^2$ )	9.81	
Turbulence model	RANS model <sup>26)</sup>	

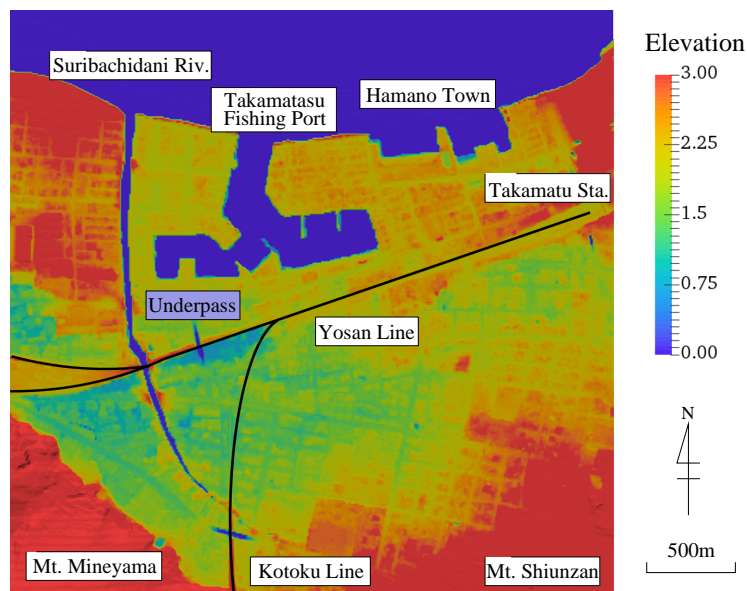


**Fig.3.3** Ground elevation

### 3.3 Boundary conditions

The boundary conditions set for each surface are as follows **Fig.3.4**. The under surface constructed by the DEMs is the nonoutlet boundary surface, the top surface is the atmosphere boundary surface, the north surface is the wave-making boundary surface, and the south surface is the outlet boundary surface. The rate of the pressure and the velocity are set as zero on other two surfaces.

The wave was generated by the "ihFoam" which is described in the 2nd chapter in the wave-making boundary surface. Regarding this solver, it is necessary to set the inputs: the wave height, period, phase, and initial sea level. Thus, the situation which is the typhoon 16th coming near Takamatsu in 2004 is employed as a reference in this simulation. The tide level at the Takamatsu port rose to T.P. 2.00 m<sup>27)</sup>, and flooding in the city started at 10:00 pm on August 30th when the typhoon 16th came near Takamatsu city. At around 10:40 pm on the same day, the tide level peaked to T.P. 2.46 m<sup>27)</sup>, after which the flooding spread gradually. Therefore, the initial sea level is set to T.P. 2.00 m, and the flooding analysis is carried out for 60 min. The wave height and period values are employed 1.47 m and 11.50 sec<sup>28)</sup>, respectively, as observed in the Hiketa area, east of the Kagawa Prefecture, Japan, which are not recorded in Takamatsu city. In this analysis, the wave is always produced on the wave-making boundary surface.

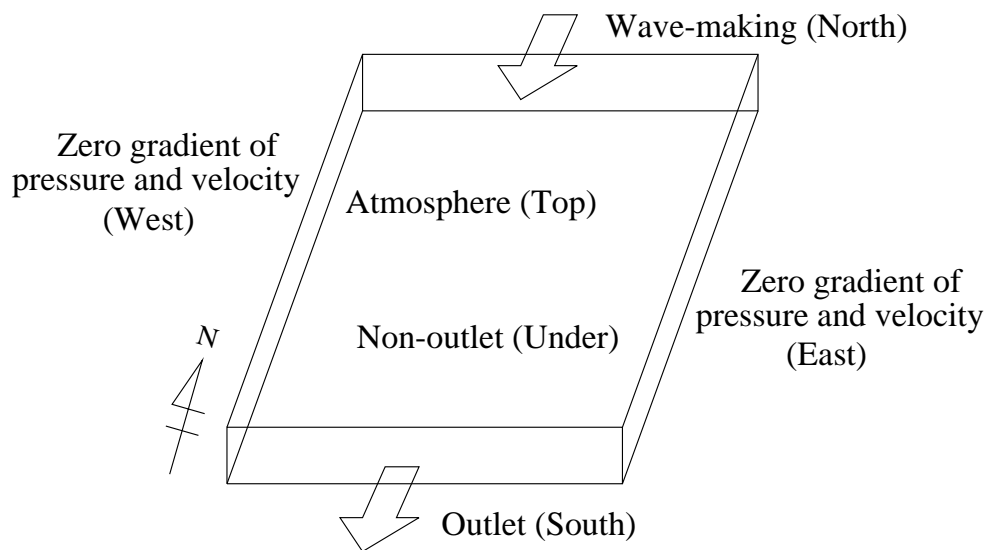


**Fig.3.4** Boudary condition

### 3.4 Results of flooding analysis

The results of the flooding analysis with a storm surge at every 300 s from 1200 s to 2700 s after the start of the analysis are shown in **Fig.3.5 - 3.10**, respectively. As mentioned earlier, the volume fraction of the liquid phase " $\alpha$ " determines whether the area in the analysis area is flooded. The flooding depth is supposed to be the value which is computed by multiplying the value of  $\alpha$  by 1.0 m since the height of each cell is 1.0 m in this analysis. According to the questionnaire survey for the people who evacuated at the time of approaching Isewan Typhoon, it was difficult for adult women to walk at the flooding depth more than 0.5 m<sup>29</sup>). Additionally, it is difficult for adult men to walk at the flooding depth more than 0.7 m<sup>29</sup>). Therefore, the area in which the volume fraction of the liquid phase " $\alpha$ " exceeds 0.5 is assumed to be flooded and this area is set as the impassable area by the flooding.

#### Result of flooding analysis at 1200 sec

Around Takamatsu Fishing Port, the value of  $\alpha$  is about 0.25 at 1200 sec after starting the flooding analysis (**Fig.3.5**). However, the agent can walk through this area at this time since the value of  $\alpha$  don't exceed 0.5. In the left side of the central area, the underpass whose elevation is lower than that in the surrounding area exists through north and south direction. This area is flooded than other area and the value of  $\alpha$  is about 0.4. However, this area is the passable area at 1200 sec after starting the flooding analysis since the value of  $\alpha$  don't exceed 0.5 as it is for around Takamatsu Fishing Port.

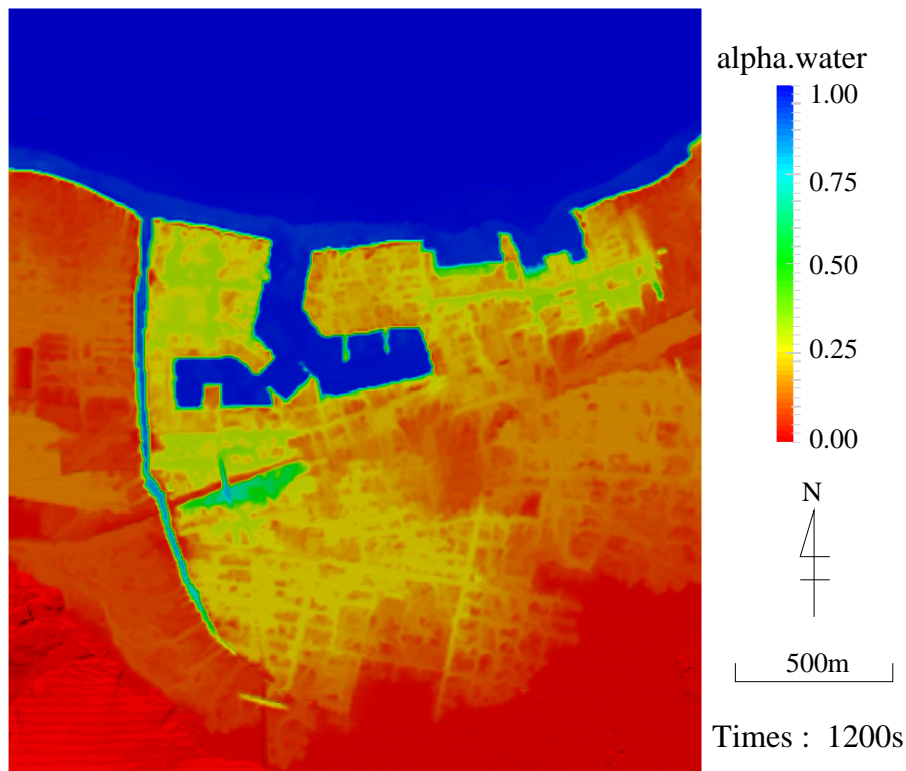


**Fig.3.5** Flooding state (T=1200 sec)

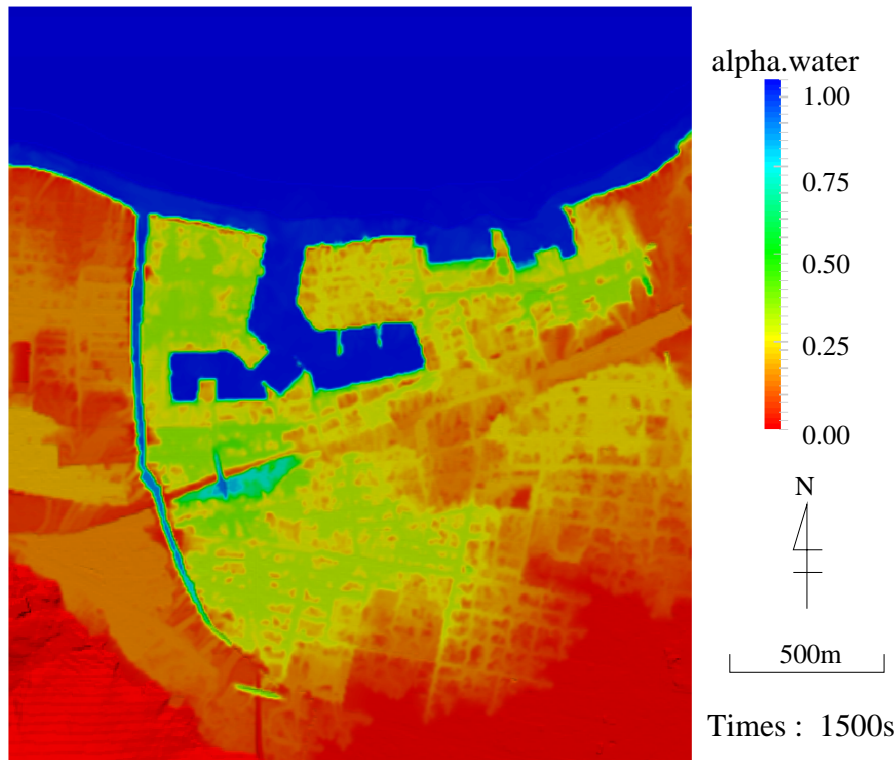


**Fig.3.6** Flooding state (T=1500 sec)

### Result of flooding analysis at 1500 sec

Outside of Takamatsu Fishing Port, the value of  $\alpha$  is 0.3 over a wide area of the south side of Takamatsu Fishing Port at 1500 sec after starting the flooding analysis (**Fig.3.6**). However, the agent can walk through this area at this time since the value of  $\alpha$  don't exceed 0.5 at this time. On the other hands, there are some areas where the value of  $\alpha$  exceeds 0.7 around the underpass. Hence, the evacuees can't already utilize as the evacuation route in this area.

### Result of flooding analysis at 1800 sec

In particular, the high-elevation area in the artificial landform north of the Kotoku Railway Line is less flooded than its surroundings 1800 s after the start of the analysis, as shown in **Fig.3.7**. On the other hand, the flooding area seems to have spread over the broad region in the center of the analysis area, where  $\alpha$  is around 0.3. In addition, it is assumed that the areas in which the value of  $\alpha$  exceedds 0.4 increase comparing the flooding state at 1500 sec with that at 1800 sec after starting the flooding analysis. It is indicated that the water which inflows to the inland area don't remain in a certain area and spreads over a wide range. Moreover, it is found that the areas where  $\alpha$  is approximately 1.0 spread around the underpass primarily because this value is equivalent to the flooding depth of 1.0 m, which implied that the underpass and southern part of this underpass becomes impassable at an early time after the start of the analysis.

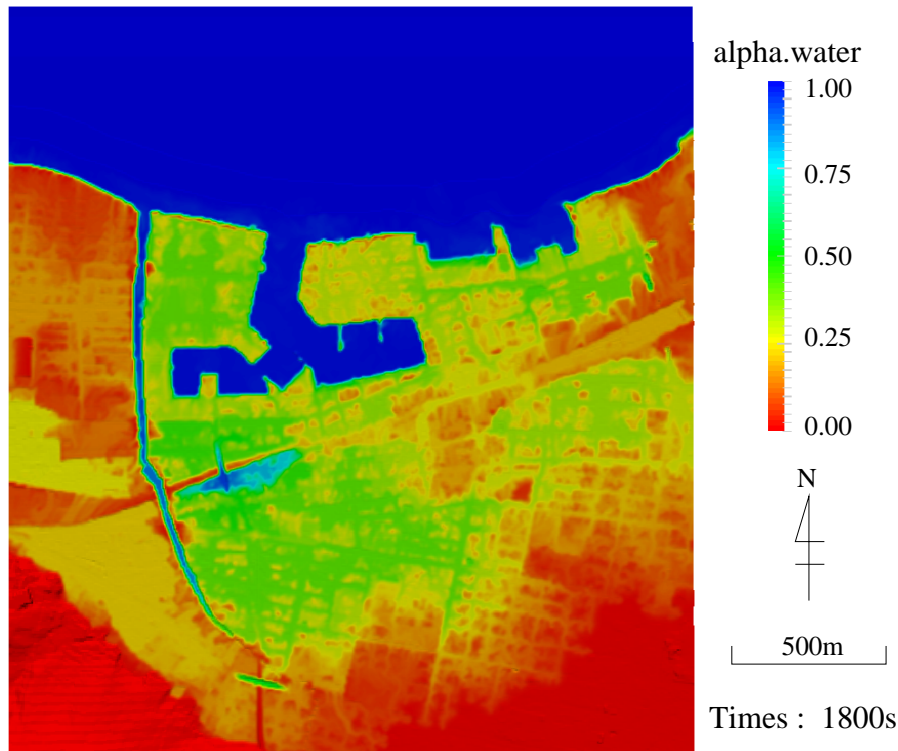


**Fig.3.7** Flooding state (T=1800 sec)

### Result of flooding analysis at 2100 sec

The value of  $\alpha$  exceeds 0.5 at 2100 sec after starting the flooding analysis in the southern part of the underpass in which the value of  $\alpha$  is around 0.3 to 0.4 at 1800 sec after starting the flooding analysis (**Fig.3.7**). Thus, most domains in the center of the analysis area become impassable area. At 2100 sec after starting the flooding analysis, the underpass is flooded and the flooded area in which the value of  $\alpha$  is 1.0 spread as it is for before. Though, the impassable areas spread over a wide range, the value of  $\alpha$  is approximately 0.2 in coastal areas of high elevation and northwest and northeast of the analysis area, implying not heavy flooding. It is indicated that the wide area is still passable around the coastal area although the impassable areas spread in the inland area. The elevation of this unflooded area around the coastal area is about 3.3 m and the elevation of the surrounding area is about 2.3 m. It is estimated that this area isn't flooded since this area is higher about 1.0m than the surrounding area.

### Result of flooding analysis at 2400 sec

As shown in **Fig.3.9**, the value of  $\alpha$  increases 2400 s after the start of the analysis in the area that is flooded at 2100 s, and the value of  $\alpha$  is 0.7 in a certain area. At 2400 sec after starting the analysis, the value of  $\alpha$  was particularly high in the center and central-eastern area with underpass and the flooding depth is deeper than that in other areas. The southern side of Takamatsu Station is passable at 2100 sec after starting evacuation simulation since the value of  $\alpha$  is 0.3. However, this area becomes impassable at 2400 sec after starting evacuation simulation since the value of  $\alpha$  exceeds 0.5. It is considered probable

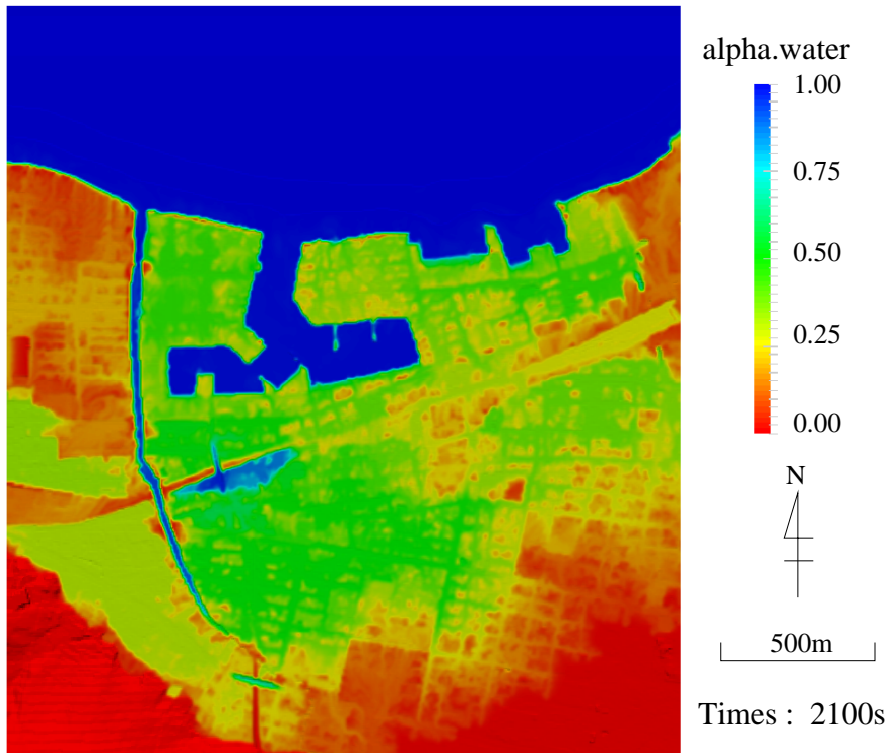


**Fig.3.8** Flooding state (T=2100 sec)

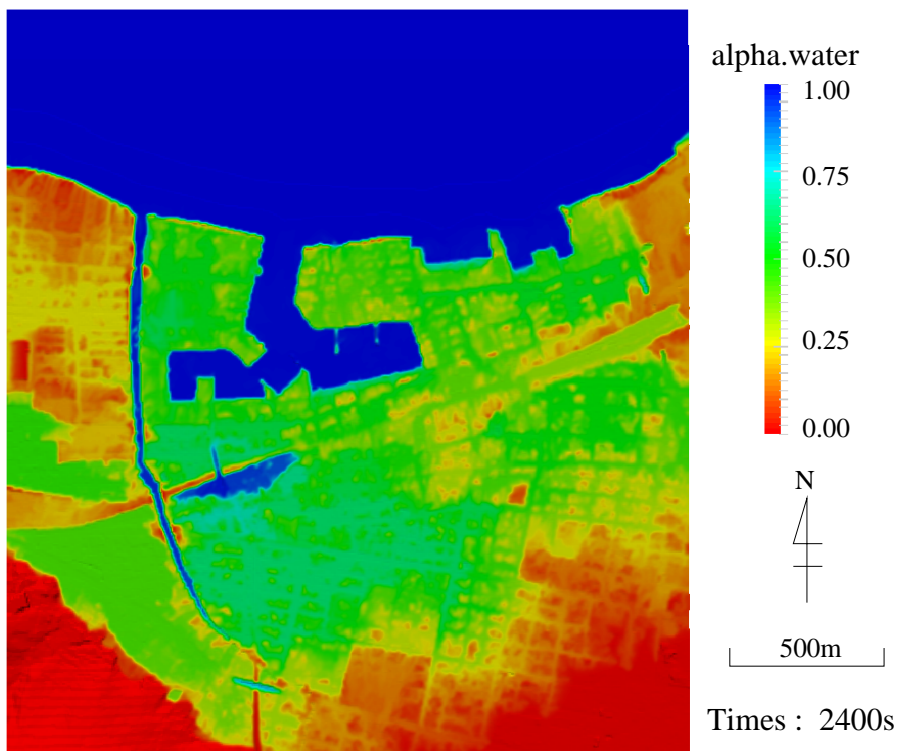


**Fig.3.9** Flooding state (T=2400 sec)

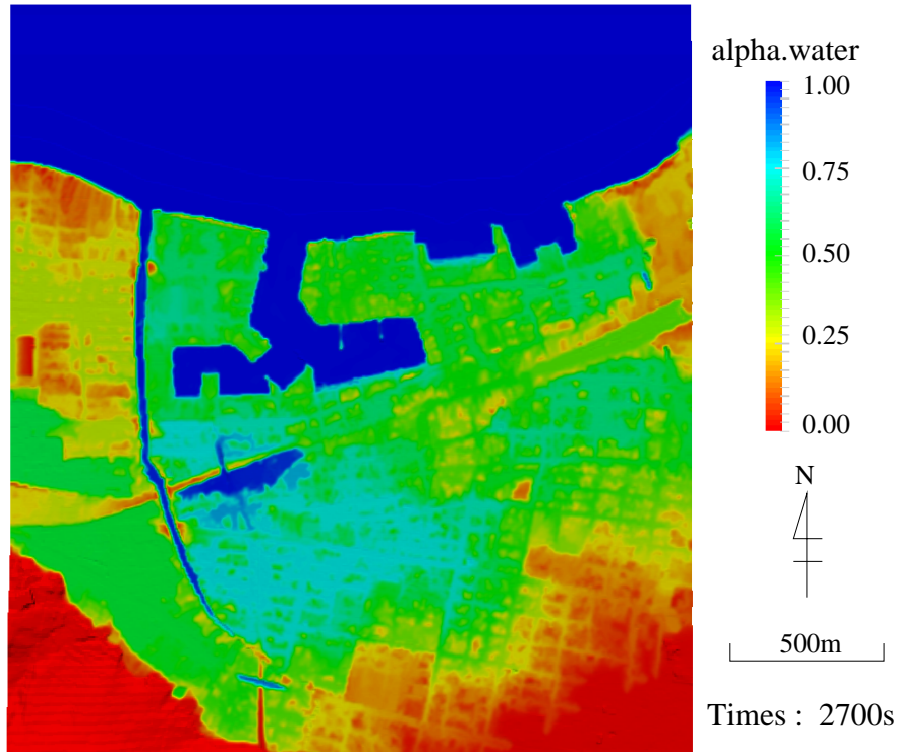


**Fig.3.10** Flooding state (T=2700 sec)

that such flooding situations are caused by the underpass in the former case and by the topography of the south area of Takamatsu Station in the latter case. The center of the analysis area where is the southern part of the underpass is particularly flooded at 1800 sec after starting the analysis under the influence of the low elevation. At the 2400 sec after starting the analysis, the water concentrates on this underpass. Thus, geographically, it can be interpreted that the southern area has a lower elevation than the northern area (**Fig.3.3**). This difference of elevation is caused by the geography. In particular, the area south of the Yosan Railway Line that runs east-west direction is a natural landform, and thus, it is lower than the artificial landform of the northern area. Therefore, the water which remains in the underpass spreads to the south side. It is found from **Fig.3.3** that the elevation of the area from Takamatsu Fishing Port to Mt. Shiunzan is higher than the surrounding area as it is for the eastern part of the central area. Thus, the water which inflows from the coastal area avoided the high elevation area goes between the south side of Takamatsu Station and the south side of the Takamatsu Fishing Port.

### Result of flooding analysis at 2700 sec

The value of  $\alpha$  exceeds 0.7 in the center and the eastern part of the central area which is already flooded at 2700 sec after starting the analysis (**Fig.3.10**). Then, the value of  $\alpha$  is particularly high and greatly exceeds 0.5 in the flooded area. However, the value of  $\alpha$  is particularly low and less than 0.3 in the unflooded area. Though the areas which are the northwest and the northeast part of analysis area are the coastal area, these areas aren't flooded than the inland area at 2700 sec after starting the flooding analysis

in the same as before. Also, in the inland area, the area which is included the center and the southeast part of the analysis area isn't almost flooded although the west side of this area is flooded. This is due to the fact that the elevation of surrounding area is higher than this flooded area as it is for the coastal area.

### **3.5 Conclusions**

As a consequence of the flooding analyses, it is found that the water inflowing from the seashore remains in the inland area whose elevation is lower than that at the coastal area. Furthermore, it is grasped that the flooded depth in and around there is deeper than that at other coastal areas since the flooding state by a storm surge depends on the elevation. It is turned out that, at this moment, the flooded area expanded rapidly after the flooding starts becomes impossible to walk over a wide range in the inland area where the elevation is low. Therefore, even people who live inland need to be aware of the storm surge if they lived in the low elevation area. It can be said the result of the flooding analysis obtained in this study is justified since this result is similar to the hazard map published by Takamatsu city. It will lead to an increase in disaster prevention awareness by presenting the disaster situation to the residents with videos and images such as this analysis result. Furthermore, it becomes possible to reflect more detailed flooding situations in the city model using for the evacuation simulations since it is clarified specifically which area was flooded and to how extent by the flooding analysis. For future tasks, the flooding analysis considering buildings and small levees, etc. is necessary to conduct in order to obtain a more accurate flooding situation.



## 4 . Evacuation simulation during storm surge

### 4.1 Introduction

In order to reduce human damage in the event of a disaster, it is necessary to provide the resident with information on disasters and evacuation behavior in advance through the hazard map and disaster prevention workshops. In recent years, various studies on evacuation behavior have been conducted. As for the research with respect to the evacuation in flood disaster, Takeda et al. carried on the flooding simulation of a storm surge and examined the evacuation difficulty in both the existence and non-existence of flooding based on the numerical results<sup>30)</sup>. The appropriate evacuation behavior of residents at the time of flooding argued in this study since the evacuation distance and number of evacuees depends on the flooding situation. In addition, Takeda et al. pointed out that it is difficult to suggest the available evacuate route owing to the difficulty to determine the evacuate routes and spots. Takahashi et al constructed the system by which the safety evacuation route to the evacuation spot considering the geography and the strength of the ground is selected<sup>31)</sup>. The temporary evacuation spot was selected based on the identify areas where evacuation is difficult through the calculations of the evacuation completion time and the distance required for evacuation by this system. It is hard to say that the evacuation spot available in the event of a disaster is selected by the proposed system since some obstacles such as the collapsed building by the earthquake and flooding by the water disaster aren't considered in selecting the proper evacuation spot. Minami et al. developed the evacuation supporting system which is indicated the quickest evacuation route to the first evacuation spot easily by calculating the horizontal moving distance and the gradient of the evacuation route the tsunami height from the arbitrary position<sup>32)</sup>. It is possible that the workable support which considers the geographic condition and building location in the target area can be proposed by the supporting system. However, it is difficult for evacuees to decide another destination of evacuation in facing with the flooded area since the city model wasn't reflected the evacuation routes which become impassable by the flooding state varying from hour to hour. In this system, it may not be possible to use that the evacuation route which is indicated by the system since changing the evacuation route due to flooding is not considered. However, it can be said that it is effective in making the hazard map useful to present the information about the disaster situation and evacuation behavior by using the simulation results such as evacuation behavior considering disaster situation since disaster prevention education and evacuation support system using these simulators are very effective. Henry et al. conducted an evacuation simulation of Balboa Island during tsunami and stated that the appropriate parameters such as population and road network should be considered according to the target area in the evacuation simulation<sup>33)</sup>. The details will be detailed later, the evacuation simulation considering the age distribution were conducted since there are many elderly people in the targeted area in this study.

In addition, the disaster simulations are actively conducted not only for the purpose of grasping the threat of disaster but also for the purpose of promoting disaster prevention education since they are very effective as a disaster prevention material<sup>34</sup>). Nikami et al. conducted the research on the effect of disaster prevention education using an evacuation simulator assuming an earthquake fire<sup>35</sup>). According to the study, it is important to enhance the image of evacuating from disasters and necessary to provide continuous disaster prevention education using a simulator in order to raise disaster prevention awareness. It is possible to reconsider the evacuation route and spot since the resident plans to utilize in the event of a disaster using the above-mentioned evacuation simulator, but this simulator isn't considered the road blockage and traffic jam caused by evacuating many residents at the same time. It is necessary to simulate evacuation behavior with considering such road blockage and traffic jam since many residents are expected to rush to the evacuation spot. In this chapter, the evacuation simulation considering the flooding state on the basis of the analysis results was conducted since the purpose of this study is to grasp the effect of the flooding state on evacuation behavior and the effect of agent's prior understanding of the flooding state in advance on the evacuation behavior.

## 4.2 Simulation summary

### Simulation area and city model

The evacuation simulation using the city model which is prepared from the road edge data in Takamatsu City provided by Geospatial Information Authority of Japan is carried. In the simulation area, the evacuation simulations are carried in the black framework of the predictable area maps in **Fig.3.1** for the storm surge flooding so as to grasp the evacuation behavior in the central area which is the residential area. A total of 12 designated evacuation spots are selected in the analysis (blue circles in **Fig.4.1**). The city models of the evacuation area in which the evacuation spots and agent are set in **Fig.4.1**. In the city model, the passable area, impassable area, evacuation spots, and flooding area are indicated, respectively, by white, black, green, and blue.

### Regarding to agent

As has mentioned above, a total of 3000 agents or "residents" are randomly placed in the city<sup>36</sup>). These agents, grouped in six according to gender and age, are assigned with different walking speeds and standard deviations to properly express certain behaviors such as overtaking<sup>37</sup>). In **Table4.1**, the numbers inside brackets for each agent type denotes the population rate in the analysis area by the gender and age of the residents in the intended area. At the time of disaster, it is expected that many evacuees don't move at the same walking speed but took action which is the crowd behavior such as the overtaking<sup>38</sup>). Thus, the standard deviations for the walking speed are set as shown as shown in **Table4.1**. In this simulation, the value of every kind which are shown in **Table4.1** were employed.

Here, the "resident" agent evacuates from an initial point to the nearest evacuation spot through the quickest route since Resident is adopted as the agent in this evacuation simulation. The flooding states

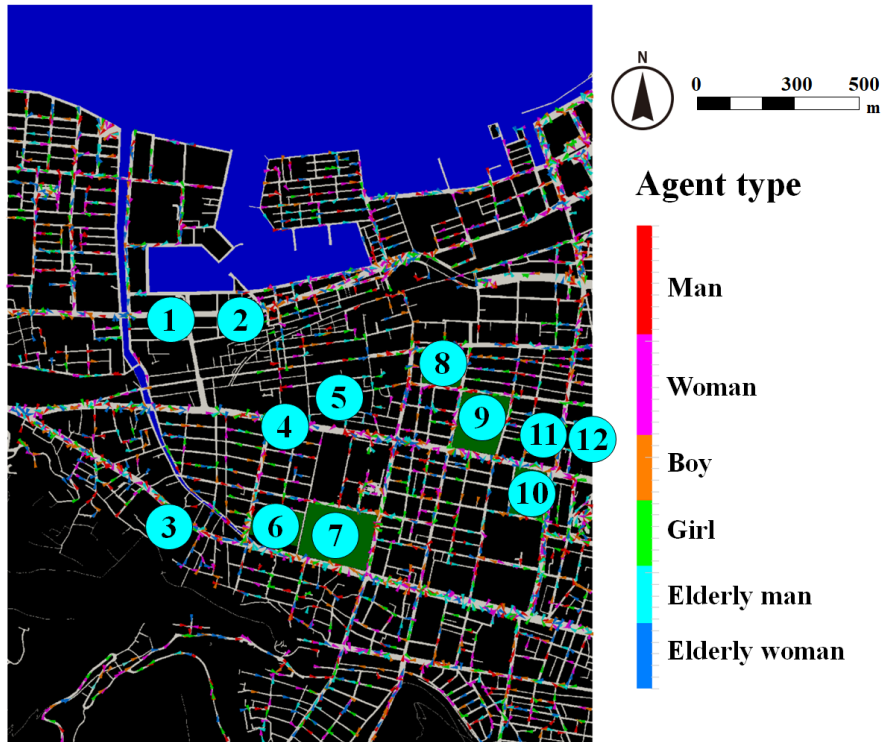


**Fig.4.1** Initial placements of agents and evacuation spots

1800, 2100, and 2400 sec after the start of the flooding analysis are reflected in the city model, which strongly affect the evacuation behavior. Since no significant change is observed in the flooding area after 2400 sec from the start of the flooding analysis, the flooding area in the evacuation simulation area is not update after that. As has mentioned above, the reference depth of the impassable area is set as 0.5 m in which adult women walk with difficulty when the flooding state is reflected the city model<sup>29)</sup>. In the flooding analysis, the area in which the volume fraction of the liquid phase " $\alpha$ " exceeds 0.5 in the flooding analyses is designated as the impassable area since the height of one mesh is set as 1.0m. The agent evacuates through the quickest route from current place to the nearest evacuation spot when the agent faces with the flooded area. As implied, the agent may not always find the quickest route or evacuate when the evacuation route is blocked by the flooding. When confronted with the area being flooded, the agent must return to the bifurcation point in the road, and from there, the agent must search a new evacuation route.

### Simulation cases

Because the main goal is to explore the effects of the flooding state and agent's prior understanding of the flooding state on the evacuation behavior, four evacuation analyses (summarized in **Table4.2**) are conducted. In Case 1 or Case 2, where the flooding state is or is not reflected, respectively, many agents can not complete evacuation. In response, simulation Cases 3 and 4 are added, in which the agent have some or good awareness (in advance) of the flooding state, respectively. In all cases, the agent's role is to

evacuate to the nearest designates spot by the quickest route determinable. As implied, the agent may not always find the quickest route or evacuate when the evacuation route is blocked by the flooding. When confronted with the area being flooded, the agent must return to the bifurcation point in the road, and from there, the agent must search a new evacuation route. Accordingly, the agent in case (b) has to search for another evacuation route every time a chosen route is flooded or when many roads around the route are inundated, whereas the agent in case (a) can search for the quickest route and evacuate while avoiding routes that are likely to be flooded. The same parameters, such as the evacuation start time and the walking speed of the agent are used in the two analyses, regardless of whether the agent know the flooded area in advance or not. In other words, the only difference between the two analyses is whether or not the agent knows the flooded area in advance before starting evacuation. In the analysis, it is impossible to pass through the flooded area as well as the structure exists, and the agent recognizes such flooded area in advance, avoids the impassable road before the evacuation start, finds the shortest route, and takes refuge action. Therefore, it is possible for the agent who grasps the flooded area in advance to evacuate quickly without taking any action such as facing the inundated area and taking a detour during the evacuation.

**Table4.1** Walking speeds and standard deviations of agent

Agent types (Rate)	Average walking speed (m/s)	Standard deviation (m/s)
Boy (15%)	1.351	0.133
Girl (14%)	1.239	0.175
Adult male (23%)	1.328	0.098
Adult female (21%)	1.247	0.144
Elderly male (12%)	1.182	0.154
Elderly female (15%)	1.113	0.125

**Table4.2** Simulation cases

Simulation cases	Flooded / Unfloded	Prior recognition of flooding state
Case 1	Unfloded	No
Case 2	Flooded	No
Case 3	Flooded	Near Suribachindani river, underpass, and northside of evacuation spot 8
Case 4	Flooded	Near Suribachindani river, underpass, northside of evacuation spot 8, and northside of evacuation spots 4, 5

### 4.3 Results of evacuation simulation

#### 4.3.1 Results of evacuation simulation: Case of the flooding state is or is not reflected

The evacuation simulation results of Case 1 and 2 are shown in this subsection. **Fig.4.2-4.11** show the simulation results for Case 1 and 2 at 1800, 2100, 2400 sec when the flooding states are uploaded and at 3600, 7200 s. Furthermore, the evacuation completion rate and number of evacuees by spot are shown in **Fig.4.12** and **Fig.4.13**.

#### Results at 1800 sec after the start of the evacuation simulations

In Case 1, most of the agent has already evacuated to the evacuation spots 3, 6, and 7 at 1800 sec after the start of the evacuation simulation (**Fig.4.2**). From **Fig.4.12**, 53% of agents complete evacuation in the whole simulation area. On the other hand, agents evacuate in a line in northern and southern area where there are few evacuation spots. At that time, there are long line of 500 m or more to evacuate to evacuation spots 1 and 2 in the northwestern area. Also, the situation is similar in the northeast area.

In Case 2, the western side of the Suribachidani River and southern side of evacuation spots 1 and 2 are flooded, and many agents are caught in the flooding around the western side of the Suribachidani River at 1800 sec after the start of the evacuation simulation (**Fig.4.3**). More than 130 agents who pass the road

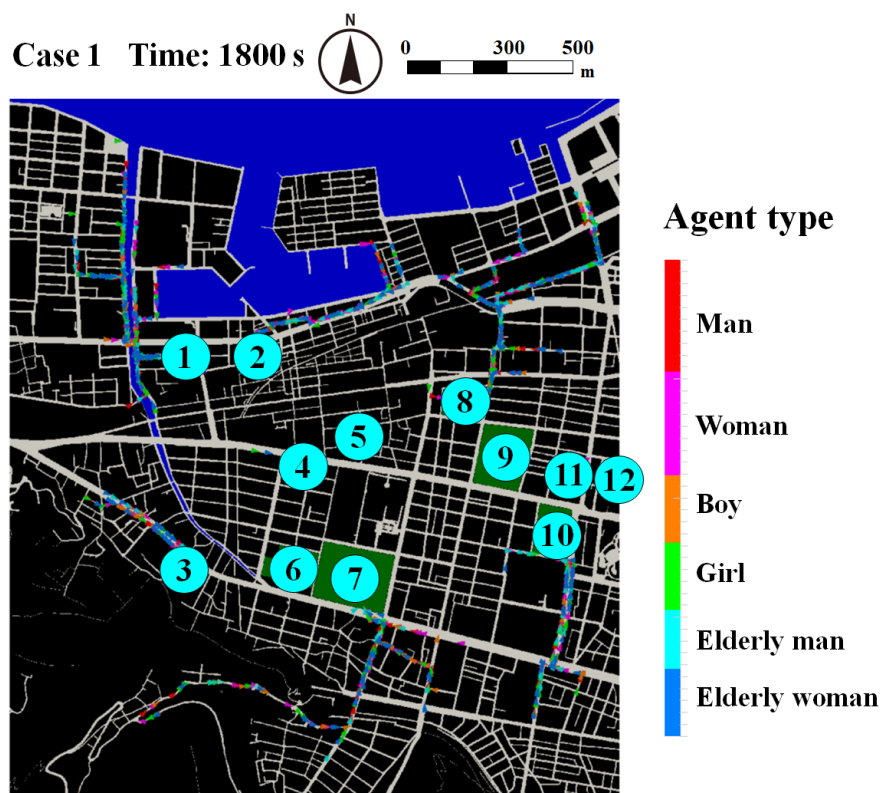


**Fig.4.2** Evacuation condition of Case 1 (T=1800s)

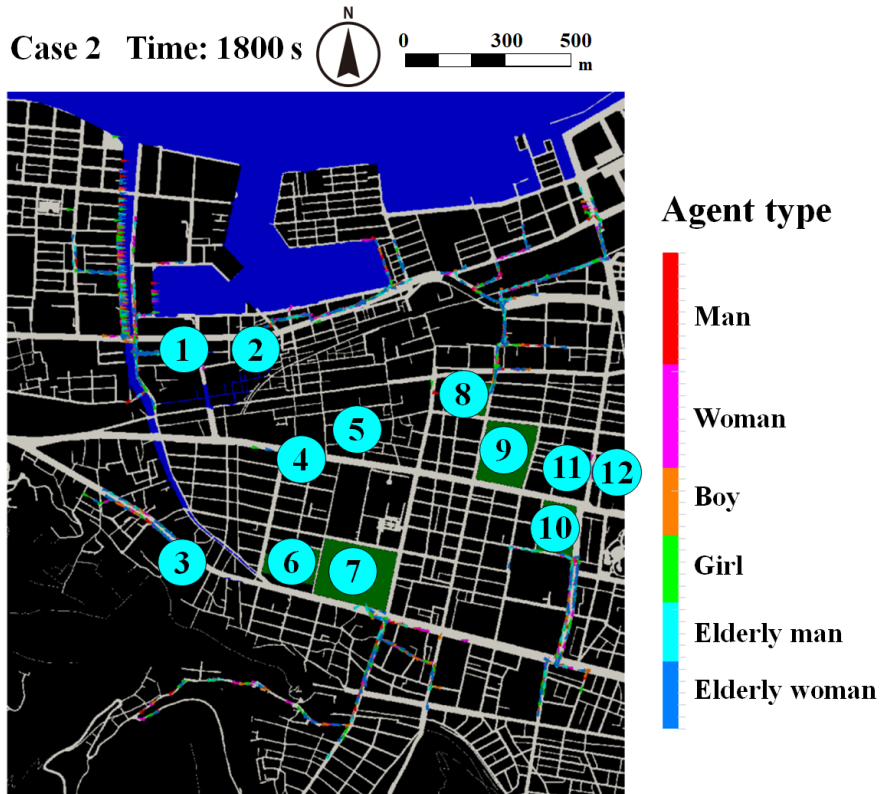


Fig.4.3 Evacuation condition of Case 2 (T=1800s)

along Suribachidani River to evacuate can't evacuate since they get caught in the flooding. In addition, the agents who are set on the south side from the evacuation spots 1 and 2 evacuate to the evacuation spot 4 further south than there since the south side of the evacuation spots 1 and 2 is impassable at the early stage from the start of flooding due to the existence of underpass. At that time, many agents are unable to evacuate around the Suribachidani River, but the evacuation behavior is the same as in Case 1 in the northeast part of the simulation area and the south side of the evacuation spot 8 since these areas have not been flooded (Fig.4.2, 4.3). Agents complete evacuation toward spots 4 and 5 in the center of the simulation area, given the many evacuation spots surrounding the area. On the other hand, many agents are caught in traffic jam since there are no other evacuation spots around the evacuation spots 1, 2 and 8 in the northern side of the analysis area and the evacuation spots 3, 7 and 10 in the southern side of the analysis area have few evacuation spots. According to the results of the flooded analyses in the previous chapter, the evacuation spots on the south side is not so flooded. Therefore, even if it takes time to evacuate, the agents are less likely to get caught in the flooding. On the other hand, it is hoped that the agent evacuates immediately since the area near the northern side of the analysis area is flooded rapidly over time and there are long traffic jams. Comparing the evacuation completion rate between Case 1 and 2, there is no difference between these two at 1800 sec after starting evacuation simulation in Fig.4.12.

## Results at 2100 sec after the start of the evacuation simulations

In Case 1, the agents walk in the long lines at 2100 sec after the start of the evacuation simulation as is the case with the state at 1800 sec (Fig.4.2, 4.4). Since the distance from the initial placement of the agent to the evacuation spot is 1000 m in the coastal area, it is expected that these agents need much time for completing the evacuation without non-existing the flooding state.

In Case 2, the area from the evacuation spot 1 to the north side of the evacuation spot 6 including the underpass which is flooded at 1800 sec after the start of the evacuation simulation becomes impassable over a wide area at 2100 sec after the start of the evacuation simulation (Fig.4.3, 4.5). Therefore, the agent can't evacuate to the evacuation spots 1, 2, 4, and 5. Most of the agents who set near the evacuation spots 4 and 5 have already completed evacuation since the evacuation spots 8 and 9 exist in about 400 m east side of the evacuation spots 4 and 5 and the evacuation spots 6 and 7 exist in about 300 m south side of the evacuation spots 4 and 5. However, many agents have evacuated even 1800 sec after the start of the evacuation simulation since there are no other evacuation spots near the evacuation spots 1 and 2, so the agents get caught in the flooding and can't evacuate in the close vicinity of these evacuation spots at 2100 sec after the start of the evacuation simulation. These agents who have been evacuating to the evacuation spot 2 start to evacuate to another evacuation spot after facing with the flooded area since the east side of the evacuation spot 2 in comparison with the flooded state near the evacuation spot 1 isn't flooded and there are agents who don't get caught in the flooding. The difference in the evacuation completion rate of

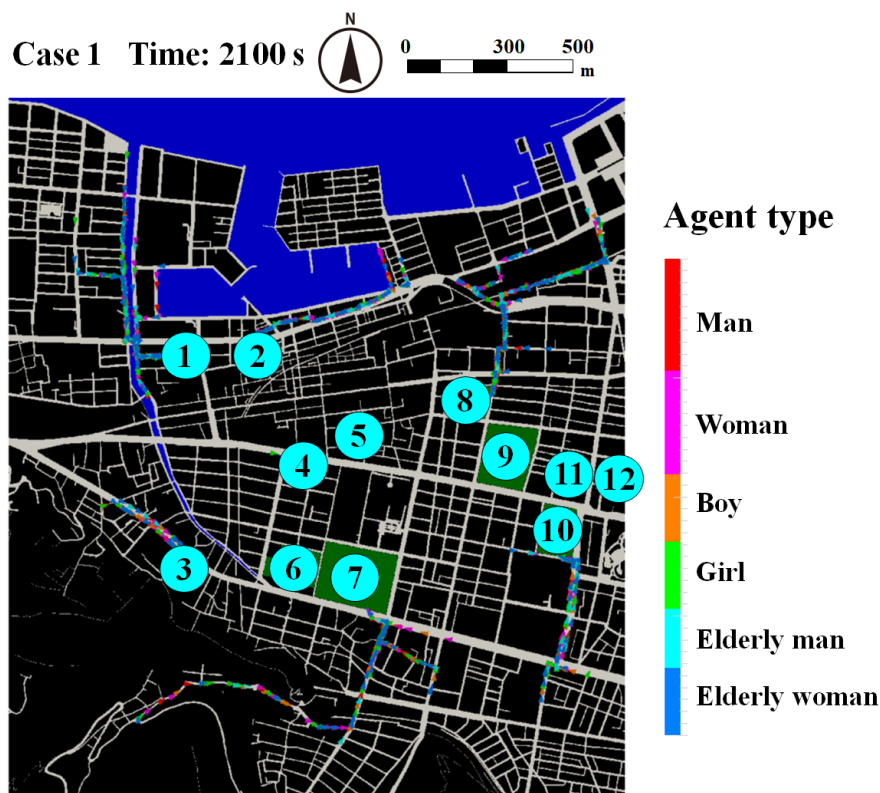


Fig.4.4 Evacuation condition of Case 1 (T=2100s)



Fig.4.5 Evacuation condition of Case 2 (T=2100s)

Case 1 and 2 had gradually widen from 2100 sec after the start of evacuation (Fig.4.12).

### Results at 2400 sec after the start of the evacuation simulations

In Case 1, most of agent who are set on the south side of the evacuation spot 10 completes evacuation at 2400 sec after the start of the evacuation simulation (Fig.4.6). However, many agents continue evacuating in the north part of the analysis area where the agents walk in a long line to evacuate before. The agents who set on the northwest part of the analysis area walked on the road along Suribachidani River to the evacuation spot 1, or the road of the south side of Takamatsu Fishing Port to the evacuation spot 2. Therefore, it is possible that many agents suffer in the flooding before completing evacuation in the case existing the flooding state.

In Case 2, the flooded area at 2400 sec is larger than that at 2100 sec and the area from the evacuation spot 1 to the evacuation spots 6 and 7 becomes impassable area (Fig.4.5, 4.7). However, the evacuation behavior is less influenced by the flooded area near the evacuation spot 4 since all agents finish evacuating there. In the north side of the evacuation spot 1, the agents who don't get caught in the flooding on the road along Suribachidani River continue evacuating. Then, they don't know which evacuation route is flooded, so they move to the road along the Suribachidani River once, but they come back to the road western side of the Suribachidani River and look for the quickest route to the evacuation spot 1 by facing with the flooded area. The north side of the evacuation spot 8 which have never been flooded is flooded at 2400 sec after the start of the evacuation simulation. It is found that many agents get caught in the



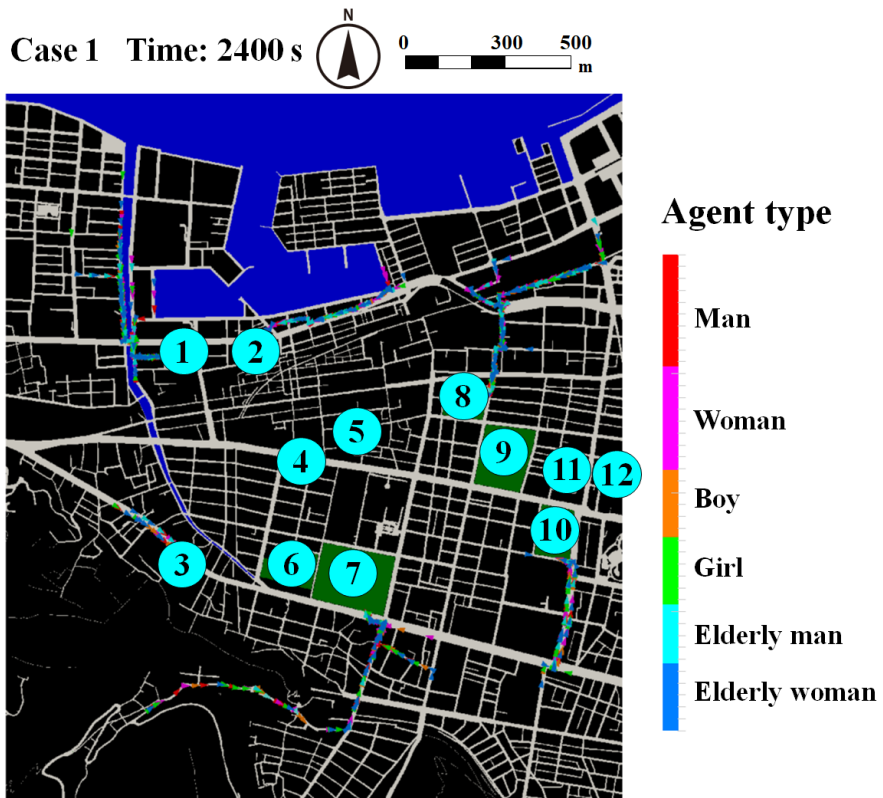


Fig.4.6 Evacuation condition of Case 1 (T=2400s)

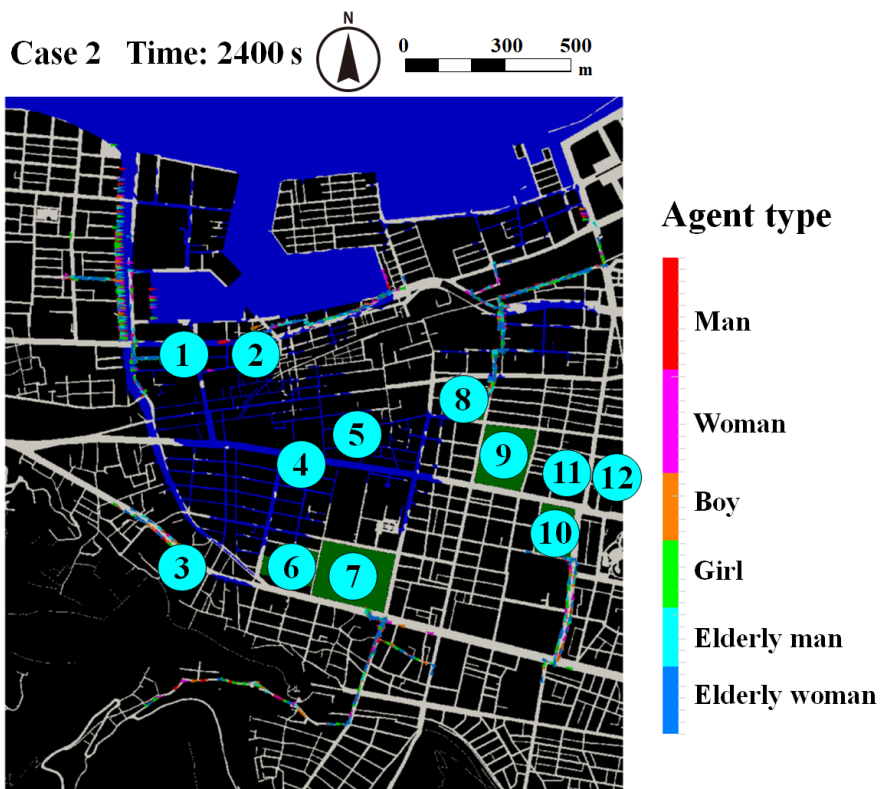


Fig.4.7 Evacuation condition of Case 2 (T=2400s)

flooding and can't evacuate in the case considering the flooding state also in this case since the agent can't complete evacuation after a long time in the vicinity of the evacuation spot 8 in Case 1 (**Fig.4.6, 4.7**). In the east side of the evacuation spot 2, many agents can't find out the passable road which lead to the evacuation spot and continued moving in the passable area which is surrounded by the flooded area, since the flooded area is spread and most of the road which leads to the evacuation spot are flooded. Therefore, the evacuation completion rate don't increase from the time when the flooded area spreads over a wide area to 2400 sec after (**Fig.4.12**). It is found that the agents who exist in the vicinity of the evacuation spots 1, 2, and 8 changed the evacuation destination or made a detour to complete evacuation for 2400 sec thereafter since these evacuation spots are not able to use by flooding. As a result, the evacuation completion rates of Case 1 and Case 2, which gradually differs from the time at 2100 sec after the start of the evacuation simulation, are 65.5% for Case 1 and 62.8% for Case 2, so the difference is about 2.7% (**Fig.4.12**).

### **Results at 3600 sec after the start of the evacuation simulations**

About 85% of agents have evacuated at 3600 sec after the start of the evacuation simulation in Case 1 (**Fig.4.12**). Comparing the evacuation simulation at 2400 sec and 3600 sec after the start of evacuation simulation, it can be seen that the agents have steadily completed evacuation, but agents evacuate from the northwestern part of the evacuation spot 1 and 8 where there are few evacuation spots still take time to evacuate and they still evacuate in line at this time (**Fig.4.6, 4.8**).

On the other hand, traffic jam still occurs on the north side of the evacuation spots 2 and 8 at the time of start the evacuation simulation in Case 2 (**Fig.4.9**). On the north side of the evacuation spot 1, the agent who searches the evacuation routes after facing with the flooded area many times at 2400 sec after the start of the evacuation simulation can't find the route to the evacuation spot and returns to the original location many times even 3600 sec after the start of the evacuation simulation (**Fig.4.7, 4.9**). If many roads become impassable due to flooding and agent won't know which road can use, it can take so much time to evacuate like this situation. In addition, the road runs north-south on the east side of the evacuation spot 8 had become unusable due to flooding. The agent who understands this situation changes the course from there to the road runs north-south on the west side of the evacuation spot 8 and gradually evacuates. In this way, while the evacuation completion rate is 71.5% when 3600 sec have passed although the agents are gradually evacuating, the rate at 1800 sec after that is 76.0% (**Fig.4.12**). That is to say, the rate increases only 4.5%. There are many agents who can't move by the flooding, but there are also many agents who face with the flooded area and change their course many times.

### **Results at 7200 sec after the start of the evacuation simulations**

In Case 1, about 99% of the agents have already completed evacuation at 6000 sec after the start of the evacuation simulation (**Fig.4.10, 4.12**). Regarding the evacuation destinations of all agents, the most frequent evacuation spot is the evacuation spot 8 which is due to the fact that there are few other evacuation spots on the north side of the evacuation spot 8 (**Fig.4.13**). The next largest number of evacuees is the evacuation spots 7, 1, and 10, but the reason why there are many evacuees to these evacuation spots is that



Fig.4.8 Evacuation condition of Case 1 (T=3600s)



Fig.4.9 Evacuation condition of Case 2 (T=3600s)

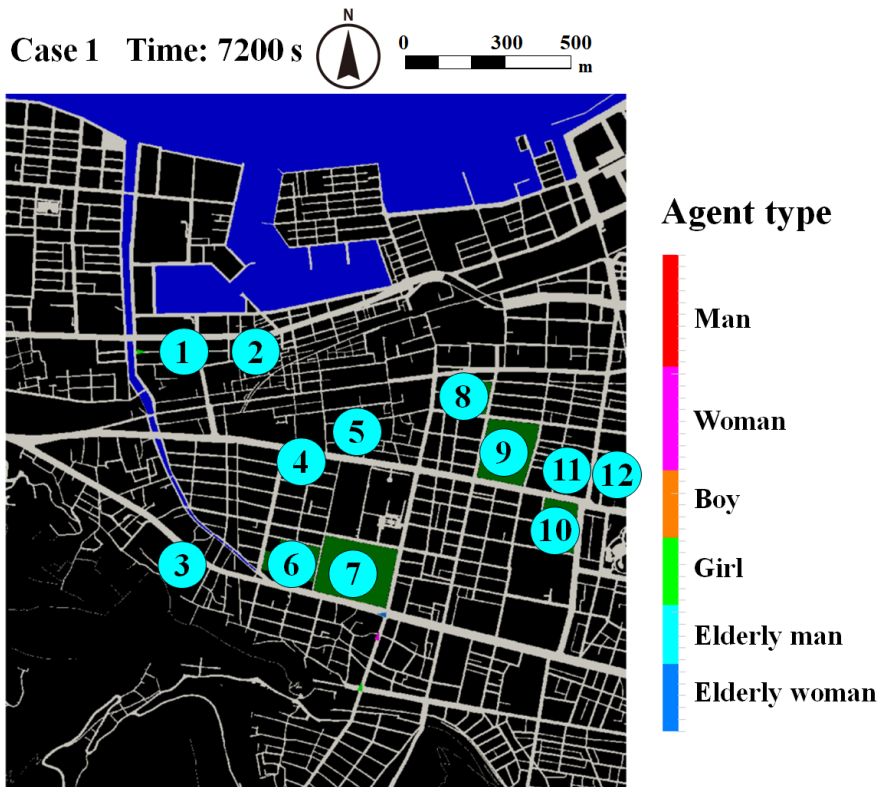


Fig.4.10 Evacuation condition of Case 1 (T=7200s)

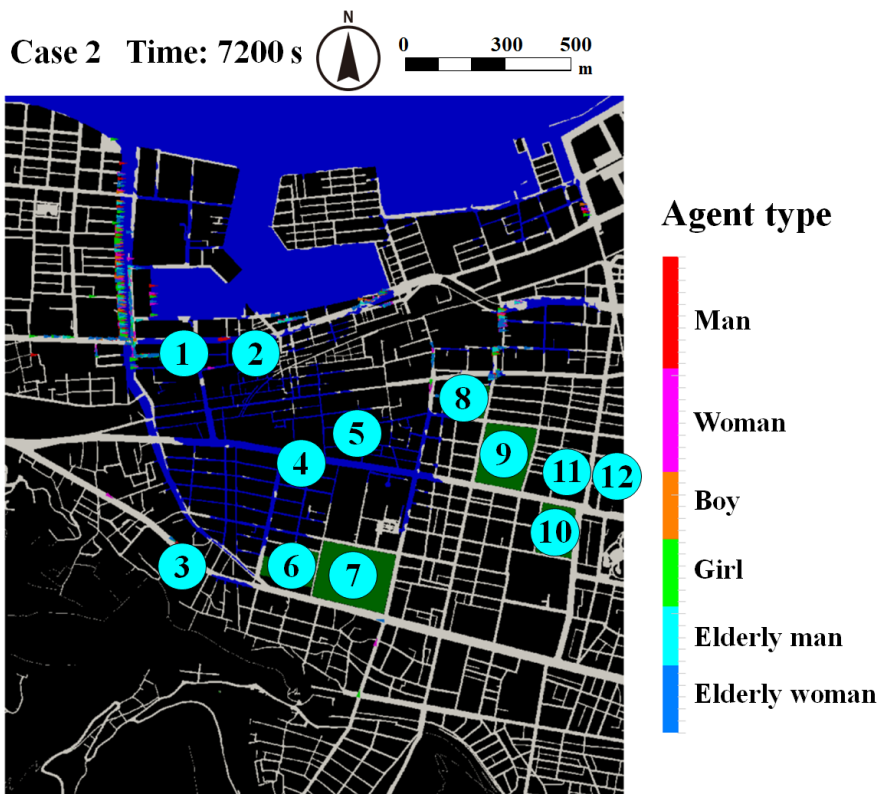
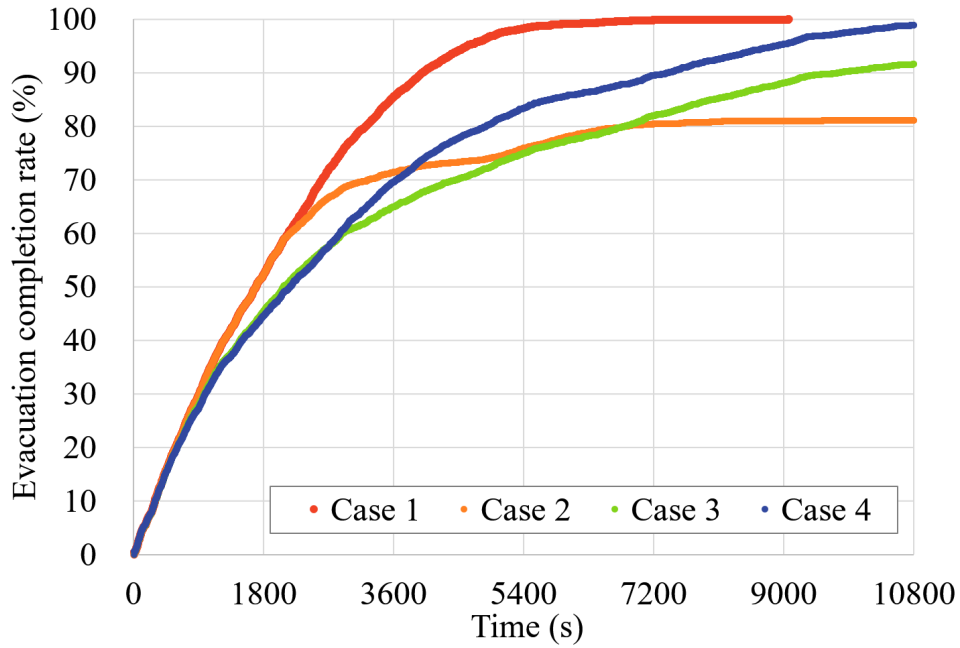
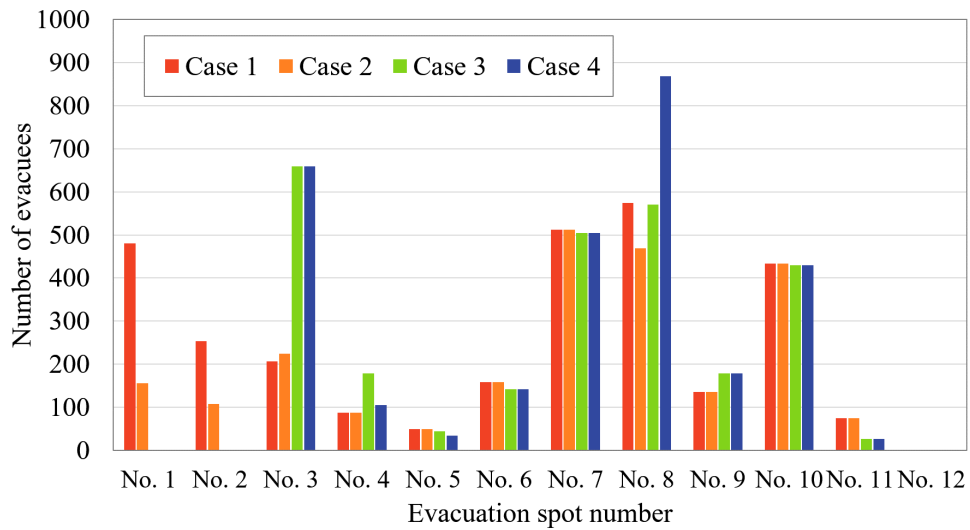


Fig.4.11 Evacuation condition of Case 2 (T=7200s)



**Fig.4.12** The evacuation completion rate



**Fig.4.13** Number of evacuees by evacuation spot

agents place in the area with few evacuation spots come to evacuate, as described above. Agents evacuate from the mountainous area located to the south of the evacuation spot 7, from the northwestern part of the evacuation spot 1, and from the southeastern part of the simulation target area to the evacuation spot 10. On the other hand, since the evacuation spots 4, 5, 9, 11, 12 are surrounded by other evacuation spots, it can be seen that there are very few evacuees to evacuate these spots.

In Case 2, almost all agents have evacuated in the southern half of the simulation target area, but

there are agents who still evacuate in the north side of the evacuation spots 1 and 8 (**Fig.4.11**). Most of the agents who are near the evacuation spot 8 at 3600 sec after the start of evacuation simulation complete evacuation, but the agents who are near the evacuation spot 1 make a round trip on the road passing through the north side of the evacuation spot 1 in the east-west direction since they don't grasp the evacuation routes to the evacuation spot 1 are flooded. The evacuation completion rate increases by 5% compared to the rate at 3600 sec after the start of the evacuation simulation since most of the agents near the evacuation spot 8 complete evacuation (**Fig.4.12**). The final evacuation completion rate is about 80% which is about 20% In addition, the number of agents who evacuates to the evacuation spots 1 and 2 which becomes unusable due to flooding is extremely small; The number of users of the evacuation spot 1 in Case 2 decreases to 32% of that of Case 1, and the number of users of the evacuation spot 2 in Case 2 decreases to 43% Although the routes to the evacuation spot 8 can't use due to flooding, the number of users at the evacuation spot 8 decreases little, and in Case 2 is 82% of that in Case 1 since there are some agents who evacuate to this spot while avoiding the flooded road. It is found that many agents get caught in the flooding and the evacuation behavior is restricted by flooding, which greatly affectes the evacuation completion rate.

### 4.3.2 Results of evacuation simulation: Case of agent grasped or don't grasp the flooding state in advance

As two cases mentioned above, it is found that the flooding states in the northwest side of the evacuation spot 1 and in the vicinity of the evacuation spot 8 have a big influenced on the evacuation behavior. The road along Suribachidani River becomes impassable in the northwest side of the evacuation spot 1 at 1800 sec after the start of the evacuation simulation. At 2100 sec after the start of the evacuation simulation, the evacuation spots 1 and 2 are flooded and the agents can't evacuate to these spots. It is found that the many agents get caught with the flooding or have to change to the destination of evacuation from the evacuation spot 1 to the faraway evacuation spot. Moreover, the agents are forced to make a detour by the flooding in the north side of the evacuation spot 8 and the agents who evacuate to the evacuation spot 2 at first changed the destination of evacuation to the evacuation spot 8. At that time, the agents have much time for completing the evacuation on the north side of the evacuation spot 8 since this area is very crowded.

In addition to Cases 1 and 2, evacuation simulations in which the agent recognizes some or most part of the flooding state in advance from, for instance, a hazard map made by a local government are carried on (hereinafter, those two are called "Case 3" and "Case 4" which correspond to "Case 1" and "Case 2", respectively). In Case 3, the agent, in advance, recognizes the area that will be flooded; the underpass flooded in an early stage of Case 1, the area near Suribachidani River; the area near the evacuation spots 1 and 2; and the northern side of the evacuation spot 8 where many agents get caught in the flooding. As well as Case 3, the agent also recognizes that the area will be flooded in advance in Case 4. In addition to Case 3, the agent in advance, recognizes the flooded area in the north side of the evacuation spots 4 and 5, which are flooded over a wide area. In these simulations, the initial placements of the agents and the walking speed are similar to Case 1 and 2. The agent does not pass through the area which is in advance recognizes as flooded area in the end even if the area is not flooded till a certain time.

**Fig.4.14-4.23** show the simulation results for Case 3 and 4 at 1800, 2100, 2400 sec when the flooding states were uploaded and at 3600, 7200 sec. The evacuation completion rate and number of evacuees by spot are already shown in **Fig.4.12** and **Fig.4.13**.

#### Results at 1800 s after the start of the evacuation simulations

In Case 3, at 1800 sec after starting evacuation simulation, there were no agent near the evacuation spots 1 and 2 which are unavailable due to flooding later (**Fig.4.14**). The agents who evacuate to these evacuation spots in Case 2 evacuated to the different evacuation spots in Case 4. In Case 2, 150 people get caught in the flooding near Suribachdani River. Since, on the other hand, the agents who are located on the west side of the evacuation spot 1 avoid Suribachidani River vicinity to the evacuation spot 3 in Case 4., they are able to evacuate without getting caught in the flooding near Suribachidani River (**Fig.4.3, 4.14**). In addition, the agent who is set on the east side of the evacuation spot 2 moved to south to evacuate to the evacuation spots 4 and 5 since they have grasped the evacuation spot 2 will be flooded. The agents in the northern side of the evacuation spot 8 avoid the roads that will be flooded later and evacuated in the east-west direction even before flooding. The evacuation completion rate in Case 3 is about 10% lower than that in Case 2 at 1800 sec after starting evacuation simulation since the agents avoid

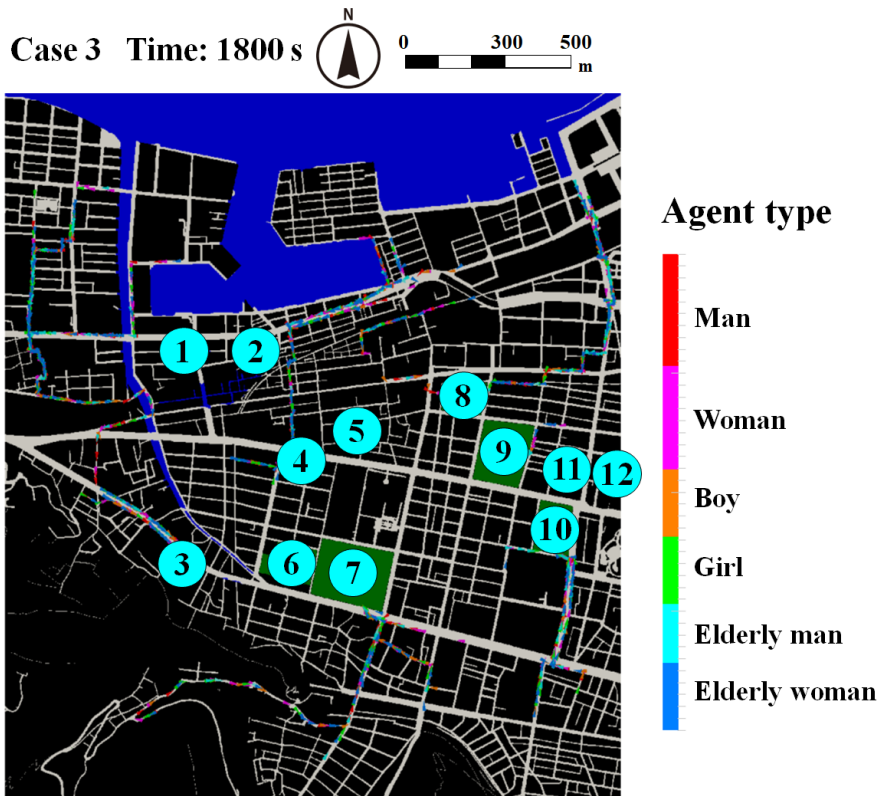


Fig.4.14 Evacuation condition of Case 3 (T=1800s)

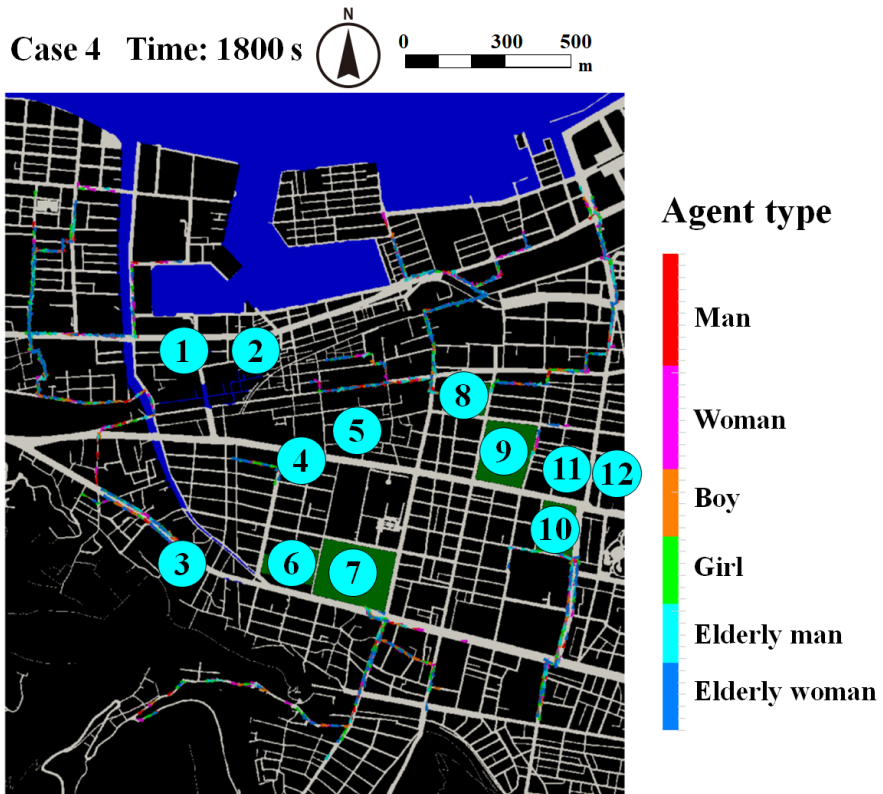


Fig.4.15 Evacuation condition of Case 4 (T=1800s)



the roads which will be flooded later (**Fig.4.12**). That is to say only 46% of agents evacuated in Case 3.

The evacuation behavior near the evacuation spot 1 in Case 4 is the same as in Case 3, and all agents avoid the Suribachidani River and goes to the evacuation spot 3 (**Fig.4.15**). On the other hand, the agent placed on the east side of the evacuation spot 2 evacuated to the evacuation spot 8 instead of the evacuation spots 4 and 5 as in Case 3 since they recognize that the north side of the evacuation spots 4 and 5 will be flooded later. Also, the agents who are located on the east side of the Takamatsu Fishing Port avoid the center of the target area and road on the south of the Takamatsu Fishing Port which will be flooded, and move to the evacuation spot 8 in this simulation. As described, the evacuation completion rate is low and 44% since the agents avoid the area that would be flooded later and made a detour in advance as in Case 3 (**Fig.4.12**).

## Results at 2100 s after the start of the evacuation simulations

In Case 3, many agents have moved to the evacuation spot without being flooded at 2100 sec after the start of the evacuation simulation (**Fig.4.16**). As has mentioned about the evacuation behavior at 1800 sec, it takes time because the agent makes a detour in the north side of the evacuation spot 8 but the agent steadily completes to evacuation. However, it can be seen that the area east of the Suribachidani River is extremely congested since the number of agents set on the northwest side of the evacuation spot 1 is very large and there are few available roads through the north and south. It can be said that it isn't very realistic to evacuate from the northwest part of the evacuation spot 1 to the evacuation spot 3 since the line of agent continues from such place to the evacuation spot 3 for more than 1 km in a straight line. Some of the agents who move from the east side of the evacuation spot 2 to the evacuation spots 4 and 5 got in the flooding. Moreover, in Case 2, the agents from the vicinity of Takamatsu Fishing Port evacuate to the evacuation spot 2 or the evacuation spot 8, and no agents get caught in the flood around the spot 4 and the spot 5 (**Fig.4.5, 4.16**).

However, in Case 3, this is the result because the agents who have already known that the area around the evacuation spot 1, the evacuation spot 2 and the north side of the evacuation spot 8 will be flooded tries to evacuate to the spot 4 and the spot 5.

At 2100 sec after the start of the evacuation simulation, many agents are able to evacuate without flooded in Case 4 as well (**Fig.4.17**). The agent who get caught in the flooding near the evacuation spots 4 and 5 in Case 3 moves to the evacuation spot 8 and continues evacuating without flooded in Case 4 (**Fig.4.16, 4.17**). In summary, it is found that the agent located far from the evacuation spot is less likely to be flooded by moving to the evacuation spot that will certainly not be flooded even if they take a detour. As has mentioned above, the evacuation completion rates in Case 3 and 4 are low and less than 50% at 2100 sec after the start of the evacuation simulation since agent make a detour to evacuate without flooded (**Fig.4.12**).

## Results at 2400 s after the start of the evacuation simulations

The agent who evacuates from the east side of the evacuation spot 2 avoiding the evacuation spot 2 to the evacuation spots 4 and 5 can't move by flooded since the flooded area gradually spreads in the central

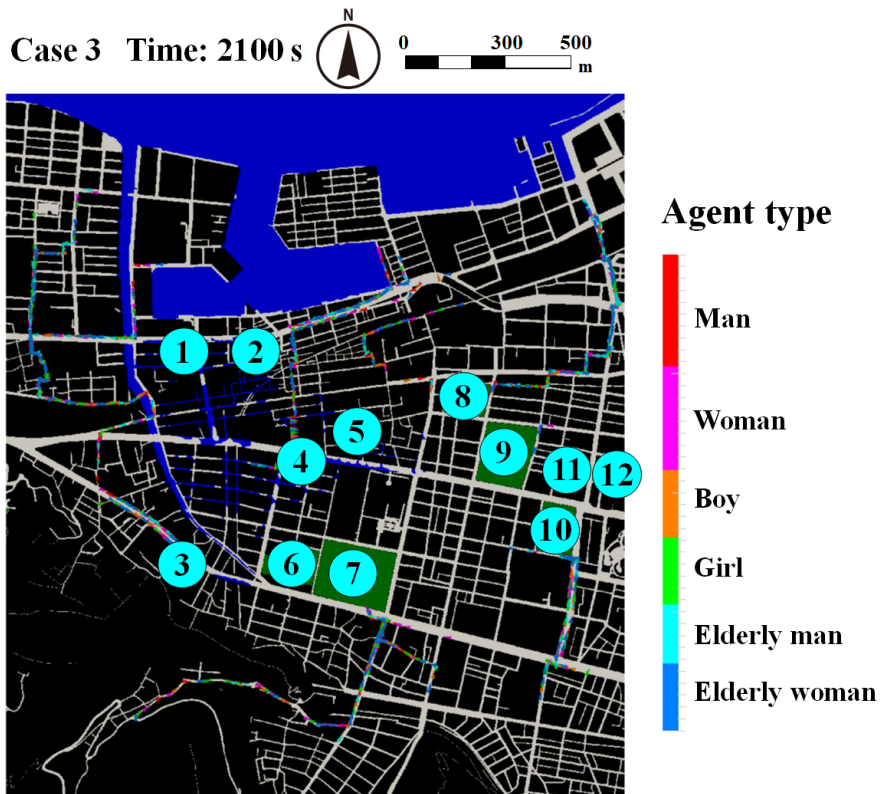


Fig.4.16 Evacuation condition of Case 3 (T=2100s)

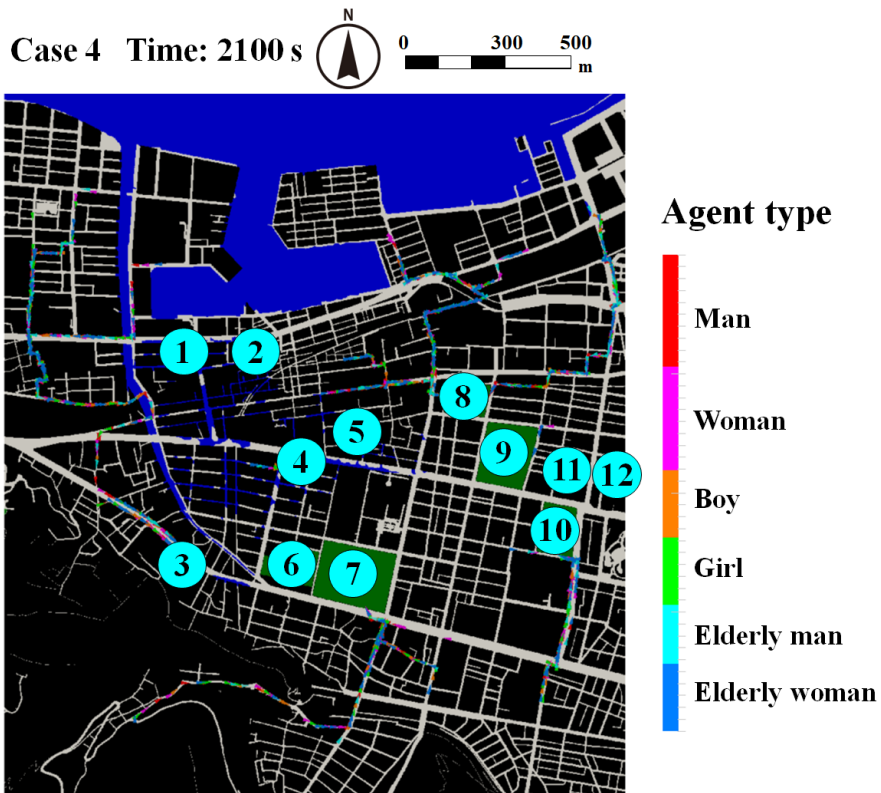
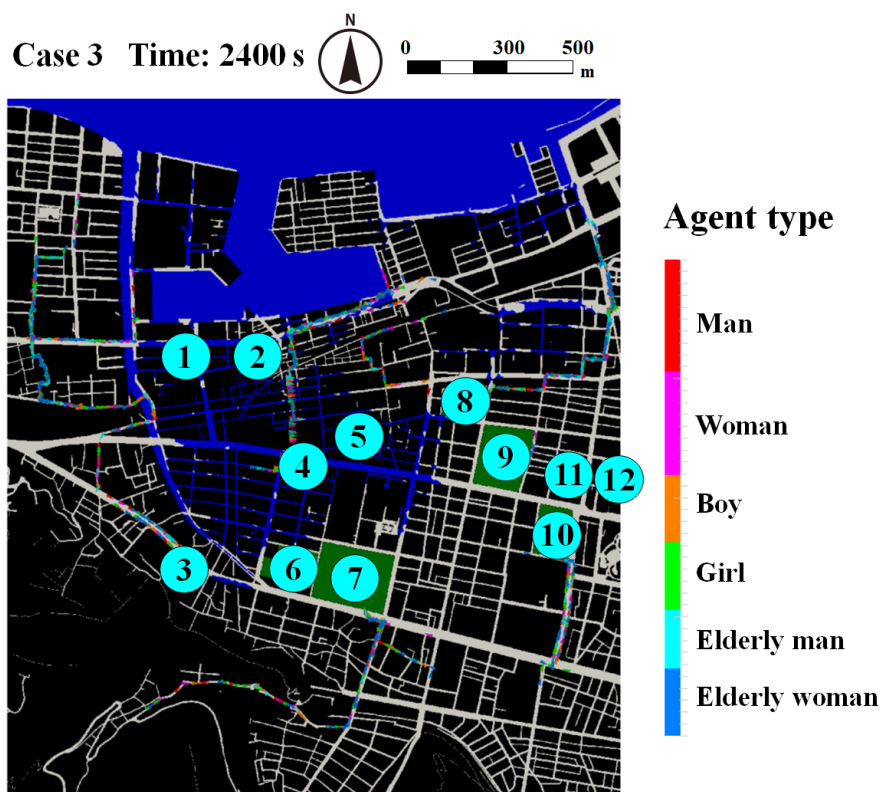


Fig.4.17 Evacuation condition of Case 4 (T=2100s)

part of the simulation target area at 2400 sec after the start of the evacuation simulation (**Fig.4.18**). It is found that the agent can get caught in the flooding as in Case 3 even if the agent grasps the flooded area in advance. In particular, there are a large number of agents got caught in the flooding on the road that run from the evacuation spot 2 to 4, and it's hard to say that the agent have been evacuated properly. On the other hand, although the traffic is still congested near the evacuation spot 1, the line is gradually shortened, and the agents gradually complete evacuation also near the evacuation spot 8. Therefore, the evacuation completion rate increases even if many agents can't move by flooded near the evacuation spots 4 and 5 (**Fig.4.12**).

In Case 4, most of the agent continues evacuating without flooded at 2400 sec after the start of the evacuation simulation (**Fig.4.19**). There is no agent at 2400 sec after the start of the evacuation simulatino and moves to other evacuation spots on the road from the evacuation spot 2 to 4 which is flooded in Case 3 (**Fig.4.18, 4.19**). However, there are about 10 agents who get caught in the flooding in the west side of the evacuation spot 4. As a result, they can't reach the evacuation spot 4 and get caught in the flooding although they move to the evacuation spot 4 from an early stage since they located on the east-west road passing from the evacuation spot 4 to Suribachidani River.



**Fig.4.18** Evacuation condition of Case 3 (T=2400s)

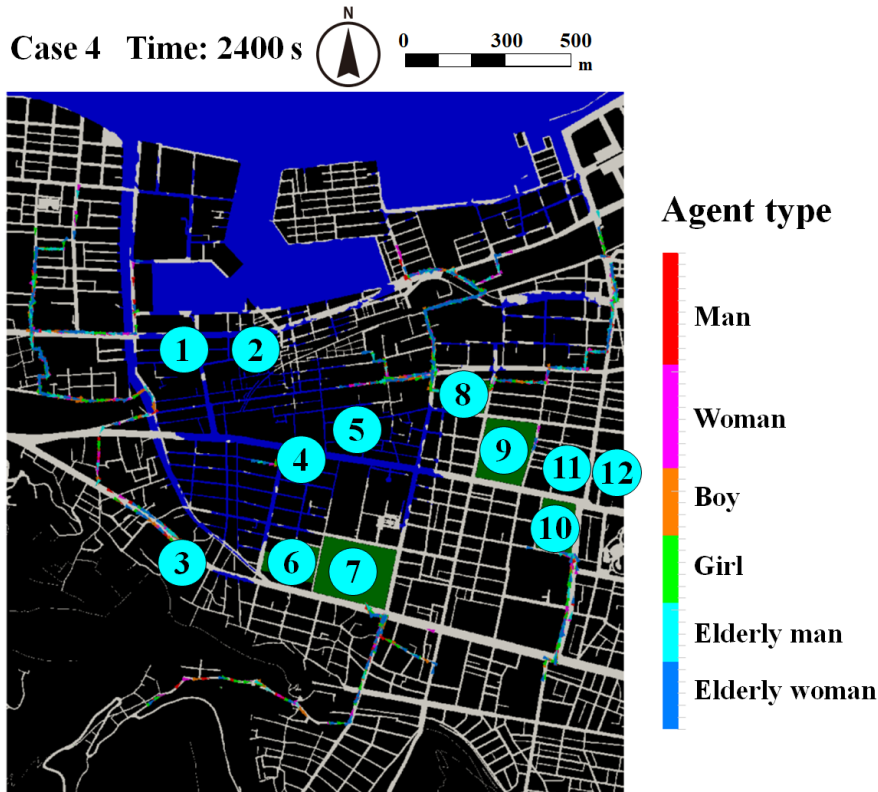


Fig.4.19 Evacuation condition of Case 4 (T=2400s)

### Results at 3600 s after the start of the evacuation simulations

In Case 3, the agents who get caught in the flooding near the evacuation spot 1 in Case 2 at 3600 sec after evacuation simulation don't get caught in the flooding and evacuate to the evacuation spot 3 (Fig.4.9, 4.20). As the agents don't grasp which road is flooded or not in Case 3, they face the flooded area with proceeding to the road which is not flooded. They repeat similar actions until they find an evacuation spot. The agents grasping the areas which will be flooded in advance need much time to evacuate in the early stages since they avoid the roads which will be flooded later. However, they don't get caught in the flooding and complete evacuation as soon as possible since they evacuate appropriately before the flooded area expands. In the eastern side of the evacuation spot 2, the agents don't get caught in the flooding and gradually complete evacuation since they evacuate to the evacuation spot 8 before the flooding spreads. As has mentioned above, in the north side of the evacuation spot 8, the agents avoid the flooded roads because they grasp the flooding state in advance. Most of agents already moved to the south-north road in Case 3 at 3600 sec after the start of the evacuation simulation, although most agents are stuck on the east-west road in the north of the flooded area in Case 2. It is expected that the agents near the evacuation spot 8 in Case 3 can evacuate earlier than those in Case 2 after 3600 sec. It is possible for the agent to complete evacuation in a short time without being caught in the flooding by grasping the flooding state in advance. The evacuation completion rate at 3600 sec after the start of the evacuation simulation in Case 3 is the lowest among the four simulation cases, which is about 65% since many agents get caught in the flooding near the evacuation spots 4 and 5 (Fig.4.12).

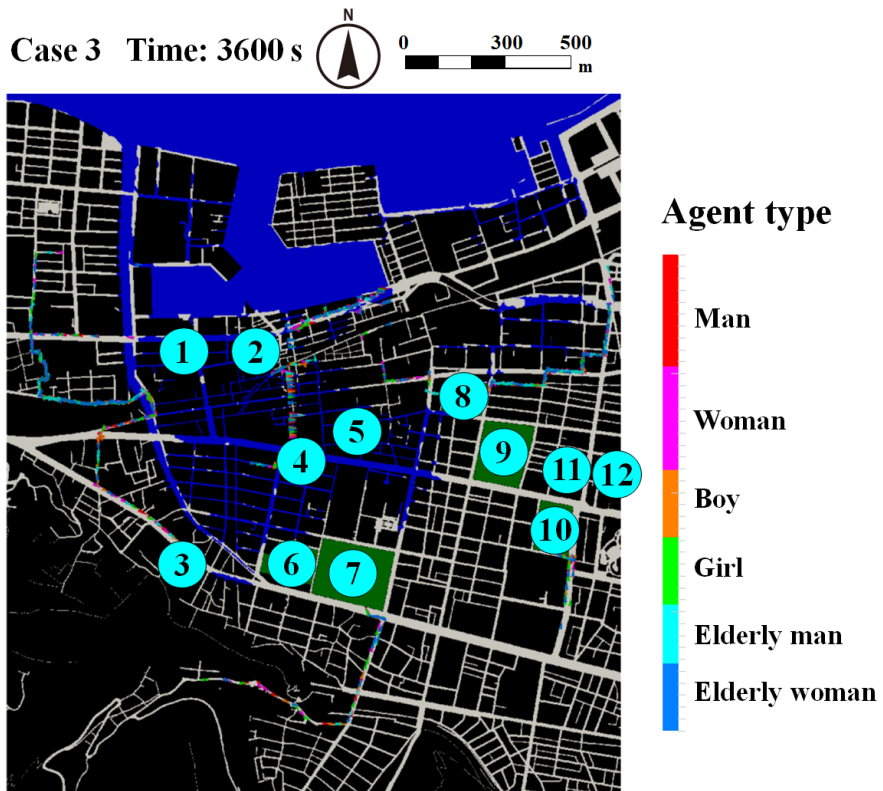


Fig.4.20 Evacuation condition of Case 3 (T=3600s)



Fig.4.21 Evacuation condition of Case 4 (T=3600s)

In Case 4, the agent takes time as in Case 3 near the evacuation spots 1 and 8 at 3600 sec after the start of the evacuation simulation, but the agent who is flooded in Case 3 continues evacuating without flooded and gradually completes evacuating to the evacuation spot 8 (Fig.4.20, 4.21). The evacuation completion rate in Case 4 gradually increases and exceeded the rate in Case 2 at 3900 sec after starting evacuation simulation (Fig.4.12). It is expected the evacuation completion rate continues increasing beyond 3900 sec because most of agents don't get caught in the flooding and can evacuate to the evacuation spot 3.

### Results at 7200 s after the start of the evacuation simulations

Almost all agents excluding get caught in the flooding, agents have completed evacuation except near evacuation site 3 completed evacuating at 7200 sec after the start of the evacuation simulation (Fig.4.22). In Case 2, many agents get caught in the flooding near the evacuation spots 1 and 2, and the northern side of evacuation spot 8. The evacuation completion rate increases even at 3600 sec after starting evacuation simulation since these evacuees complete evacuating in Case 3 at 3600 sec after starting evacuation simulation (Fig.4.12). The evacuation completion rate is more than 90% in the end in spite of the fact that the flooding is considered. Similarly, the number of evacuees who evacuate to evacuation spot 3 increase in Case 3 since the agent who evacuates to evacuation spots 1 and 2 in Case 2 evacuated to evacuation spot 3 in Case 3 (Fig.4.13). It can be said that it is effective to evacuate after grasping the flooded area in advance since the evacuation completion rate in Case 3 finally exceeds 90% (Fig.4.12). However, it is also find that it isn't enough to grasp the flooded area in advance and may get caught in the flooding in

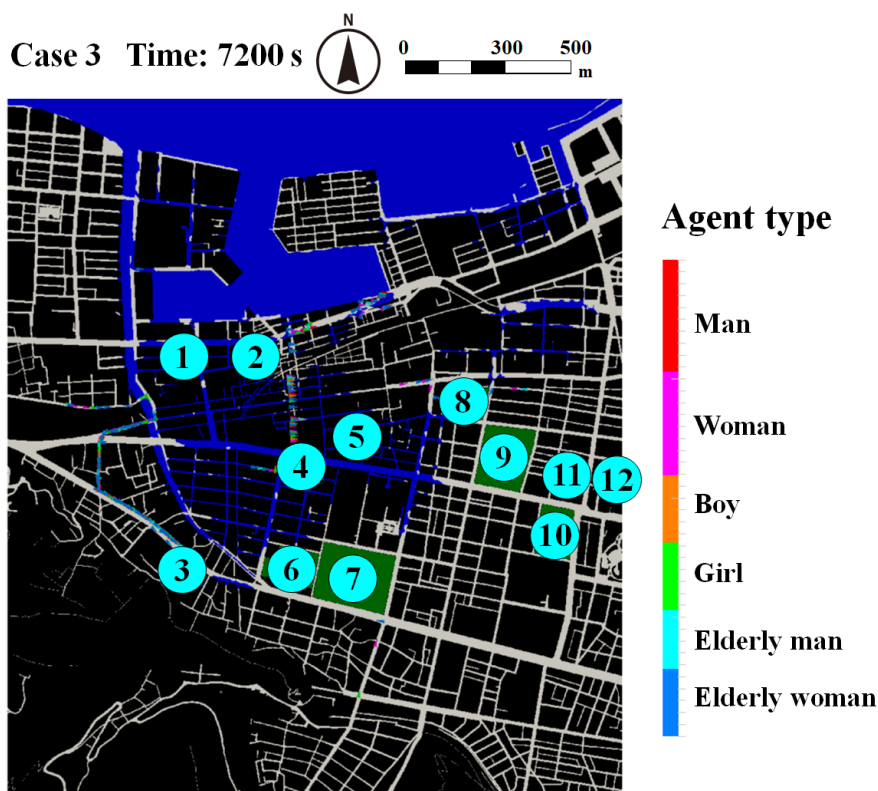


Fig.4.22 Evacuation condition of Case 3 (T=7200s)



Fig.4.23 Evacuation condition of Case 4 (T=7200s)

some cases; the nearest evacuation spot is flooded or there is a distance to the evacuation spot, etc.

There is no evacuee who evacuates to the evacuation spots 1 and 2 since the agent grasps that they can't evacuate to the evacuation spots 1 or 2 by flooding in Case 4 (Fig.4.23). They evacuate to the evacuation spot 3 or 8 instead of the evacuation spot 1 or 2 in Case 4. Therefore, the number of evacuees who evacuates to the evacuation spots 3 and 8 increases. However, as has already described above, the number of evacuees to the evacuation spot 8 don't increase in case 3, unlike in case 4, because there are many agents who get caught in the flood in the north side of the spot 4 and the spot 5. The number of evacuees who evacuates to the evacuation spot 3 increases from about 200 evacuees in Case 2 to about 650 evacuees in Case 4 (Fig.4.13). In addition, the number of evacuees who evacuates to the evacuation spot 8 increases from about 470 in Case 2 evacuees to about 870 evacuees in Case 4. However, it takes a long time for the evacuees in Case 4 to complete the evacuation to the evacuation spot 3 (Fig.4.12). As has already mentioned, the agent near the evacuation spot 8 can complete evacuation in a short time without being caught in the flooding by grasping flooded areas in advance. However, it is found the agent can't complete evacuation in a short time near the evacuation spot 1 and 2 even if the agent grasps the flooding state in advance. This is because that the evacuation spots 1 and 2 as well as their surroundings are flooded though the evacuation spot 8 around which the flooding occurred isn't flooded. In addition, the fact that there are very few south-north roads because the Kotoku Railway Line runs between the evacuation sites 1, 2, and 3 is one of the causes. The agents who evacuate to the evacuation spot 1 in Case 2 and to the evacuation spot 3 in Case 4 are located in the northwest part of the analysis area. This area isn't flooded in the flooding analyses since the elevation of the area is about 3m and it is higher than

the surrounding area. According to the analyses results, it may be better to evacuate to the second floor of their home for the elderly people or disabled persons who have difficulty in walking long distances or evacuating quickly.

## 4.4 Conclusions

Many agents get caught in the flooding in front of the evacuation site and cannot complete evacuation when there is an evacuation spot in a low-altitude area or an area prone to flooding. The coastal evacuation spot is flooded in the early stage and many agents get caught in the flooding when the storm surge disaster occurred in Takamatsu in 2004. Similar results are obtained in the flooding analysis conducted in this study. It is found to take time to complete evacuation in the area few evacuation spots since the congestion is caused by the concentration of many agents due to the flooding of the road. Thereby, the evacuation simulation is carried out with assuming that the agent recognizes in advance the flooding area which greatly affects the evacuation behavior in the above evacuation simulation. When the agent recognizes the flooded state in advance, they can complete the evacuation in a short time without being caught in the flooding. At the same time, the evacuation completion rate is much higher than that in the case where the flooded state is not recognized in advance. However, in the case that the evacuation spot itself is flooded in the area where there are few evacuation sites and few possible evacuation routes, the agents are forced to evacuate for a long time before reaching the evacuation spot even if the agents grasp the flooded area beforehand. In this research, only pedestrians are dealt with, but even when agent evacuates using vehicle, the time to complete evacuation can be very long in such an area where there are few shelters around and few evacuation spots available. Therefore, it is effective to grasp the flooding area in advance and evacuate avoiding the area in order to take appropriate evacuation action. However, it is also necessary to consider an evacuation at home in areas where there are few evacuation sites. In order to reduce the risk of disasters, it is important to enable all evacuees to evacuate to a safe place. Therefore, it is necessary to discuss measures for areas with few evacuation spots or evacuation spot around which there is the possibility of flooding as has mentioned above. Though the agents are randomly placed in the city, it is desired to carry out appropriate agent placement from the results of the census, etc., which leads us to discuss the proper arrangement of an evacuation spot in densely populated areas or depopulated areas. In addition, it is anticipated that the disaster prevention consciousness of the agent who grasps the inundation situation beforehand is higher than that of the agent who does not grasp it. Therefore, it is necessary to appropriately reflect the level of disaster prevention consciousness in the parameters of agents, because the level of disaster prevention consciousness has a large effect on the time required for evacuation and the time of the start of evacuation.



## 5 . Satellite image analysis during heavy rainfall

### 5.1 Introduction

Conference on the Use of Earth Observation Satellites for Disaster Prevention was held in September 2014 since prompt information acquisition is necessary to enable smoother recovery and relief activities in the event of a disaster. The purpose of this conference is to verify the effectiveness of satellites for disaster prevention and ALOS-2 disaster prevention utilization experiment plan was implemented through this conference. As a result, a lot of studies have been conducted on grasping the disaster situation utilizing satellite image. Ueda et al. made it possible to classify the disaster and non-disaster areas since he detected the disaster areas caused by sediment disaster using SAR images and DEM data<sup>39)</sup>. Additionally, Hasekura et al. extracted the tsunami flooded area caused by the 2011 off the Pacific of Tohoku Earthquake using optical satellite images and SAR images<sup>40)</sup>. In recent years, various methods for recognizing the disaster situations such as the damage situation in a wide range such as flooded area and sediment-related disaster areas using satellite images have been studied. Although it is necessary to grasp the damage situation on roads since the damage situation mainly on the roads hindered the recovery and relied on activities in the event of the heavy rain disaster. Also, it is difficult to recognize the disaster area from optical satellite images since it is often bad weather on the day after the disaster when a heavy rain disaster or a storm surge disaster occurs due to a typhoon. For such disasters, it is common to use SAR images that aren't affected by the shooting time and weather condition. There are some methods used to grasp the disaster situation from SAR images such as the extraction using the method of the additive color mixture<sup>41)</sup>, the extraction of changing area by difference processing which is used the images before and after the disaster<sup>42)</sup>, and the extraction of the flooded area by detecting the outline of the flooded area using only images after a disaster<sup>43)</sup>. If it is necessary to quickly grasp the damage situation, it may not be possible to use the method of the extraction of the outline of the flooded area since this method has a complex processing process and it is expected that it will take time to detect the disaster area. In this chapter, in addition to extracting the disaster area by the method of the additive color mixture which has fewer steps using the SAR images before and after a disaster, the road areas are also analyzed in order to a smooth recovery and relief activities after the disaster.

## 5.2 Analysis summary

### Target area and disaster

The target water disaster of this study is the heavy rain in July 2018 that caused widespread damage, mainly in western Japan. The damaged area of Mabi-cho, Kurashiki city, Okayama prefecture (the area of 8922 m east-west  $\times$  5572 m north-south) which is particularly severely damaged by this disaster is grasped in this study. In order to grasp the damaged area, the satellite images before the disaster took around 0:00 on July 10th, 2016, and after the disaster taken around 0:00 on July 8th, 2018 was used. Other details of satellite images are shown in Table5.1. In this study, these images were taken in the same season so that the flooded area isn't affect by the paddy fields. In addition, the same satellite and sensor are used to take the satellite image before and after the disaster.

**Table5.1** Condition of satellite image shooting

	Shooting date and time	Satellite	Sensor
Before a disaster	Midnight on July 10th, 2016	ALOS-2	PALSAR-2
After a disaster	Midnight on July 8th, 2018	ALOS-2	PALSAR-2

## 5.3 Results of satellite image analysis

### 5.3.1 Extraction of damaged areas by the method of the additive color mixture

#### Additive color mixture of satellite images

As has already mentioned in Chapter 2, the SAR image is analyzed by the method of the additive color mixture of which extracts areas changed before and after a disaster as color changing, and extract the area that changed before and after a disaster as a color change.

The pre-disaster image and post-disaster image are converted from grayscale to red and cyan scale, respectively, and additional processing is performed on these two images. The gray and red scale images of the pre-disaster are shown in Fig.5.1 and Fig.5.2, the gray and cyan scale images of the pre-disaster are shown in Fig.5.3 and Fig.5.4, and the image obtained from these red and cyan scale images is shown in Fig.5.5, respectively. In this study, paddy fields located on the north side of Oda River, which passes through the target area from east to west, are shown in black in the images of before and after the disaster since two images are taken in the same season in order not to be affected by paddy fields to grasp the flooded area as has mentioned above. That is to say, the water is filled in the paddy fields regardless of the flooded (Fig.5.2, 5.4).



**Fig.5.1** Satellite image of before a disaster (Gray scale)

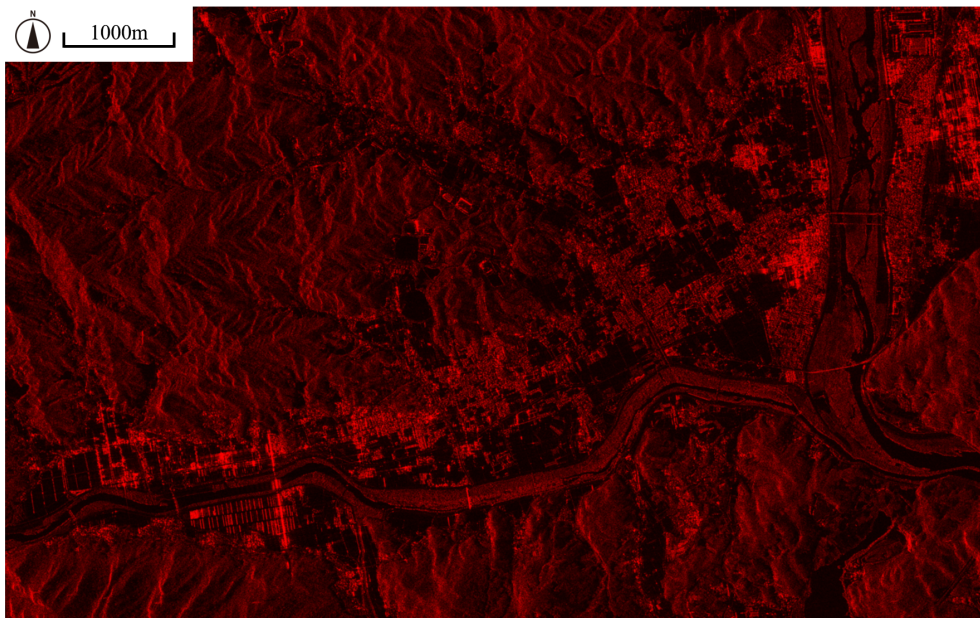


**Fig.5.2** Satellite image of after a disaster (Red scale)

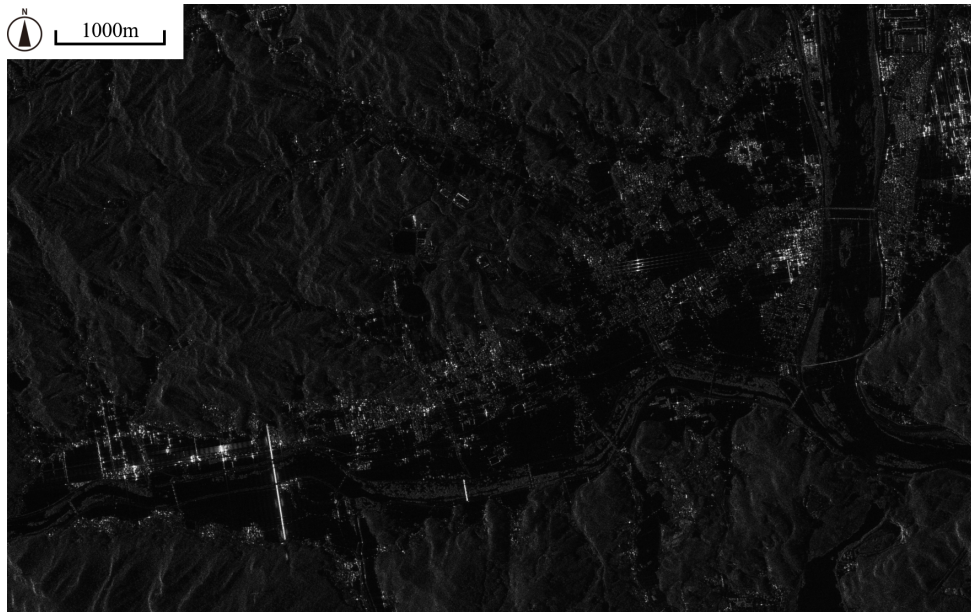


**Fig.5.3** Satellite image of before a disaster (Gray scale)

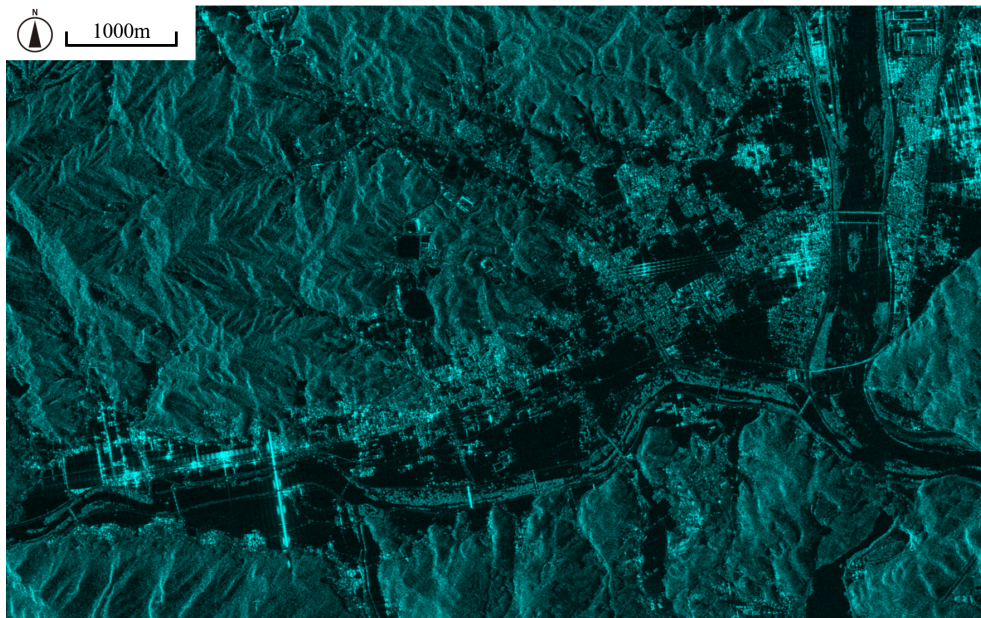


**Fig.5.4** Satellite image of after a disaster (Cyan scale)

## Examining the validity of additive color mixture images

In Takahashi River through the north-south direction in the eastern part of the analysis target area, the central part of this river is shown in black which indicates that the water area remains unchanged before and after the disaster. On the other hand, there are many areas around the riverbank that are shown in red. It means that the water area of this river have expanded due to heavy rain. A blue area extended outside the red area, which means that it have become a bare area due to the inflow of the sediment. The eastern side of the Takahashi River is shown in white which indicates that there is no change due to flooding or sediment in those areas. On the other hand, the north side of Oda River, the area around Kurashiki Makibi Support School, and the west side of Takahashi River excluded the paddy fields are extensively shown in red over a wide area and such areas where the intensity of reflected waves have decreased after the occurrence of the disaster (Fig.5.5). The estimated flooded range of Mabi-cho, Kurashiki city, Okayama prefecture due to the heavy rain in July 2018 which is provided by the Geospatial Information Authority of Japan is shown in Fig.5.6. Comparing the black area in Fig.5.6 with the flooded area which is the black and red area in Fig.5.5, it is considered these areas are almost the same. According to the estimated flooding stage color map around Mabi-cho, Kurashiki city (Fig.5.7), also provided by the Geospatial Information Authority of Japan, the flooding depth of the east side of Takahashi River was shallower than other areas, and it seems that it isn't so flooded. Even if the image after the addition processing (Fig.5.5), there are many white areas on the east side of Takahashi River, and the area is less flooded than the surrounding area. In summary, it is reasonable to think that the extraction result of the

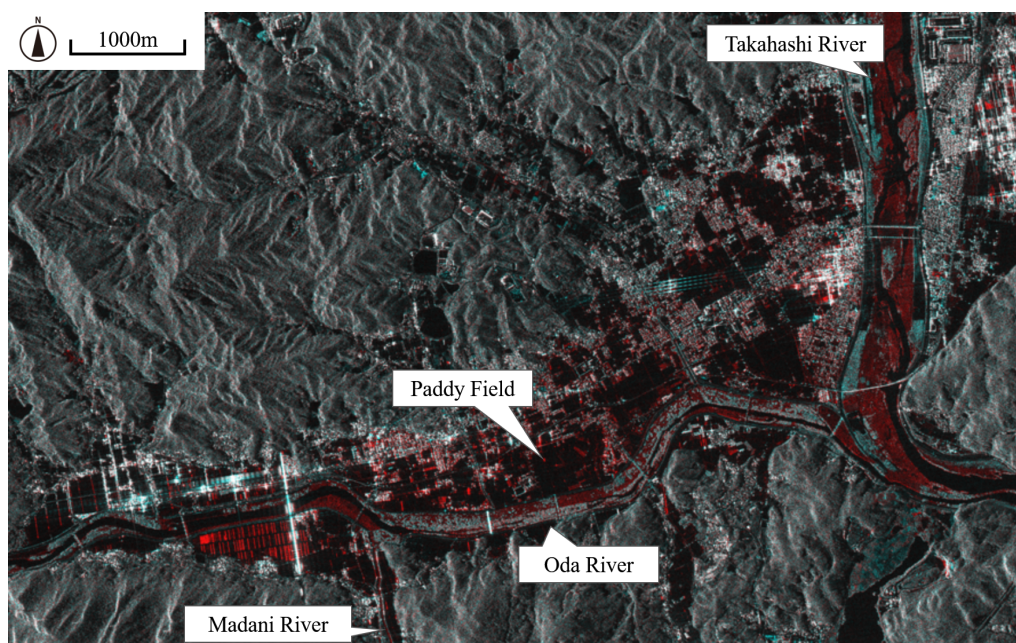


**Fig.5.5** Satellite image using additive color mixture

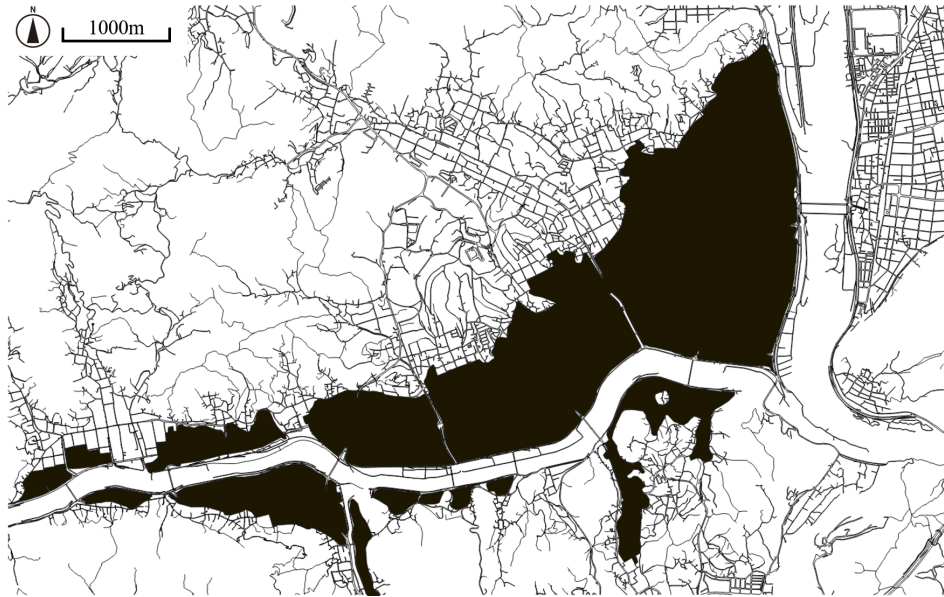


**Fig.5.6** The estimated inundation range at Mabi-cho

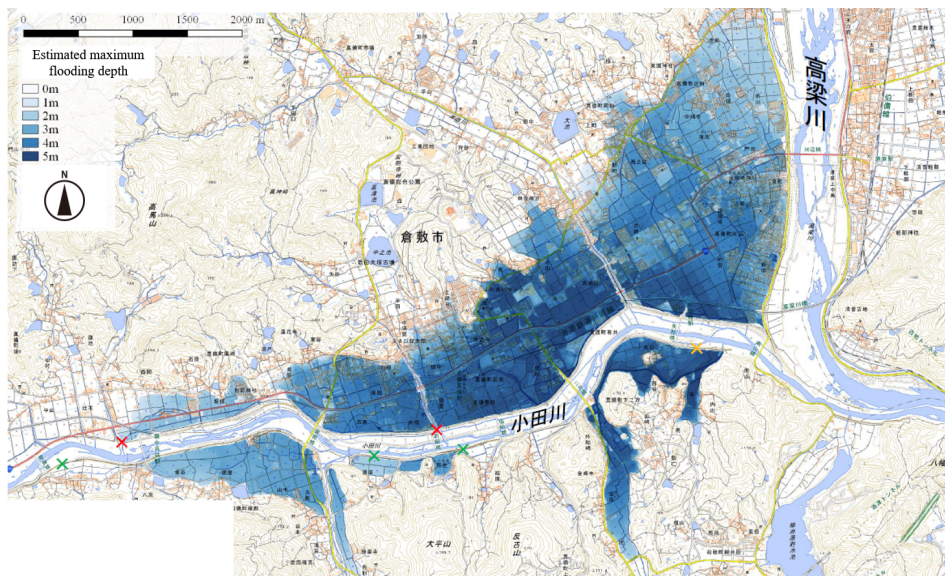


**Fig.5.7** The estimated flooding stage color map around Mabi-cho<sup>44)</sup>

change region using the method of the additive color mixture is useful since the change region obtained by this analysis is consistent with the area in the estimated flooding stage color map around Mabi-cho, Kurashiki city.

### 5.3.2 Extraction of road area in addition processing images

In this subsection, the disaster area in the road is extracted using the image obtained by the method of the additive color mixture. The road area is extracted by the procedure shown in Section 2.3. First, the image of road edge data and the image divides into the roads and non-road areas from the road edge data are shown in **Fig.5.8** and **Fig.5.9**, respectively. Next, the image in which the road area is extracted by Fig.5.5 and **Fig.5.9** is shown in **Fig.5.10**. Only the more clearly colored areas are judged as the changed area since most of the road area is colored black as shown in the enlarged view of **Fig.5.10**, and it is difficult to find the part of colored in red or cyan. Therefore, as shown in Chapter 2.3, the area where the

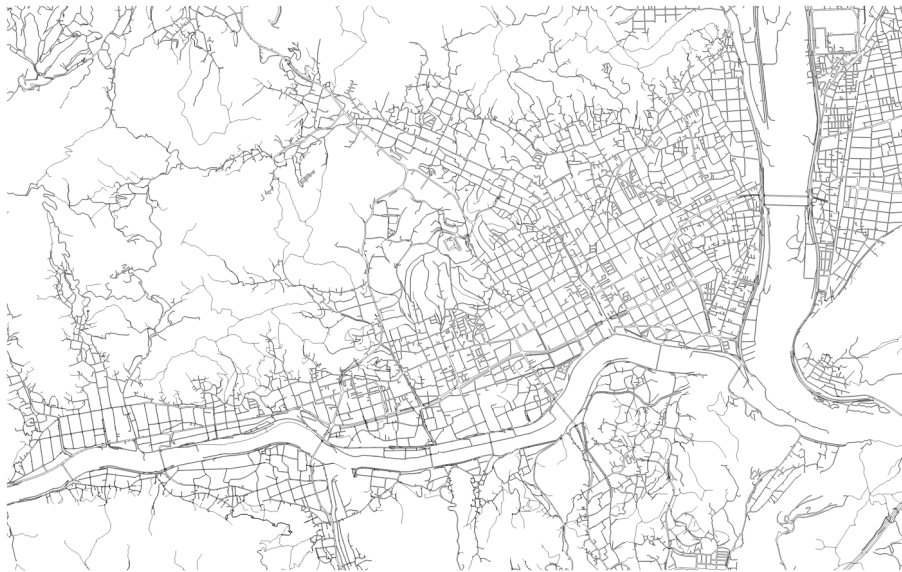


**Fig.5.8** Vector data of road edge



**Fig.5.9** Distinguishing road parts



**Fig.5.10** Extraction of road parts in satellite images

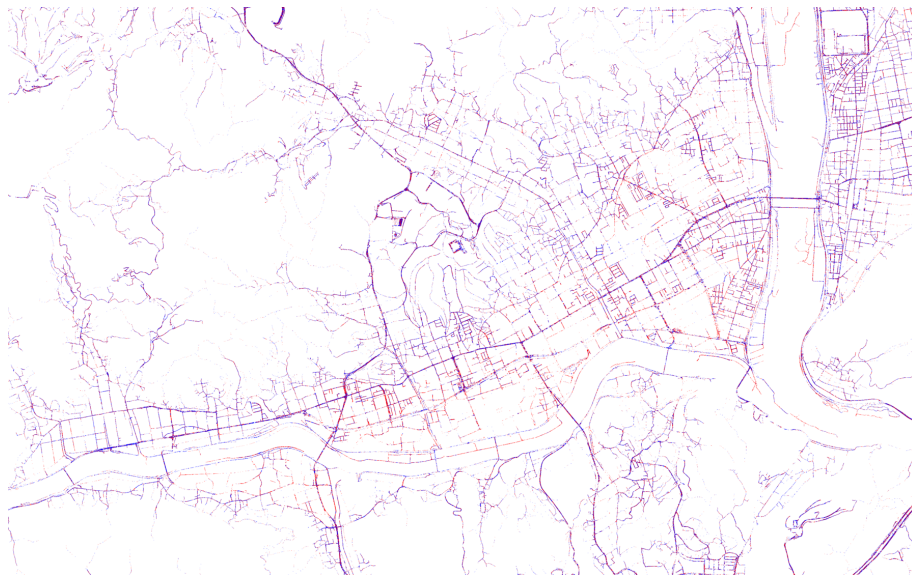


**Fig.5.11** Emphasizing colored parts

$R$  value is more than 50 and the values of  $G$  and  $B$  are less than  $R$  value is shown in red, where the value  $G$  and  $B$  are more than 50 and the  $R$  value is less than the values of  $G$  and  $B$  is shown in cyan. In addition, other parts are shown in white. By performing the above processing, the result of setting a threshold and recoloring is shown in **Fig.5.11**. This process made it possible to grasp only the places where large changes are seen on the road. The above threshold is adopted in this study from several thresholds in order to make it easier to see the change area and to gain the same result as the actual situation.



### 5.3.3 Extraction results of damaged areas in the road area

#### Extraction results of damaged areas in the road area

Aerial photographs in arbitrary areas and extracted image of the disaster situation such as flooded and sediment area obtained by the method of additive color mixture are compared in order to examine the validity of the extraction result obtained by the method of the additive color mixture. The aerial photographs and the results of extracting the damage situation such as flooded and sediment area before and after the disaster from two satellite images by the method of the additive color mixture are shown in Fig.5.12-5.20 and Fig.5.13-5.21, respectively. The aerial photographs are published by the Geospatial Information Authority of Japan (<https://maps.gsi.go.jp/>) and are taken on July 9th, 2018. In addition, the enlarged view of the arbitrary area in Fig.5.13-5.21 are shown in Fig.5.14-5.16, Fig.5.19, and Fig.5.22,5.22, respectively.

#### Analysis results of the area around Kurashiki Makibi Support School

Fig.5.12 and Fig.5.13 show the aerial photograph around Kurashiki Makibi Support School located on the north side of Oda River and the result of extracting the changed area on the road, and Fig.5.14-5.16 show the north side of Kurashiki Makibi Support School, Prefectural Road 281, and the vicinity of Oda River, respectively. A large number of roads are flooded such as the road on the east side of Kurashiki Makibi Support School and Prefectural Road 281 runs north and south from Fig.5.12. In the extraction results (Fig.5.13,5.14,5.15), these roads are also colored in red indicating that the flooded areas can be extracted appropriately. In the vicinity of Oda River, it is found that the flood occurs at the point near the river and sediment occurred at a distance from the river from (Fig.5.16) since the sidewalk near the river

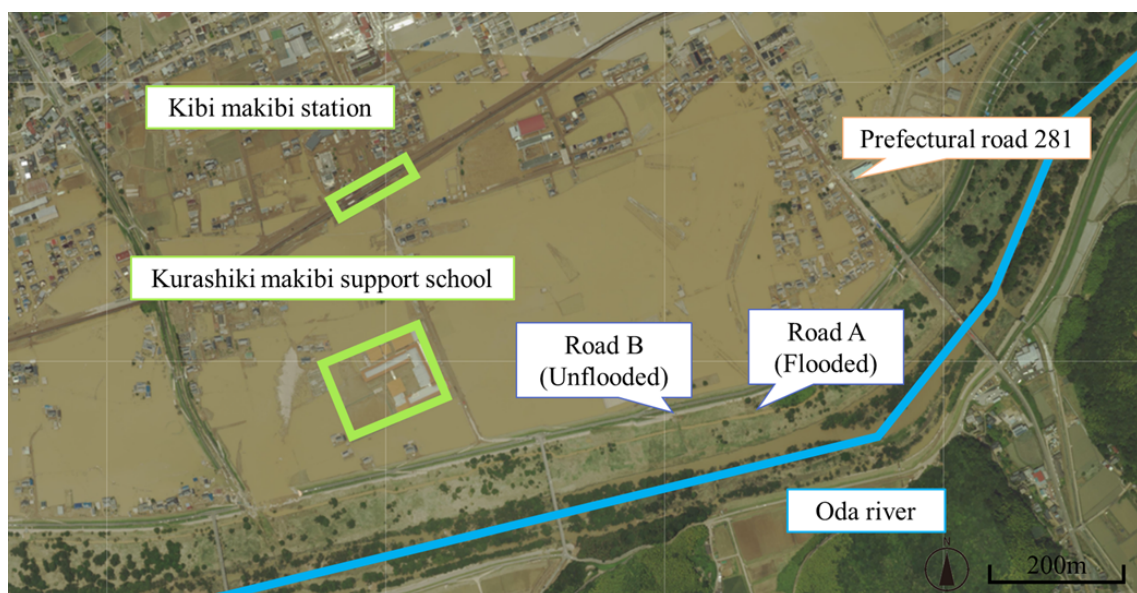
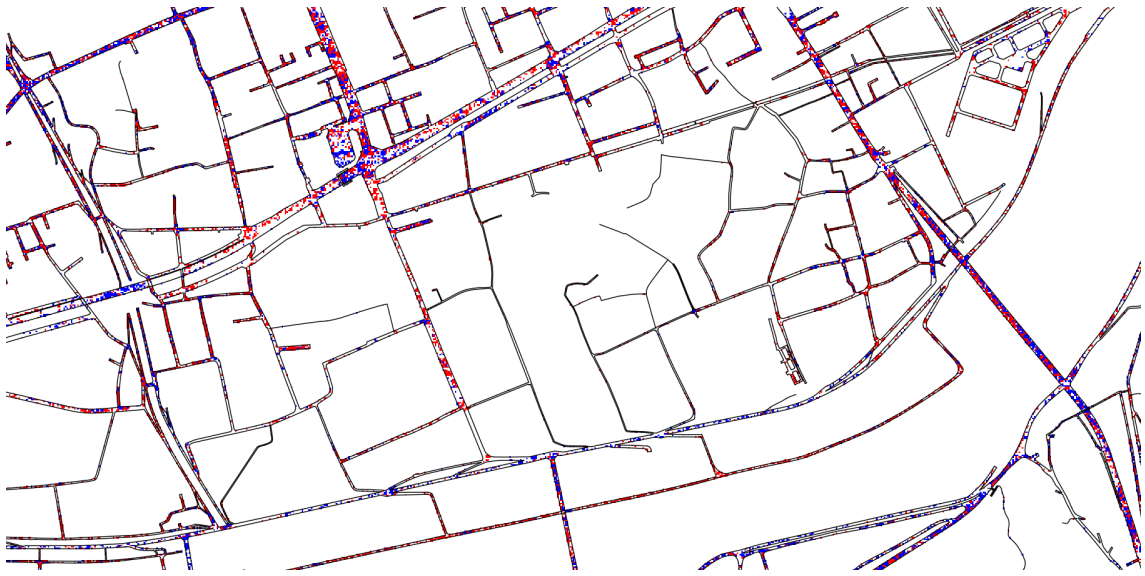
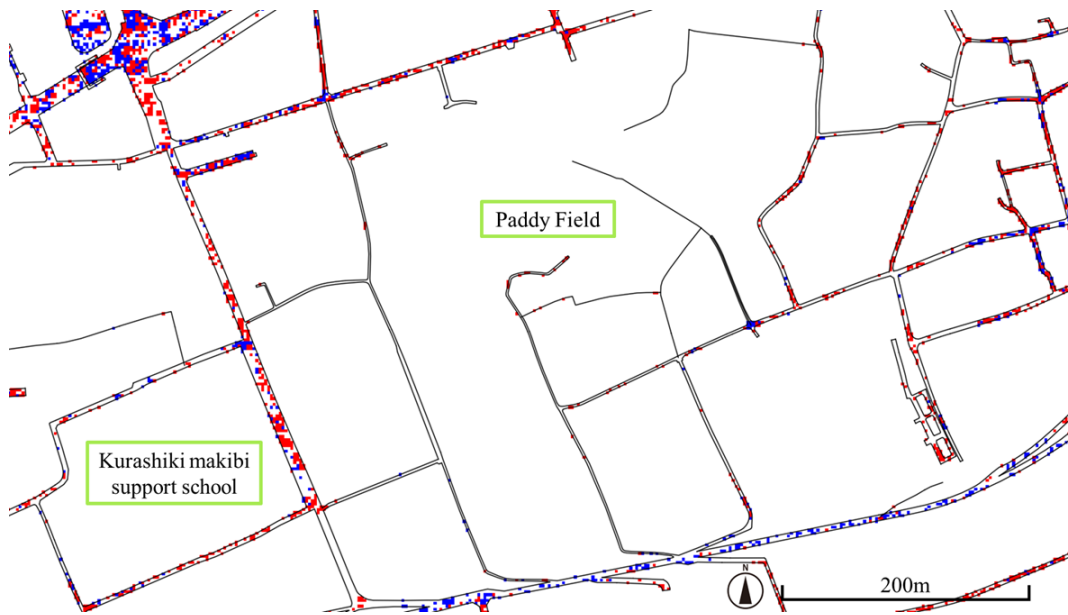


Fig.5.12 Aerial photogrammetry after a disaster (Near Kurashiki makibi support school) <sup>45)</sup>



**Fig.5.13** Extraction of damaged area on road (Near Kurashiki makibi support school)



**Fig.5.14** Extended figure (East side of Kurashiki makibi support school)

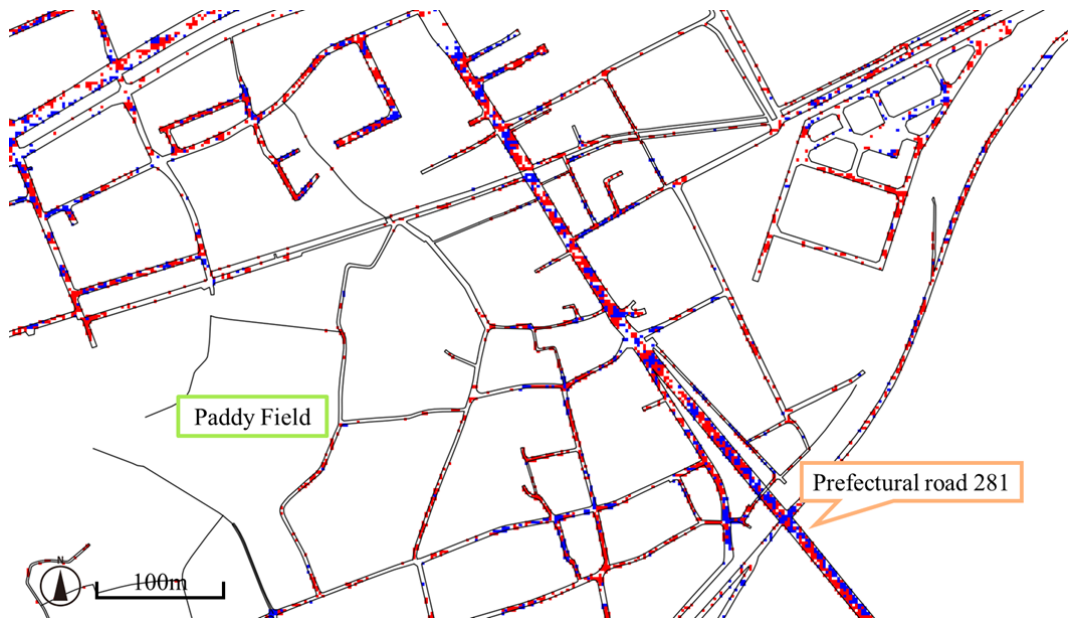


**Fig.5.15** Extended figure (Near prefectural highway 281)

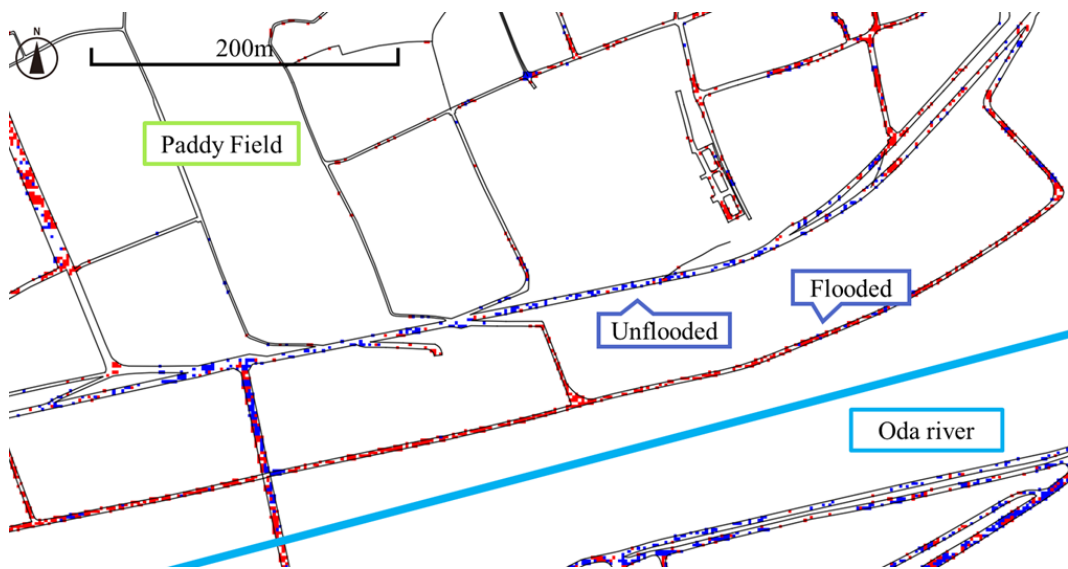


**Fig.5.16** Extended figure (Near Oda river)

is colored red (Fig.5.16, Road A), and the road several meters away from it colors blue (Fig.5.16, Road B). The road near the river in the extraction result (Fig.5.16) is flooded since this road's color is darker than other roads and the same color as the water surface from the aerial photograph (Fig.5.12). However, at least the road colored in blue in the extraction results (Fig.5.13) haven't been flooded, whether or not there is sediment can't be confirmed, since this road is brighter than the road which considered to be flooded and the water surface in the aerial photograph (Fig.5.16). The road near Kibi Makibi Station's color is darker than other roads and flooded and the same applied to the extraction result (Fig.5.12), there are many places colored in red near the same road and railroad track (Fig.5.13). In summary, the flooding state on some roads can be grasped from the extraction result, but the widespread flooding in the central part of Fig.5.12 (the east side of Kurashiki Makibi Support School) can't be properly reflected in the extraction result (Fig.5.13, 5.14). It is caused that the roads width are small and difficulty in extracting flooded areas on the roads using satellite images with a resolution of 2.5 m. This area colors in red and judged as flooded including the road area which isn't really flooded even in the satellite image before the disaster since paddy fields spread out in this area and were filled with water in both pre-disaster and post-disaster periods.

### **Analysis results of the area near the north side of Prefectural road 486**

The aerial photograph on the north side of Prefectural road 486 is shown in Fig.5.17, and the result of extracting the change area on the road is shown in Fig.5.18. Additionally, the enlarged view of the vicinity of Yata Elementary School is shown in Fig.5.19. The flooded area could be properly extracted since the target area is flooded over a wide area according to the aerial photograph (Fig. X) and the same areas are also colored as red in the extraction results (Fig.5.18). The extraction result is valid since the road running in a north-south direction about 200 m west from the irrigation canal located in the center of the

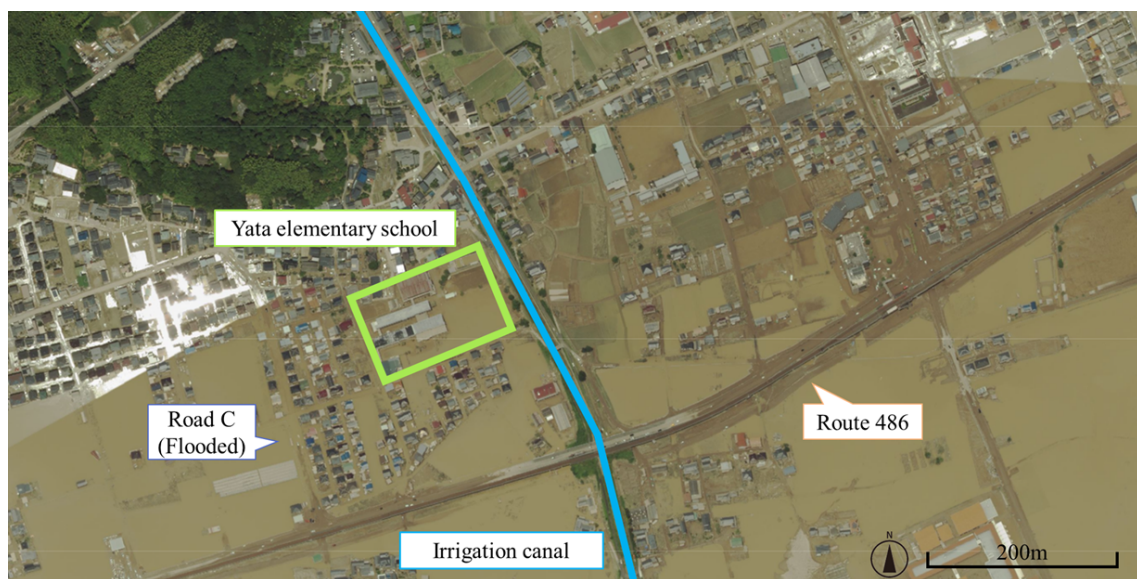


**Fig.5.17** Aerial photogrammetry after a disaster (North side of Route 486) <sup>45)</sup>

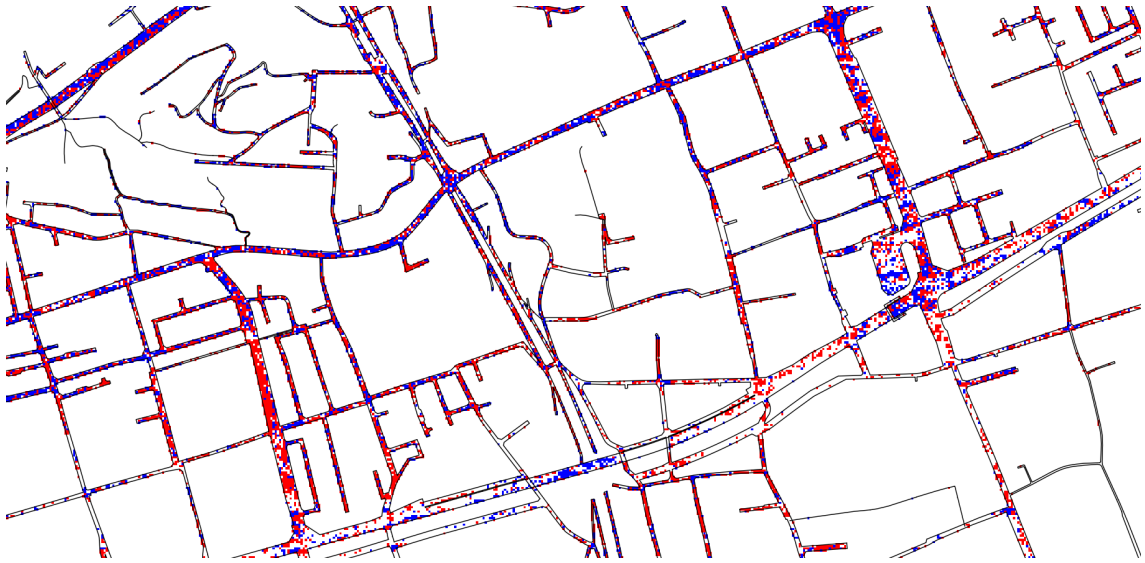


**Fig.5.18** Extraction of damaged area on road (North side of Route 486)

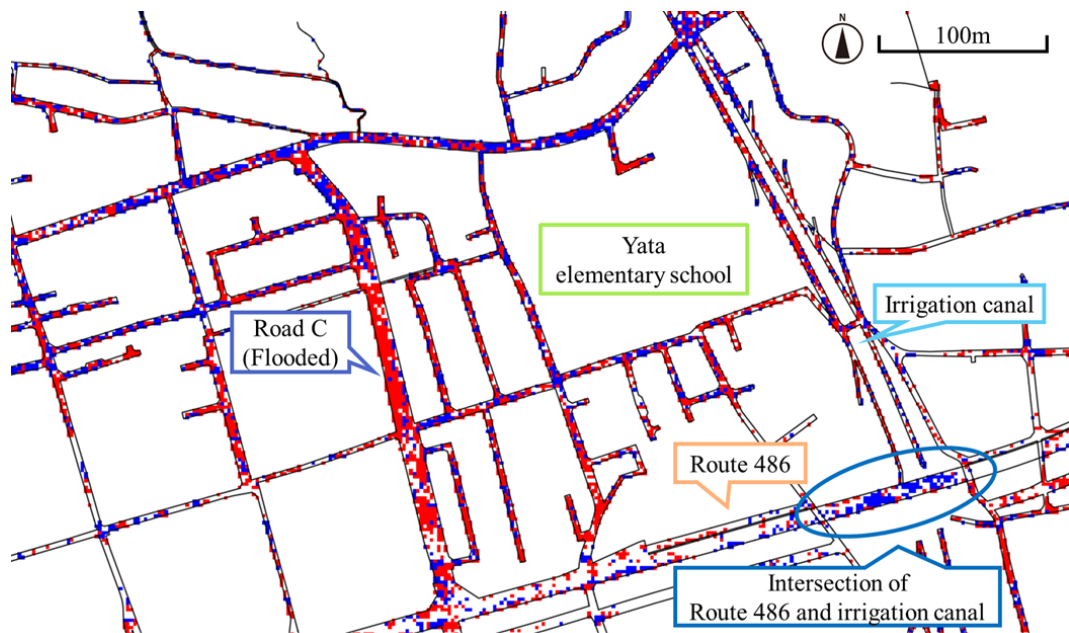


**Fig.5.19** Extended figure (Near Yata elementary school)

target area is colored red in the extraction result (Fig.5.19, Road C) and can be seen the flooded area in the aerial photograph (Fig.5.17). The color of the intersection of the irrigation canal and Route 486 is brighter than the surrounding area (Fig.5.17), and this area isn't flooded. Similarly, this area isn't flooded but covered with sediment since there are no areas colored in red near the intersection and there are more blue areas than the surroundings in the extraction result (Fig.5.18, 5.19).

## Analysis results of the area around Mabi Community Center Hattori Branch

The aerial photograph around Mabi Community Center Hattori Branch located on the south side of Oda River is shown in Fig.5.20, and the result of extracting the change area on the road is shown in Fig.5.21. Additionally, the enlarged view of the paddy fields located on the west side of the target area and Madani River are shown in Fig.5.22, 5.22, respectively. Most of this area is the paddy fields, and

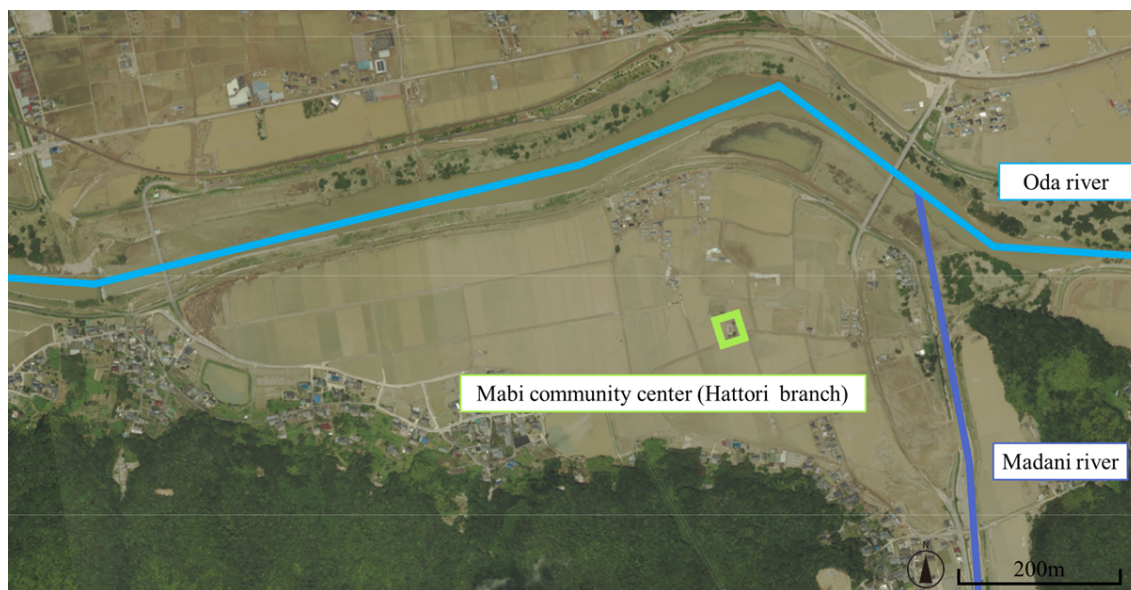


**Fig.5.20** Aerial photogrammetry after a disaster (South side of Oda river) <sup>45)</sup>



**Fig.5.21** Extraction of damaged area on road (South side of Oda river)

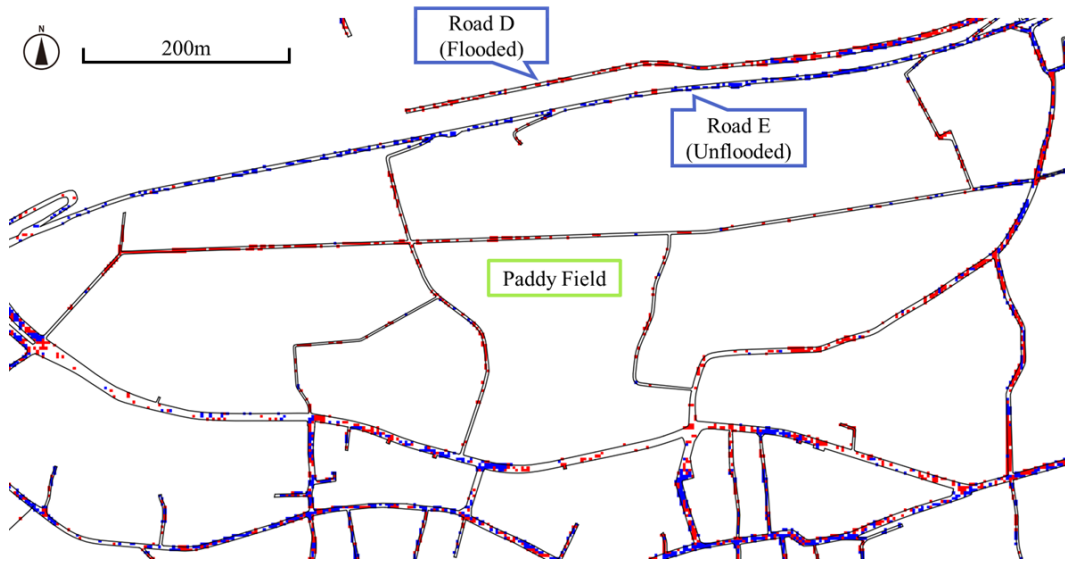


**Fig.5.22** Extended figure (South side of Oda river)

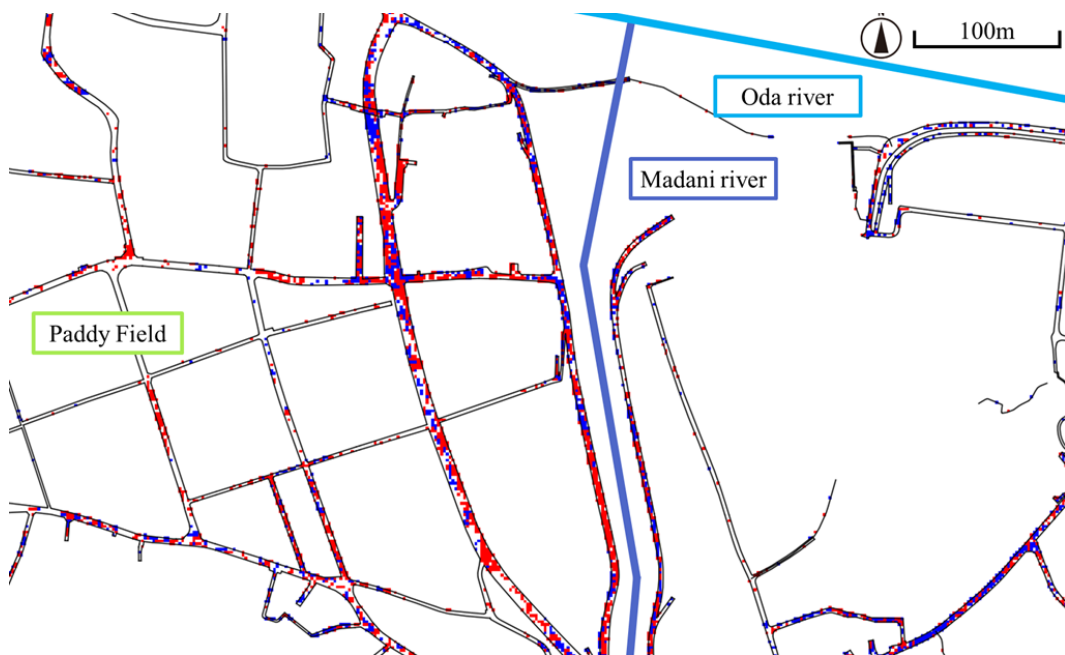


**Fig.5.23** Extended figure (Intersection of Madani and Oda river)

the roads surrounding them are also flooded extensively (Fig.5.20). There is a possibility that it can't be judged correctly since there are more uncolored areas than other wide roads although there are some areas

colored in red by the extraction results (Fig.5.21, 5.22). It is caused that the road width is small and there are paddy fields in the vicinity as is also the result of extraction around the Kurashiki Makibi Support School. The sidewalk near Oda River is colored in red (Fig.5.22) and another sidewalk several meters away from it is colored in blue. Therefore, the road can be judged whether it is damaged by the disaster if the roads are significantly affected by flooded and sediment even if the road width is small (Fig.5.12, 5.13).

There are a lot of the flooded areas at the confluence of Madani River run north-south direction located in the center of the target area and Oda River runs east-west direction, and a lot of flooded area can be also grasped from Fig.5.20. Similarly, there are also more colored areas around the confluence of Madani River and Oda River than the surrounding area in the extraction result (Fig.5.21, 5.23).

## 5.4 Conclusions

It is possible whether or not there is flooded on wide roads can be judged appropriately. As the results of grasping the disaster situation using SAR images, it is found that the extensive changes such as flooded areas can be extract by the method of additive color mixture used in this study. Focusing on only the roads, it is found that the effects of the flooded and sediment on the road can be grasped correctly in the wide road. However, it is difficult to recognize the effects of the flooded and sediment on the narrow road or a road around the water area regardless of with or without a disaster since the resolution of the SAR image used in this study is 2.5m and it is necessary to consider the influence of abandoned vehicles, etc. It is necessary to analyze using the satellite with high resolution in order to recognize whether or not there is a flooded in the road with a small width. In recent years, the spatial resolution of SAR images has improved remarkably, and Terra SAR-X and COSMO-SkyMed with a resolution of 1 to 5 m have been launched, and also it became possible to shoot SAR images with a resolution of 0.25 m in this year. It can be said that there is a good possibility that such high-resolution SAR images can be used in the event of a disaster in the future. In the future, it is desirable to automatically extract the flooded area and the area with sediment by machine learning in order to make it easier to grasp the changing area.



## 6 . Discussion and conclusions

In this study, the evacuation simulation considering the flooding state by a storm surge on the basis of the result of flooding analysis by the OpenFOAM which is one of the Computational Fluid Dynamics (CFD) tools is conducted so as to grasp the proper evacuation behavior when a storm surge occurs. Next, the additional evacuation simulation in which the agent grasps the flooding state beforehand was carried out under the same conditions as those used in the analysis in which the agent doesn't grasps the flooding state in advance so as to understand the effect of grasping the inundation place beforehand on the evacuation action. The damage situation on the road was extracted using SAR image and road edge data in order to grasp the damaged area on the road necessary for smooth recovery and relief activities after the disaster since the purpose of this study is not only to provide the useful information on disaster mitigation measures, but also to promptly grasp the disaster area immediately after a disaster and to provide the information of leading to more rational recovery activities.

As mentioned in Chapter 1, the awareness of hazard map is currently as low as about 50%, and there are many people who feel that it is useless. However, this research revealed that it is very important to know the flooding state in advance. Also, it is possible to grasp the flooding status which changes every moment from the flooded analysis and the information such as the evacuation route according to the flooding status and the place where the evacuation spot is insufficient from the evacuation simulation. Therefore, as one of the disaster mitigation method, it is necessary to prepare and publish a highly useful hazard map reflecting the information obtained in this study, and also to make efforts to improve the awareness of the hazard map. In order to protect the community and residents from disaster in the long term, it is needed to take structural measures such as the construction of new evacuation spot and non-structural measures such as the making the hazard map useful and raising awareness of the hazard map. By the simulation carried out in this study, it is possible to obtain the timeline information on the flooded state and the area information in which the refuge place is insufficient in addition to the disaster prior information which should be described in the hazard map. As issues of the hazard map, the improvement in usefulness and recognition is mentioned. As has already mentioned above, it is considered that adding the information grasped in this study to the hazard map may lead to the improvement of usefulness and recognition of the hazard map.

In the meantime, the recognition of the hazard map can be improved by the actions that students of the local area university and NPO on the disaster volunteer positively carry out the workshop and citizen lecture about disaster prevention and present disaster prevention measures to the resident with the hazard map. At present, the workshops using tsunami inundation analysis have been held <sup>46)</sup>, and the residents have come to revise the evacuation destination or rethink to advance the evacuation start time through the workshops. The presentation of the simulation result in the workshop and lecture on the disaster prevention

seems to be very effective. Therefore, by presenting the result of evacuation behavior simulation in addition to the storm surge flooding analysis carried out in this study, it is possible not only to grasp the threat of storm surge flooding and the time required for flooding, but also to discuss the appropriate evacuation start time and evacuation route, as well as the measures to be taken when evacuation is delayed. It is desirable to present the results of simulations conducted by the authors in the past on evacuation behavior in early evacuation<sup>47)</sup> since it is also important to consider the evacuation preparation time in grasping the time required for evacuation in a disaster<sup>48)</sup>. In addition, by carrying out simulations considering regional characteristics such as the age distribution of the target region, the problems to be solved and points to be considered at the time of disaster can be set for each region, so that the residents can discuss the disaster prevention measures and evacuation actions based on such simulations. The simulation carried out in this study can be applied not only in Japan but also in various places in the world, since it is easy for the simulation to obtain and it is analyzed using cheap or free data, and as already mentioned above, the issues to be solved such as regional characteristics and regional problems at the time of disaster can be reflected in the analysis parameters. Even residents without specialized knowledge can easily understand the disaster situation and appropriate evacuation behavior since this simulation can visualize the flooded situation and the movement of evacuees. So that more concrete disaster prevention measures will be taken by informing residents of the disaster prevention information and conducting evacuation drills based on the simulation results. In recent years, various disasters have occurred in various places in Japan, and it seems that the disaster prevention consciousness of the nation is improving. On the other hand, no large-scale disasters have occurred in Takamatsu City, Kagawa Prefecture since 2004. Therefore, it is considered that the weathering of disasters and enhance the momentum to prepare for disasters from a long-term perspective not only by actively tackling disaster prevention and mitigation using simulations as shown in this paper but also by reconsidering past disasters.

These information not only enhance the current hazard map, but also enable us to suggest more appropriate location of the evacuation sites which are newly added. As a future task, it is needed to examine where to add an evacuation spot in areas where there is a shortage of the spots so as to ensure safety and economy, and what is a safer and faster way to evacuate when such an additional spot is added. In Japan, the evacuation of the elderly is also a problem because of the aging of the population. Therefore, not only workshops and evacuation drills in the local government, but also individual disaster prevention measures for each region in the long term such as the utilization method of evacuation supporters and disaster prevention workers will be developed by carrying out the evacuation behavior simulation according to the features of each region such as the region with many elderly people and the depopulated region. Additionally, it is possible to find the problem in present countermeasure through the verification of evacuation behaviors or to take the useful disaster prevention countermeasure which matches the region more through the trial of the solution plan by conducting the similar simulation, when the disaster occurs regardless of large and small. For example, the simulation carried out in this study is also practiced in local governments, etc., and it leads to the proposal of long-term disaster prevention measures policy in the object region. It is necessary to reflect more realistic parameters for simulation, such as evacuation using vehicles, tourists who are not familiar with the intended area, and people who cannot move independently, in consideration of the fact that the agents in many local cities tend to evacuate using vehicles, that the information presentation to tourists is insufficient, and that the consideration is necessary for the elderly.

As described above, it is found that the disaster analysis and evacuation simulation conducted in this study are effective as disaster prevention and mitigation measures. In addition, the satellite images are analyzed in this study as recovery and reconstruction measures after the disaster. Although the resolution of the satellite images used in this study is not high resolution, it becomes possible to grasp the changes before and after the disaster even with such satellite images. The extraction of change areas on the roads using SAR images used in this study may lead to rapid restoration activities since the blockage status on wide roads where special vehicles can pass is necessary to grasp for the first report and promptness is required for restoration and rescue. It is easy to obtain satellite images before a disaster and satellite images are taken quickly even after a disaster occurs since a lot of satellite images have been taken in recent years. Information on the road area may be delivered to the disaster area more quickly by analyzing the satellite images immediately after a disaster using this analysis method. It is easy for residents to recognize the disaster situation since the road condition is shown in only two colors: cyan and red in the analysis results. Therefore, it can inform the available roads in the event of the disaster or returning home temporarily by providing information not only the experts of the disaster giving direction in the disaster spots but also the residents who evacuated to the evacuation spots Based on the above, the research on disaster prevention/mitigation measures before a disaster and recovery/reconstruction measures in the event of a disaster based on mathematical engineering is conducted in this study. As a result, it becomes possible to consider the disaster reduction and recovery measures in large-scale cities, which cannot be grasped by experiments. It is an issue to develop the results of this research into more elaborate ones and to apply them to the social world in collaboration with local governments.

# REFERENCES

## Chapter 1

- 1) Committee and Verification of water disaster in Joso City, "Verification report of supporting for the water disaster in Kinugawa River in 2017", 92p, 2016
- 2) Research group of the heavy rainfall disaster in Tohoku in 2015, "Research report of the disaster by the heavy rainfall in Kanto area on September 2015", 173p, 2016
- 3) Takamatsu City, "Disaster information about Tokai and Tonankai earthquake" <https://www.city.takamatsu.kagawa.jp/1334.html> (accessed 2021-01-06)
- 4) Kagawa prefecture, "The historical records of inundation, The flooding damage caused by storm surge which is generated by typhoon No.0416", <http://www.pref.kagawa.lg.jp/kasensabo/kasen/02-suigai/index.html> (accessed 2021-01-06)
- 5) T. Suzuki "Damage situation of house and public facilities in Takamatsu City by 16th typhoon in 2004", Report of NILIM, No. 268, pp.1-6, 2005
- 6) A. Tanaka, J. Ichizawa, Y. Miyagawa, H. Yoshii, Y. Jibiki, S. Udagawa, N. Sekiya, I. Nakamura, I. Matsuo, "A survey for residents' behavior affected by a torrential rain: a case study from the town of Sayo in Hyogo prefecture in 2009, [http://www.iii.u-tokyo.ac.jp/manage/wp-content/uploads/2016/03/20110427-rsrNo27\\_2.pdf](http://www.iii.u-tokyo.ac.jp/manage/wp-content/uploads/2016/03/20110427-rsrNo27_2.pdf) (accessed 2021-01-06)
- 7) Takamatsu City, "Hazard Map in Takamatsu City", <http://www.city.takamatsu.kagawa.jp/takamatsu-bosai/> (accessed 2021-01-06)
- 8) M. Ushiyama, F. Imamura, T. Katayama, K. Yoshida, "Investigation of people's behavior at heavy rainfall disaster in the highly flood disaster information age -A case study on the typhoon No.0206 July, 2002-", Journal of Japan Society of Hydrology and water resources, Vol.17, No.2, pp.150-158, 2004
- 9) Road Management Division of Kanto Regional Development Bureau, Ministry of Land, Infrastructure and Transport, "Application of the Disaster Countermeasures Basic Law in Heavy Rainfall Disaster in Kanto-Tohoku Region in September 2015", March issue of Road Administration Seminar in 2015, 5p, 2016

- 10) H. Murakami, "Study on flood disaster in Mabi Area, Kurashiki City by torrential rains in West Japan 2018 -Some lessons from Arii questionnaire-", Chugoku Region Division Research of Natural Disaster Research Council, No.5. pp.19-pp.22,2019

## Chapter 2

- 11) OpenFOAM Foundation : OpenFOAM User Guide 2.3 Breaking of a dam, <http://www.openfoam.org/docs/user/> (accessed 2021-01-06)
- 12) Brackbill, J. U., D. B. Kotrhe and C. Zemach, "A Continuum Method for Modeling Surface Tension", *J.Comp.Phys*, Vol.100, pp.335-354, 1992
- 13) Y. Inukai, K. Oguni, M. Hori, "Development of Measurement-based Multiagent Simulator for Evacuation Process", *Journal of Applied Mechanics*, Vol.8, pp.629-636, 2005
- 14) M. Hori, Y. Inukai, K. Oguni, T. Ichimura, "Study on Developing Simulation Method for Prediction of Evacuation Processes after Earthquake", *Sociotechnica*, Vol.3, pp.138-145, 2005
- 15) M. Oshino, "Evacuation Simulation Based on Multi-agent Model", Graduation thesis in Chuo University, 42p, 2005
- 16) K. Watanabe, A. Kondo, "Development of Tsunami Evacuation Simulation Model to Support Community Planning for Tsunami Disaster Mitigation", *Journal of Architecture and Planning*, Vol.71, No.637, pp.627-634, 2009
- 17) Takamatsu City; "The number of households and households by size of household segregated by sex and age", <https://www.city.takamatsu.kagawa.jp/7729.html> (accessed 2021-01-06)

## Chapter 3

- 18) K. Kawaike, H. Maruyama, S. Yoshimoto, M. Noguchi, "Inundation Flow Analysis in the Isahara Low-lying Area and its Application to Strategies Reducing Flood Damage", *Proceedings of Hydraulic Engineering*, Vol.49, pp.565-570, 2005
- 19) K. Tachi, K. Takedomi, K. Kawamoto, M. Kaneki, S. Iida, R. Hirakawa, Y. Tanioka, "Development of Inundation Flow Analysis Model Considering Landside Water, -Study in Ogaki City-", Vol.8, pp.145-150, 2002
- 20) R. Uchida, "Development of Highly Accurate Simulator of Inundation Flow for Water Disaster Measure Support", *Research Report for Hydrosience and Hydraulic Engineering of 2006 in Hiroshima University*, March issue, pp.466-471, 2007
- 21) E. Ohsita, H. Kume, "Investigations on Storm Surge and Tsunami Hazard Map to Minimize Casualties", *Report of the Coastal Development Institute of Technology*, No.3, pp.9-12, 2003

- 22) Takamatsu City, "Hazard Map Produced by Takamatsu City", <http://www.city.takamatsu.kagawa.jp/takamatsubosai/pdfmap/takasio.pdf> (accessed 2021-01-06)
- 23) T. Tomita, K. Honda, H. Kawai, T. Kakinuma, "Damage in Takamatsu by Storm Surge Inundation of Typhoon No.0416", Proceedings of Coastal Engineering, Vol.52, pp.1326-1330, 2005
- 24) Kagawa prefecture, "Port Planning Map in Takamatsu", [http://www.pref.kagawa.jp/kowan/ports/map/big/01\\_takamatsu.pdf](http://www.pref.kagawa.jp/kowan/ports/map/big/01_takamatsu.pdf) (accessed 2017-02-08)
- 25) D. Tomihara, Y. Takagi, "Analysis of Milk Crown Formation by Using the Adaptive Mesh Refinement of OpenFOAM", Proceedings of the 25th Symposium on Computational Fluid Dynamics, Vol.31, pp.175-179, 2012
- 26) Y. Kawasaki, H. Nakao, K. Izuno, "Multi-phase Flow Analysis of Tsunami Forces and Associated Pressures on a Rectangular-section Bridge Girder", Journal of Japan Society of Civil Engineers, Ser.A1, Vol.71, No.2, pp.199-207, 2015
- 27) Y. Oikawa, M. Mukaitani, "Characteristics of Human Behavior in High Tide Disaster by Typhoon 0416 and 0418", Papers of Research Meeting on Civil Engineering Planning, Vol.31, CD-ROM, 179, 2005
- 28) F. Kato, S. Inagaki, K. Noguchi, M. Hukuhama, "Coastal Disaster in 2004", Technical Note of National Institute for Land and Infrastructure Management, No.273, pp.9-10, 2005
- 29) Ministry of Land, Infrastructure and Transport, "Guide to making figure of expected inland inundation area", pp.11-12, 2015

## Chapter 4

- 30) M. Takeda, K. Inoue, K. Toda, K. Kawaike, "Consideration of Hazard Map and Evacuation for Storm Surge", Proceedings of Coastal Engineering, Vol.44, pp.356-360, 1997
- 31) M. Takahashi, H. Imanishi, K. Abe, "A study on the Selection of Refuge Facilities Using GIS in Local Plan for Disaster Prevention", Papers of the 32th Tohoku Branch of Japan Society of Civil Engineering, CD-ROM, IV-53, 2013
- 32) M. Minami, A. Ando, R. Akatani, "Tsunami Disaster Evacuation Planning Considering with Vertical Drop of the Evacuation Route", Papers of the 32th Research Meeting on Civil Engineering Planning, 216, 2005
- 33) Henry, K. D., Wood, N. J., and Frazier, T. G., "Influence of road network and population demand assumptions in evacuation modeling for distant tsunamis", Natural Hazards, 85(3), pp.1665-1687, 2017.
- 34) T. Katada, N. Kuwasawa, "Development of tsunami comprehensive scenario simulator for risk management and disaster education", Journal of Japan Society of Civil Engineers, Ser. D2 (Historical Studies in Civil Engineering), Vol.62, No. 3, pp.250-pp.261, 2006

- 35) T. Futagami, K. Ide, M. Imanishi, "Practice research for disaster prevention education promotion utilizing disaster simulator", Journal of Japan Society of Civil Engineers, Ser. F6 (Safety Problem), Vol.71, No. 2, I.153-I.160, 2015
- 36) Takamatsu city, "Populations classified by age and sex", <https://www.city.takamatsu.kagawa.jp/7729.html> (accessed 2021-01-06)
- 37) Oberg, T, Karsznia A, Oberg. K, "Basic gait parameters: Reference data for normal subjects, 10-79 years of age, Journal of Rehabilitation Research and Development", Vol.30, No. 2, pp.210-223, 1993
- 38) J. Kiyono, F. Miura, K. Takimoto, "Simulation of emergency evacuation behaviour during disaster by using distinct element method", Journal of Japan Society of Civil Engineers, No.537, pp.233-244, 1996

## Chapter 5

- 39) D. Ueda, S. Mabu, T. Kuremoto, "Landslide Detection Using CNN with SAR Images before/after the Disaster and DEM", The 32nd Annual Conference of the Japanese Society for Artificial Intelligence, Proceedings of the Annual Conference of JSALI, No.32, 1D1-02, 2018
- 40) K. Hasekura, H. Gokon, K. Meguro, "Developing a new method to detect tsunami inundation area by integrating optical satellite image and SAR data", SEISAN KENKYU, Vol.70, No.4, pp.229-233, 2018
- 41) T. Komuro, Y. Akamatsu, K. Yamaguchi, P.E. Yastika, N. Simizu, Y. Nihei, "Identification of damaged ponds using SAR images after a heavy rainfall in northern Kyushu, 2017", E-journal GEO, Vol.14, pp.271-287, 2019
- 42) W. Liu, F. Yamazaki, H. Gokon, S. Koshimura, "Extraction of Tsunami Inundation Areas and Damaged Buildings for the 2011 Tohoku, Japan Earthquake from High-resolution SAR images", Journal of Japan Association for Earthquake Engineering, Vol.12, pp.73-85, 2012
- 43) M. S. Horritt, "A statistical active contour model for SAR image segmentation", Image and Vision Computing, Vol.17, pp.213-224, 1999
- 44) Geospatial Information Authority of Japan, Estimated flooding gradient tints map around Mabi-cho, Kurashiki city due to heavy rain in July 2018, <https://www.gsi.go.jp/common/000208572.pdf> (accessed 2021-01-06)
- 45) Geospatial Information Authority of Japan, Geographical Survey Institute Map, Orthogonal image taken after the heavy rain in July 2018 (Takahashi River district) <https://maps.gsi.go.jp/> (accessed 2021-01-06)

## Chapter 6

- 46) A. Nonomura, A. Tani, M. Masumoto, "Tsunami evacuation buildings designated by local community", *Journal of Natural Disaster Science J. JSNDS*, 37-4, pp.407-418, 2019
- 47) S. Kubo, M. Wada, H. Yoshida, M. Hori, T. Ichimura, M.L.L. Wijerathne, "Numerical study on influence of first motion of evacuation onto evacuation behavior in storm surge flooding", *Journal of Structural Engineering*, Vol.64A, pp.155-168, 2018
- 48) Lindell, M. K., Sorensen, J. H., Baker, E. J., and Lehman, W. P., "Community response to hurricane threat: Estimates of household evacuation preparation time distributions", *Transportation research part D: transport and environment*, 85, 102457, 2020



## Acknowledgment

I spent almost 6 years at Yoshida Laboratory, Graduate School of Kagawa University, and worked on the research. I suffered from a lack of ability every day, but I was finally able to complete my doctoral thesis. When I was in the first and second years of the doctoral program, I was worried about the direction of my research and the course of my future. Even in such a hard time, I was able to obtain satisfactory results by virtue of a lot of advice and strict guidance from Professor Yoshida, my supervisor. I learned not only about research but also how to teach juniors and how to manage my own mind and time during 6 years at Yoshida Laboratory. I am very grateful to Professor Yoshida. I also appreciate Professor Ishizuka and Associate Professor Nonomura, who are subadvisors. I was able to receive clear directions at each research report meeting and reconsider my own research. Additionally, Professor Hori of Japan Agency for Marine-Earth Science and Technology, and Professor Ichimura and Associate Professor Lalith of the University of Tokyo have also provided guidance many times since I started my research. They taught me not only the research methods and how to use the programs but also about awareness and approach for research. Also, I am grateful to my friends, seniors, and juniors who belonged to the laboratory during the same period as me. When I got stuck on my research, I was able to refresh myself by talking with them. I am also grateful to my parents who allowed me to do what I wanted to do without denying my path. I may cause a lot of worries to my parents as I continue to pursue my career as a researcher, but I will commit to getting the results of my research and return the favor. I would like to express my gratitude to everyone who has been supporting me.

This work was supported by JSPS Grant-in-Aid for JSPS Fellows Grant Number 19J14428.